Experimental verification of multi-antenna techniques for aerial and ground vehicles' communication

Izydorczyk, Tomasz

Publication date:
2020

Document Version
Publisher's PDF, also known as Version of record

EXPERIMENTAL VERIFICATION OF MULTI-ANTENNA TECHNIQUES FOR AERIAL AND GROUND VEHICLES' COMMUNICATION

BY

TOMASZ IZYDORCZYK

DISSERTATION SUBMITTED 2020

AALBORG UNIVERSITY

DENMARK

Experimental verification of multi-antenna techniques for aerial and ground vehicles' communication

Ph.D. Dissertation

Tomasz Izydorczyk

Aalborg University
Department of Electronic Systems,
Wireless Communication Network Section
Fredrik Bajers Vej 7A, 9220 Aalborg Øst, Denmark

Dissertation submitted:	May 2020
PhD supervisor:	Professor Preben Mogensen Aalborg University
Assistant PhD supervisors:	Associate Professor Gilberto Berardinelli Aalborg University
	Assistant Professor Fernando M.L. Tavares Aalborg University
PhD committee:	Associate Professor Jimmy Jessen Nielsen (chairman) Aalborg University
	Professor Christian Wietfeld TU Dortmund University
	Research Manager Johan Torsner Ericsson Research
PhD Series:	Technical Faculty of IT and Design, Aalborg University
Department:	Department of Electronic Systems

ISSN (online): 2446-1628
ISBN (online): 978-87-7210-645-8

Published by:
Aalborg University Press
Langagervej 2
DK – 9220 Aalborg Ø
Phone: +45 99407140
aauf@forlag.aau.dk
forlag.aau.dk

Printed in Denmark by Rosendahls, 2020

Curriculum Vitae

Tomasz Izydorczyk

Tomasz Izydorczyk received B.Sc. degree in Electrical Engineering from Silesian Technical University, Poland and M.Sc. degree in Mobile Communications from Télécom ParisTech/Eurecom, France in 2015 and 2017 respectively. In 2016, he was a research intern with Intel Mobile Communications. He is currently pursuing a doctorate degree at Aalborg University (AAU). His research interests include MIMO techniques, V2X and UAV communications, focusing on their experimental verification.

Curriculum Vitae

Abstract

In the last years, the need for vehicular communications has been growing rapidly. Ground vehicles are experiencing higher and higher levels of autonomy and with the help of the Vehicular to Everything (V2X) communication, in the future, can potentially become fully autonomous. Cellular-connected Unmanned Aerial Vehicles (UAVs), popularly known as drones, will be used for package delivery, TV broadcasting and many other applications. Both types of vehicles demand high data throughput as well as reliable connectivity.

The design of vehicular communication systems faces multiple challenges. For aerial vehicles, the high probability of line-of-sight communication with serving base station may result in severe interference conditions. Ubiquitous coverage and the expected amount of data traffic due to a large number of vehicles are instead the main challenges for ground-level vehicular communications.

Nonetheless, increased space and reduced power constraints of the vehicles with respect to the typical handheld device offer the opportunity to install multiple antennas on a vehicular device. These extra degrees of freedom can be used to potentially mitigate interference and ensure reliable vehicular connectivity. This thesis focuses on an experimental investigation on how multi-antenna technologies can be most efficiently used to improve vehicular connectivity. The manuscript contains experimental results focused on the performance of multi-antenna systems operating over live 4G networks to improve vehicular communication.

The first part of this thesis focuses on downlink vehicular communication. A 16-antennas software-defined radio measurement tool capable to record cellular signals has been designed for analysis of different multi-antenna combining techniques. Using offline post-processing, the potential of Maximum Ratio Combiner (MRC) and receive beamforming is studied, by comparing Signal-to-Interference plus Noise Ratio (SINR) of the decoded cellular signals. To further correlate the gains of the multi-antenna techniques, spatial channel characterization is performed, analyzing the impact of angular spread, the stability of Angle of Arrival (AoA) over time and interference pat-

tern on the performance of multi-antenna receivers. Finally, different methods of choosing the beamforming direction are analyzed. The results indicate that both multi-antenna techniques outperform a single antenna system with an SINR increase by more than 7 dB. For ground-level vehicular communication, the relative performance of both multi-antenna techniques is comparable, though receive beamforming has clear advantages in high dominant interference ratio (DIR) scenarios. Meanwhile, beamforming outperforms MRC for the downlink UAV communications due to better spatial interference mitigation properties stemming from antenna directionality and low angular spread of the incoming signals.

The second part of this thesis is devoted to uplink vehicular communication and is focused on the performance of uplink beamforming. For the evaluation purposes, a real-time measurement tool based on a directional antenna switching system operating in live cellular networks has been designed and built for both V2X and UAV studies. During the studies, the focus is on understanding the achievable uplink throughput of a vehicle as well as the mobility management system performance. Furthermore, the spatial filtering of uplink interference is studied for UAV communication. This study is later extended by an extensive system-level simulation campaign, in which the potential of uplink beamforming for a scenario with a large number of UAVs is investigated. The obtained results show the potential of uplink beamforming for coverage extension due to antenna directionality. However in good channel conditions, the antenna gain may potentially be compensated by uplink power control, limiting uplink throughput improvements. Beamforming is found to reduce the number of successful handovers by maintaining longer connectivity with the same base station due to antenna gain. Simulation results show how the spatial filtering of interference due to uplink beamforming, improves overall network performance leading to improved throughput and ensuring a fair coexistence with ground-level users.

Resumé

Behovet for vehicular kommunikation er hastigt vokset de seneste år. Vores jordbaserede fartøjer, bliver i øget grad selvkørende ved hjælp af Vehicular to Everything (V2X) kommunikation og i fremtiden bliver de potentielt fuldkomment autonome. Unmanned Aerial Vehicles (UAV), eller populært sagt droner, der er forbundet til det cellulære mobilnetværk, vil kunne anvendes til blandt andet pakkeaflevering og TV signal transmissioner. Begge typer af fartøjer, kræver høj datarate samt en pålidelig trådløs radio forbindelse.

Der er mange udfordringer forbundet ved at designe kommunikationssystemer til vehicular kommunikation. Ved luftbårne fartøjer, kan den øgede sandsynlighed for line-of-sight kommunikation med dens serving base-station resultere i kritiske interferenssituationer. For jordbaserede fartøjer er de store udfordringer at opnå dækning alle-steder og at håndtere de meget store mængder af data fra højt antal af fartøjer.

Ikke desto mindre, giver de større skala ved fartøjerne, sammenlignet med en normal håndholdt enhed, mulighed for at montere multiple antenner på fartøjet. De resulterende ekstra frihedsgrader kan potentielt anvendes til at begrænse interferens og sikre en pålidelig vehicular kommunikation. Denne afhandling, fokusere på eksperimentel undersøgelse af hvordan multiantenneteknologi best muligt kan anvendes til at forbedre vehicular kommunikation. Manuskriptet indeholder eksperimentelle resultater af multiantennesystemer der opererer over et live 4G netværk, med formålet at forbedre vehicular kommunikation.

Den første del af afhandlingen fokusere på downlink vehicular kommunikation. Med formålet at analysere multiantennekombinationsteknikker, er et 16-antenne software-defined radio målingsværktøj, i stand til at optage cellulære radiosignaler, blevet udviklet. Ved hjælp af offline post-processering, er potentialet ved Maximum Radio Combiner (MRC) og modtager beamforming multiantenneteknikker blevet studeret, ved at kombinere Signal-to-Interference plus Noise Ratio (SINR) af de afkodede cellulære radiosignaler. Spatial channel characterization er anvendt for at korrelere de observerede forbedringer af multiantenne teknikkerne mod angular spread, stability of Angle of Arrival (AoA) over tid samt interferensmønstre hos den modta-

gende multiantenne enhed. Yderligere er forskellige metoder for valg af beamforming retninger analyseret. Resultaterne indikere at begge multiantenneteknikker overgår singleantenneteknikker med et øget SINR på mere end 7 dB. For jordbaserede vehicular kommunikation er den relative performance af begge multiantenneteknikker sammenlignelige, men modtager beamforming har en klar fordel ved høj dominant interfence ratio (DIR) scenarier. I mellemtiden udkonkurrere beamforming MRC for downlink UAV kommunikation på grund af bedre rumlige interferensbegrænsende egenskaber, der stammer fra antennens retningsbestemmelse og lav vinkeludbredelse af de indgående signaler.

Den anden del af afhandlingen er dedikeret til uplink vehicular kommunikation med fokus på performance af uplink beamforming. Et realtids måleværktøj baseret på et direktionelt antenneskiftningssystem som er udviklet til at operere i et live cellulært netværk og til anvendelse ved både V2X og UAV studier. Under studierne i denne del af afhandlingen har vores fokus har været på at forstå hvad er den opnåelige uplink datarate er for et fartøj og dets performance under mobility management. Derudover har vi studeret spatial filtrering af uplink interferens ved UAV kommunikation. Studiet er senere udvidet med en omfattende system-level simuleringskampagne, for at afdække potentialet for uplink beamforming ved et stort antal af UAVs. Vores opnåede resultater viser potentialet for at udvide dækningen ved uplink beamforming ved hjælp af antennens retningsbestemmelse. Ved gode signal betingelser er den opnåede forbedring ved beamforming dog opvejet af uplink power kontrol mekanismen og derved er der ikke opserveret en forbedring af uplink dataraten. Det er fundet, at beamforming er i stand til at reducere antallet af succesfulde handovers, ved at muliggøre vedligeholdelsen af forbindelsen til den samme base-station længere ved hjælp af det opnående antenne gain. Simuleringsresultaterne viser hvordan spatial filtrering af interferens forårsaget af uplink beamformining, forbedre den overordnede netværks performance og resultere i en forbedret datarate og samtidig sikre en fair coexperience for jord-baserede brugere.

Contents

List of Abbreviations

3GPP 3rd Generation Partnership Project

5G Fifth Generation

A2G Air-to-Ground

AoA Angle of Arrival

AS Angular Spread

BS Base Station

BVLOS Beyond Visual Line of Sight

C-V2X Cellular-V2X

C2 Command and Control

DoF Degrees of Freedom

DSRC Dedicated Short-Range Communication

GdUE Ground User Equipment

HPBW Half Power Beamwidth

IoT Interference over Thermal noise

IRC Interference Rejection Combining

KPI Key Performance Indicator

LoS Line of Sight

LTE Long Term Evolution

MIMO Multiple Input Multiple Output

MRC Maximum Ratio Combiner

MUSIC Multiple Signal Classification

QoS Quality of Service

RF Radio Frequency

RSRQ Reference Signal Received Quality

RSRP Reference Signal Receive Power

RSU Road Side Unit

SAGE Space-Alternating Generalized Expectation-maximization

SINR Signal-to-Interference-plus-Noise Ratio

SDR Software-Defined Radio

SVD Singular Value Decomposition

UAV Unmanned Aerial Vehicle

UE User Equipment

V2V Vehicle-to-Vehicle

V2X Vehicle-to-Everything

VUE Vehicular User Equipment

Thesis Details

Thesis Title:	Experimental verification of multi-antenna techniques for aerial and ground vehicles' communication
Ph.D. Student:	Tomasz Izydorczyk
Supervisors:	Prof. Preben Mogensen, Aalborg University, Denmark Assoc. Prof. Gilberto Berardinelli, Aalborg University, Denmark Assist. Prof. Fernando M.L. Tavares, Aalborg University, Denmark

The research described in this manuscript has been carried out at the Wireless Communication Networks (WCN) section at Aalborg University, Denmark. This work was conducted in parallel with the mandatory courses and teaching activities required to attain the PhD degree.

The main body of this thesis consists of the following papers:

[A] T. Izydorczyk, F. M.L. Tavares, G. Berardinelli and P. Mogensen, "*A USRP-based multi-antenna testbed for reception of multi-site cellular signals*", IEEE Access 2019.

[B] T. Izydorczyk, M. Bucur, F. M.L. Tavares, G. Berardinelli and P. Mogensen, "*Experimental evaluation of multi-antenna receivers for UAV communication in live LTE networks*", IEEE GLOBECOM workshops proceedings 2018.

[C] T. Izydorczyk, F. M.L. Tavares, G. Berardinelli, M. Bucur and P. Mogensen, "*Angular Distribution of Cellular Signals for UAVs in Urban and Rural Scenarios*", The 13th European Conference on Antennas and Propagation (EUCAP) 2019.

[D] T. Izydorczyk, F. M.L. Tavares, G. Berardinelli, M. Bucur and P. Mogensen, "*Performance evaluation of multi-antenna receivers for vehicular communications in live LTE networks*", IEEE 89th Vehicular Technology Conference (VTC2019-Spring) 2019.

[E] T. Izydorczyk, G. Berardinelli, F. M.L. Tavares, M. Bucur and P. Mogensen, "*On the potential of uplink beamforming in vehicular networks based on experimental measurements*", IEEE 90th Vehicular Technology Conference (VTC2019-Fall) 2019.

[F] M. M. Ginard, T. Izydorczyk, P. Mogensen and G. Berardinelli, "*Enhancing vehicular link performance using directional antennas at the terminal*", IEEE GLOBECOM workshops proceedings 2019.

[G] T. Izydorczyk, M. M. Ginard, S. Svendsen, G. Berardinelli and P. Mogensen, "*Experimental evaluation of beamforming on UAVs in cellular systems*", submitted to IEEE 92nd Vehicular Technology Conference (VTC2020-Fall) 2020.

[H] T. Izydorczyk, G. Berardinelli, P. Mogensen, M. M. Ginard, J. Wigard and I. Z. Kovács, "*Achieving high UAV uplink throughput by using beamforming on board*", IEEE Access 2020.

This dissertation has been submitted for assessment in partial fulfillment of the PhD degree. The dissertation is based on the submitted or published scientific papers which are listed above. Parts of the papers are used directly or indirectly in the extended summary of the thesis. As part of the assessment, co-author statements have been made available to the assessment committee and are also available at the Faculty.

Acknowledgments

This PhD thesis is a result of hard work and invaluable help and support from many kind people. I express my sincerest and special thanks to my supervisors. To Preben Mogensen, for his guidance and support to help me grow as a researcher. To Gilberto Berardinelli for tireless discussions and corrections of every technical document and publication I ever wrote. Finally to Fernando M.L. Tavares for his technical expertise and help which allowed me to quickly settle in the role of a PhD student.

I would like to extend my gratitude to two colleagues: Mădălina Bucur and Michel Massanet Ginard for their contribution in the project and all the daily chats and discussions improving the team's atmosphere. Further I would like to thank Kenneth Knirke, Jesper Dejgaard Meyer and Steffen Hansen for all their work and commitment in preparation of the testbeds as well as the execution of the measurement campaigns.

I thank my spouse for her patience and endless support throughout these years. Last but not least, I want to credit all my colleagues in the WCN section for their helpful recommendations and words of encouragement.

Tomasz Izydorczyk
Aalborg University, May 18, 2020

Part I

Introduction

Chapter 1

Introduction

1.1 Background

During the last decade, a major shift was observed in the design of wireless communication systems. Previously almost exclusively human-centric, the demands for the next generation wireless systems are driven by so-called vertical use cases. Due to rapid development in image processing, machine learning and artificial intelligence, driving the increasing interest in autonomous vehicles, vehicular communication emerges as one of the main use cases of future communication systems. Ground and Aerial vehicles, popularly referred to as cars and drones, constitute a large group of vehicular devices potentially benefiting from increased intelligence and wireless connectivity.

In the future, ground vehicles referred interchangeably as Vehicular User Equipments (VUEs), connected using Vehicle-to-Everything (V2X) communication, can potentially become fully autonomous. Self-driving vehicles would enable driver-less journeys leading to increased safety while reducing pollution and traffic jams [1]. IHS Markit [2] predicts that in 2040 more than thirty million autonomous vehicles will be sold globally. Further, as predicted in [3], already in 2030, the vehicles with a high level of autonomy will drive more than a half trillion miles worldwide!

While VUEs are expected to take over ground-level commuting services, Unmanned Aerial Vehicles (UAVs) will emerge in our skies. Autonomous or remotely pilot UAVs, using Beyond Visual Line of Sight (BVLOS) control enabled by wireless connectivity, will give rise to a plethora of services including delivery of goods, multimedia production, security or surveillance missions [4]. Market analysts forecast huge growth of the UAV market in upcoming years, reaching twelve billion dollars for sales of UAVs [5] and more than seventy billion dollars by 2022 in services offered using UAVs [6].

Table 1.1: Performance requirements for different types of safety-related vehicular messages

Use case	Latency	Reliability	Data Rate
Cooperative awareness	100 ms	90–95%	5–96 Kbps
Cooperative sensing	3 ms	$>$ 95%	up to 25 Mbps
Cooperative maneuvers	3–100 ms	$>$ 99%	up to 5 Mbps
Vulnerable road user	100 ms	95%	10 Kbps
Traffic efficiency	1 s	$<$ 90%	up to 2 Mbps
Teleoperated driving	5–20 ms	$>$ 99%	$>$ 20 Mbps

Table 1.2: UAV traffic requirements for C2 link

Downlink/Uplink throughput	60-100 kbps
Latency	50 ms
Reliability	Up to 10^{-3} packet error rate

1.1.1 Requirements of vehicular communication

VUEs in order to become more and more autonomous, require to gather information about the environment from its on-board sensors, from other vehicles as well as from other elements of road architecture (static information hubs as Road Side Units (RSUs), traffic lights or any other sensors). Table 1.1 presents the requirements imposed on the wireless network to support different types of messages [7]. They were defined during the 3rd Generation Partnership Project's (3GPP) Release 15 study on service requirements for enhanced V2X scenarios. Most of the use cases require highly reliable, low latency services delivered continuously with high availability. In emergency situations, VUEs may need to send the live video camera view for teleoperated driving. This would require a constant bit rate, high uplink throughput exceeding 20 Mbps. On top of safety-related features, a driver-less vehicle will become an infotainment platform providing digital content to its passengers which would require high downlink throughput scheduled as the best-effort traffic.

UAVs require a Command and Control (C2) link to efficiently steer the aircraft. Table 1.2 presents the requirements imposed on the wireless network by the C2 link, defined by 3GPP during Release 15 study on enhanced LTE support for aerial vehicles [8]. In addition, the payload-related communication imposes extra requirements, especially on the uplink communication. As presented in Table 1.3, continuous uplink throughput higher than 10 Mbps will be required to transmit a real-time video feed in cases of surveillance or real-time broadcasting UAVs [9].

Table 1.3: UAV traffic requirements for payload communications

Use case	Uplink throughput
Surveillance	10 Mbps
Infrastructure inspection	10 Mbps
Drone delivery	200 Kbps
Precision agriculture	6 Mbps
Real-time multimedia services	Minimum 10 Mbps

1.2 Cellular vehicular communication

Different wireless networks are considered to serve vehicular demands. Dedicated Short-Range Communications (DSRC) and Cellular-V2X (C-V2X) are two competing technologies designed for vehicular communications [10]. UAVs can be connected using among others WiFi, dedicated (proprietary) technologies or cellular networks [11].

This thesis is focused on the applicability of cellular networks to connect both ground and aerial vehicles. As argued in the previous section, vehicular networks demand high availability and ubiquitous connectivity. Cellular networks such as Long Term Evolution (LTE) or Fifth Generation (5G) can provide widespread coverage around the globe. In comparison with DSRC which is designed as a direct Vehicle-to-Vehicle (V2V) communication system, C-V2X technology can be also used to communicate with other elements of the road environment due to increased communication range [12]. The already-deployed cellular networks are also regarded as a cost-saver for the UAV communications with respect to the dedicated networks which would have to be designed and deployed from scratch.

1.2.1 Challenges of cellular vehicular communication

When trying to incorporate vehicles within a cellular network, it is worth recalling the differences between the users of the system: Ground User Equipments (GdUEs), VUEs and UAVs. The first difference is the traffic pattern. For GdUEs it is irregular, downlink oriented, served commonly as a best-effort type of traffic. For the VUEs, the downlink-uplink ratio is more balanced. A vehicle needs to receive information from other vehicles as well as share it's own. As presented in [7], vehicles supporting information sharing for automated driving will transmit on average ten messages per second. The traffic is therefore much more periodic, and requires high Quality of Service (QoS) [13].

Balanced traffic requirements in conjunction with a possible massive concentration of vehicles due to traffic jams or even regular downtown traffic,

may create capacity and interference problems leading to decreased downlink Signal-to-Interference-plus-Noise Ratio (SINR) and worse coverage than observed by GdUEs [14]. In rural areas, coverage problems may also occur in uplink due to the limited transmit power of the vehicle terminals. Usually as shown in [15], the coverage is uplink-limited due to low maximum uplink transmit power. For the GdUEs, mostly downloading content from the Internet, this problem is negligible, however for high uplink QoS demanding vehicles it may become a potential bottleneck.

UAVs require ubiquitous connectivity in the air. Cellular systems were originally deployed for the ground-level communications (antenna downtilt, cell planning etc.). However as shown in [16], cellular coverage is still sufficient up to hundreds of meters where small quadrocopters are expected to fly. The aerial coverage is the effect of favorable propagation characteristics in the Air-to-Ground (A2G) communication link [17]. With a limited number of obstructions (lack of trees or buildings), the signal strength observed by the UAV is higher than for the GdUEs due to the high Line of Sight (LoS) probability. Contrary to ground-level systems, UAV's downlink coverage becomes interference-limited as many strong signals are received from multiple Base Stations (BSs) [18].

A similar challenge may occur also in the uplink direction. Due to favorable propagation scenarios, a signal transmitted from the UAVs is received by multiple BSs leading to increased interference levels and therefore decreased uplink SINR for other users of these cells, effectively reducing their throughput. Assuming the same spectrum is shared among UAVs and GdUEs, their uplink coexistence becomes a major challenge.

As argued in this section, the use of cellular networks to serve vehicular services imposes several new challenges on the design of the next-generation wireless systems. Figure 1.1 presents the main challenges split between ground and aerial vehicles. Different parts of this thesis address them from various perspectives. In the figure, the list of main Key Performance Indicators (KPIs), used in this thesis to quantify the system's performance is also provided. Please note, that this thesis focuses only on radio link challenges of vehicular communications. Please refer to [19], for a survey on the economic, sociological and security challenges of vehicular communications.

1.2.2 Solutions proposed in the literature

There are many methods proposed in the literature to solve the aforementioned challenges. A complete literature review is provided, depending on the addressed challenge, in the introduction of each publication. At this point, it is beneficial to indicate the main research directions by grouping and shortly describing some of the proposed solutions.

To cope with downlink capacity problems for the ground vehicles, the

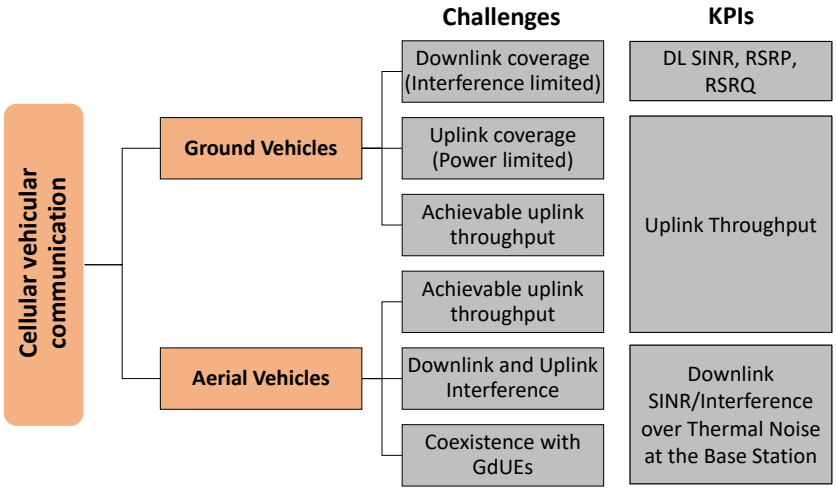

Fig. 1.1: Challenges of cellular vehicular communication

research direction is to maximize the spectral efficiency of the cell by spatially multiplexing multiple users using massive Multiple Input Multiple Output (MIMO) and mm-wave frequencies [20–22]. Benefiting from narrow beam shapes, the downlink inter-cell interference is reduced. Another, very similar solution, assumes installing the RSUs which are simple remote radio heads [23,24]. By using RSUs, the communication distance can be further reduced leading to the increased system's capacity, while the network intelligence can remain in the BS [25].

To mitigate interference and improve uplink capacity, it is envisioned that vehicles will have sidelink capabilities to send the uplink sensor data directly to the nearby vehicles with limited or no assistance from cellular infrastructure [26–28]. In this way, the communication distance is shortened, the system's capacity increased and interference reduced, due to limited transmit power. Finally, to avoid mutual interference with other incumbents of cellular systems, the European Union designated a 30 MHz spectrum in the 5.875-5.905 GHz frequency band for Intelligent Transport Systems [29].

The challenges of UAV communication such as downlink and uplink interference as well as coexistence with GdUEs are mostly addressed using one of the following three methods. Sub 6-GHz massive MIMO, due to beamforming at the BS is expected to greatly improve the coverage and mitigate interference, by focusing the BS antennas to transmit/receive only from the desired direction [30–32]. Based on the results of many measurement campaigns [16,18,33], 3GPP in Release 15 proposed a set of enhancements of LTE services for UAV communications [34]. Among others, different power con-

trol settings for the UAVs to limit their uplink transmit power and therefore mitigate interference; or UAV identification signaling were standardized. Finally, UAV's path planning can be seen as an optimization problem where the position of a UAV can be optimized to improve its SINR as well as limit interference caused to the network [35–37].

1.2.3 Drawbacks of proposed solutions

All presented research activities are shown capable of solving one or many challenges of vehicular communications. Unfortunately most of them require major investments in cellular infrastructure. Installation of RSUs, exchanging antenna panels or deployment of a new dedicated network for VUEs or UAVs will be expensive and may only be profitable in the large metropolitan areas or along main transit routes [25]. However VUEs and UAVs should be able to operate everywhere where needed, regardless of the state of the cellular infrastructure. In rural areas, where vehicle density is low, the proposed solutions may not be able to match the availability and throughput requirements.

1.3 Benefits of multi-antenna vehicles

1.3.1 Problem statement

The development of autonomous vehicular technologies depends on wireless communications' quality. While investing in cellular networks just to match the vehicular demands may not be profitable, the question arises:

What can be done to improve the connectivity of the vehicles without the need for expensive changes in the network infrastructure?

To answer this question, it is worth to once again recall the differences between a typical GdUE and a vehicular terminal. The one standout difference is the form factor. A typical GdUE is a handheld device, small enough to be placed in the pocket. This imposes practical constraints on the physical size of the battery or number of antennas together with respective Radio Frequency (RF) chains. On the other hand, VUEs and UAVs have a much bigger (and heavier) frame size. This observation leads to the hypothesis:

Multiple antenna systems, operating in sub-6 GHz frequencies can be installed on a vehicle terminal due to sufficient available space and power.

The main objective of this thesis is to understand the potential of multi-antenna systems installed on a vehicle terminal for dealing with the challenges of VUE and UAV communications. The theoretical foundation of the

multi-antenna systems is already well-established [38]. However, their performance benefits and practical applicability to vehicular scenarios are yet to be fully understood.

1.3.2 Multi-antenna techniques

Using multiple antennas provide extra Degrees of Freedom (DoF), which can be used to boost data rates or improve the system's reliability. The maximum throughput can be increased by sending multiple streams over the antennas (spatial multiplexing) and relying on well-conditioned channel matrices for retrieving the streams at the receiver [39]. Robustness can be achieved via diversity schemes, that can constructively exploit uncorrelated channels or beamforming schemes, that steer the transmit or receive signal over the desired direction, thus improving its strength as well as mitigating interference coming from unwanted directions.

To mitigate the challenges of vehicular communication, this work is focused on the use of multi-antenna techniques to improve the reliability, increase the coverage and thus meet the throughput demands imposed on vehicular communications. Therefore, two multi-antenna diversity techniques are studied: Beamforming and Maximum Ratio Combiner (MRC). They are further described in the remainder of this section.

Beamforming algorithms are usually used to increase the SINR for signals received (or transmitted) from the desired direction due to directional antenna gain. Knowing the optimal beamforming direction, a maximum theoretical gain B of:

$$B = 10 \log_{10}(N_{Ant}) \tag{1.1}$$

in dB can be achieved, where N_{Ant} is the number of antennas. Beamforming can also be used to cancel out up to $N_{Ant} - 1$ sources of interference by positioning antenna nulls towards their direction [39]. To realize the beamforming system in a practical design, a maximum antenna spacing of half-wavelength is needed, to avoid spatial aliasing.

Using a beamforming system installed on a vehicle terminal is expected to increase the network's coverage (SINR) and therefore the throughput. Due to directional beamforming gain, the desired signal power can be increased, while a narrow beam pattern may reduce the power of interference by spatially filtering signals from unwanted directions. However these benefits will only be observed, if optimal beamforming direction is known and Half Power Beamwidth (HPBW) is optimally designed based on the observed channel characteristics. On the other hand, vehicle-side beamforming may impact mobility management procedures. Using a directional pattern may lead to suboptimal handover decisions, as the received power from some cells will be increased while from others attenuated.

MRC is a method of diversity combining in which each receive branch is phase-corrected and weighted proportional to the experienced fading [40]. It is an optimal technique when no interference is present. However, in practical cellular systems like LTE, this assumption may not be valid as strong neighbor cell interference is often present. In such a case, Interference Rejection Combining (IRC) can be applied as it uses also the interference covariance matrix to account for the presence of interference [41]. However, to fully benefit from IRC, the interference covariance matrix would need to be correctly estimated. Such estimation becomes increasingly difficult with an increased number of interfering sources such as in the UAV's A2G channel. Therefore, in this work only the potential of MRC is studied.

1.4 Thesis objectives and scope

In this thesis, the focus has been placed to understand the potential benefits of receive and transmit beamforming techniques in the vehicular scenarios, their performance gains as well as practical concerns such as finding optimal beamforming direction or HPBW. For the downlink communication, the beamforming performance is compared with an MRC as well as a single antenna system. In the uplink, transmit beamforming is compared with a single transmit antenna.

The main part of this thesis is focused on the experimental evaluation of multi-antenna techniques in vehicular scenarios. As the potential techniques are well understood in theory, the experimental verification is the next important step needed to understand their performance in the real world vehicular scenarios. In such situations, usually oversimplified or easily tunable simulation settings (including but not limited to a number of antennas, perfect beamforming angle estimation, channel models, etc.) are confronted with real propagation conditions and their practical implementation. Hence, below there is a list of hypotheses and studied research questions:

- **Hypothesis:** Multi-antenna techniques such as MRC and receive beamforming can improve the performance of downlink vehicular communication by addressing downlink coverage and throughput challenges.
  - RQ1: What is the performance of a multi-antenna vehicular receiver with respect to a single antenna system? Does the performance differ regarding the operational scenarios of the two vehicle types?
  - RQ2: Which multi-antenna technique yield the best performance improvements in downlink signal reception in terms of received SINR?

  - RQ3: What is the best approach to choose beamforming direction and HPBW?

- **Hypothesis:** Transmit beamforming can improve uplink performance of vehicular systems.
  - RQ1: Can beamforming be used to improve uplink throughput in vehicular scenarios?
  - RQ2: Can beamforming techniques be used to meet UAV traffic requirements for payload communications while ensuring coexistence with GdUEs?
  - RQ3: What is the effect of using beamforming on the mobility management performance?

1.5 Methodology

To study the presented hypotheses and answer the stated research questions, it was decided that an experimental approach should be used. There were many reasons why measurements were chosen over system-level simulations. First, at the beginning of this PhD project, there were no standardized channel models for UAV communication that can be easily implemented in the simulator. It was assumed that using ground-level channel models may have a great influence on the observed results and may have led to the wrong conclusions. The second reason was related to yet another assumption that the performance of multi-antenna techniques will vary depending on the interference conditions. By measuring the signals directly from the live cellular networks, the interference pattern from the real deployment can be observed leading to the most realistic conclusions drawn regarding the performance of multi-antenna techniques.

As presented in Figure 1.1, multiple KPIs were chosen to address the challenges of vehicular communication. Downlink SINR and Reference Signal Receive Power (RSRP) are two metrics used throughout this thesis to assess the cellular coverage observed by the vehicle. SINR, together with Reference Signal Received Quality (RSRQ), are two metrics quantifying not only desired but also interfering signals. They are used to study the potential of downlink interference mitigation when using beamforming. Uplink throughput and Interference over Thermal noise (IoT) measured at the BSs (provided by a collaborating mobile network operator) are two KPIs that are used to assess the uplink performance of the multi-antenna techniques.

The study presented in this thesis is divided into two parts: downlink and uplink or in other words multi-antenna receiving and transmitting techniques. First, in the downlink part, a sixteen antennas Software-Defined Radio (SDR) measurement testbed was designed and used in two measurement

campaigns: ground-level (VUE scenario) and aerial-level (UAV scenario), both performed using live cellular networks. The main reason for designing an SDR testbed, was the capability to record and store raw unprocessed signals, such that the same data can be used for different research activities. In this work, after the measurements, the recorded data was used to study the performance of receive beamforming and MRC for both VUE and UAV communications. As this study was conducted during the first part of the project, it also contains several sub-studies related to the practical implementation of multi-antenna systems, such as how to acquire optimal beamforming direction, the impact of mobility on multi-antenna techniques or simply how many antennas to use.

Second part of this thesis is devoted to uplink vehicular communication and focuses on the performance of transmit beamforming. In this study, lessons learned from downlink evaluation are used to design a new measurement tool, that is based on the LTE modem and six directional antennas. The capability of real-time connection to the cellular network was the main reason driving the development of the new measurement tool, such that the uplink interference generated from a vehicle to the network can be studied. Another set of measurement campaigns was conducted. The analysis focuses mostly on the performance comparison of transmit beamforming with relation to a single antenna omni-directional system.

Further, in the final part of the PhD, studies related to the UAV uplink are followed by system-level simulations that are used to study the scalability of the proposed beamforming solution to multi-UAV scenarios. At this point of time, the suitable channel models for UAV communications, such as the height-dependent Path Loss model [42], already existed, removing the main challenge of using simulations, as argued at the beginning of this section. Simulations were conducted instead of the measurements as it was deemed impractical to perform real experiments with a large number of vehicles.

Please note that a great part of this PhD was spent on the actual development of the measurement setups used in the conducted experiments. Two different setups were developed for downlink and uplink studies. They were later adapted to match the practical constraints of VUE and UAV available for the measurements. Each of the presented topics is further discussed in the subsequent chapters and publications. Figure 1.2 presents the visual mapping of the related research activities to the remaining chapters and publications.

1.6 List of contributions

This thesis is organized as a collection of publications. Below the list of the publications that constitute the main body of this thesis is presented. Please

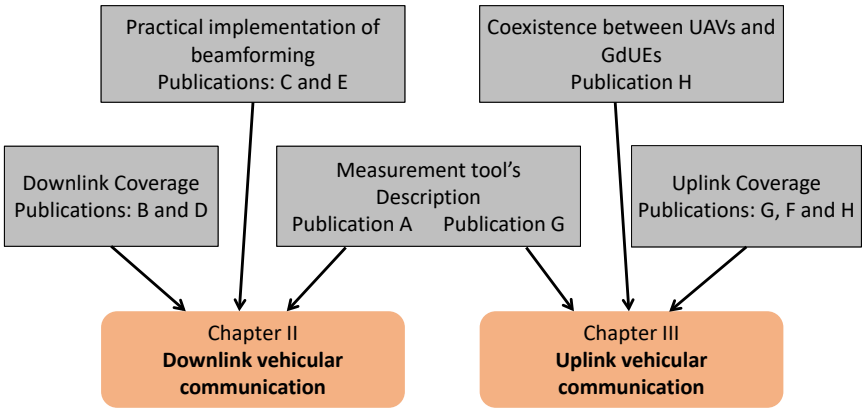

Fig. 1.2: Mapping of studied vehicular challenges to remaining chapters of the thesis

note that the order in which the publications are listed is not necessarily chronological, but follows the presentation structure used in the next chapters:

- **PAPER A:** T. Izydorczyk, F. M.L. Tavares, G. Berardinelli and P. Mogensen, "*A USRP-based multi-antenna testbed for reception of multi-site cellular signals*", IEEE Access vol. 7, November, 2019.
- **PAPER B:** T. Izydorczyk, M. Bucur, F. M.L. Tavares, G. Berardinelli and P. Mogensen, "*Experimental evaluation of multi-antenna receivers for UAV communication in live LTE networks*", IEEE GLOBECOM workshops proceedings, December, 2018.
- **PAPER C:** T. Izydorczyk, F. M.L. Tavares, G. Berardinelli, M. Bucur and P. Mogensen, "*Angular Distribution of Cellular Signals for UAVs in Urban and Rural Scenarios*", The 13th European Conference on Antennas and Propagation (EUCAP), April, 2019.
- **PAPER D:** T. Izydorczyk, F. M.L. Tavares, G. Berardinelli, M. Bucur and P. Mogensen, "*Performance evaluation of multi-antenna receivers for vehicular communications in live LTE networks*", IEEE 89th Vehicular Technology Conference (VTC2019-Spring), April, 2019.
- **PAPER E:** T. Izydorczyk, G. Berardinelli, F. M.L. Tavares, M. Bucur and P. Mogensen, "*On the potential of uplink beamforming in vehicular networks based on experimental measurements*", IEEE 90th Vehicular Technology Conference (VTC2019-Fall), September, 2019.

- **PAPER F:** M. M. Ginard, T. Izydorczyk, P. Mogensen and G. Berardinelli, "*Enhancing vehicular link performance using directional antennas at the terminal*", IEEE GLOBECOM workshops proceedings, December, 2019.

- **PAPER G:** T. Izydorczyk, M. M. Ginard, S. Svendsen, G. Berardinelli and P. Mogensen, "*Experimental evaluation of beamforming on UAVs in cellular systems*", submitted to IEEE 92nd Vehicular Technology Conference (VTC2020-Fall), April 2020.

- **PAPER H:** T. Izydorczyk, G. Berardinelli, P. Mogensen, M. M. Ginard, Jeroen Wigard and István Z. Kovács, "*Achieving high UAV uplink throughput by using beamforming on board*", IEEE Access, April, 2020.

Furthermore, as a part of this thesis, three patents were filed in collaboration with Nokia Bell Labs in Aalborg. All of them concern the practical use of beamforming to enhance UAV communication. None of the patents would be filed without the experimental work that constitutes this thesis.

1.7 Thesis outline

This thesis is divided into four chapters, where the main contributions and findings are presented. First chapter is the introduction, followed by two chapters related to the downlink and uplink performance of multi-antenna systems for vehicular communications. The last chapter summarizes the main findings and contributions of this thesis. Finally, in appendices all relevant publications are provided. Below the more detailed list of contributions for each chapter is discussed:

- **Chapter I: Introduction**
  This is the current chapter discussing the background of vehicular communications. The challenges of vehicular communications and potential solutions to cope with them are presented. Further, the main hypothesis of this thesis is provided and followed by a detailed list of research objectives studied in this work.

- **Chapter II: Downlink vehicular communication**
  This chapter discusses the potential of multi-antenna receivers to improve downlink coverage for VUEs and UAVs, interleaved with remarks on the practical implementation of beamforming. It begins with the description of a designed measurement tool. Further the performance of MRC and receive beamforming is discussed. Finally the spatial channel characterization is used to study practical aspects of beamforming.

- **Chapter III: Uplink vehicular communication**
  This chapter covers both measurement efforts as well as system-level simulations used to study the performance of uplink beamforming. It starts with the description of measurement tools designed for this study. The results are presented from the single-vehicle perspective followed by a system-level approach. Finally, the coexistence with GdUEs and mobility management performance are also discussed.

- **Chapter IV: Conclusions**
  The last chapter of the thesis concludes this work. All hypotheses and research questions are recalled and tested based on the obtained results. Finally, suggestions concerning further studies are provided.

References

[1] GSMA, "Cellular Vehicle-to-Everything (C-V2X), Enabling Intelligent Transport," Available at: https://www.gsma.com/iot/wp-content/uploads/2017/12/C-2VX-Enabling-Intelligent-Transport_2.pdf, 2017, White paper.

[2] Auto Tech Insight, "Autonomous Vehicle Sales Forecast," Available at: https://autotechinsight.ihsmarkit.com/shop/product/5001816/autonomous-vehicle-sales-forecast-and-report, 2018, White paper.

[3] KPMG, "Islands of Autonomy. How autonomous vehicles will emerge in cities around the world," Available at: https://assets.kpmg/content/dam/kpmg/za/pdf/2017/11/islands-of-autonomy-web.pdf, 2017, White paper.

[4] GSMA, "Using Mobile Networks to Coordinate Unmanned Aircraft Traffic," Available at: https://www.gsma.com/iot/wp-content/uploads/2018/11/Mobile-Networks-enabling-UTM-v5NG.pdf, 2018, White paper.

[5] Business Insider Intelligence, "UK Business Insider Intelligence. Commercial Unmanned Aerial Vehicle (UAV) Market Analysis. Industry trends, companies and what you should know," Available at: https://www.businessinsider.com/commercial-uav-market-analysis?IR=T, 2017, White paper.

[6] Research and Markets, "The Global UAV Payload Market 2017-2027," Available at: https://www.researchandmarkets.com/research/nfpsbm/the, 2017, White paper.

[7] 3GPP, 3rd Generation Partnership Project, "Service requirements for enhanced V2X scenarios (release 15)," Tech. Rep. TR 22.186 V15.0.0, March 2017.

[8] 3GPP, 3rd Generation Partnership Project, "Technical specification group radio access network: study on enhanced LTE support for aerial vehicles," Tech. Rep. TR 36.777 V15.0.0, December 2017.

[9] Y. Zeng, Q. Wu, and R. Zhang, "Accessing From the Sky: A Tutorial on UAV Communications for 5G and Beyond," *Proceedings of the IEEE*, vol. 107, no. 12, pp. 2327–2375, December 2019.

[10] 5GAA, 5G Automotive Association, "V2X Functional and Performance Test Report. Test Procedures and Results," Tech. Rep. P-180106, 2018.

[11] S. Hayat, E. Yanmaz, and R. Muzaffar, "Survey on Unmanned Aerial Vehicle Networks for Civil Applications: A Communications Viewpoint," *IEEE Communications Surveys Tutorials*, vol. 18, no. 4, pp. 2624–2661, 2016.

[12] 5G Americas, "Cellular V2X Communications Towards 5G," Available at: https://www.5gamericas.org/wp-content/uploads/2019/07/2018_5G_Americas_White_Paper_Cellular_V2X_Communications_Towards_5G__Final_for_Distribution.pdf, Tech. Rep., March 2018, White paper.

[13] 5GAA, 5G Automotive Association, "C-ITS Vehicle to Infrastructure Services. How C-V2X technology completely changes the cost equation for road operators," 2018.

[14] M. Boban, A. Kousaridas, K. Manolakis, J. Eichinger, and W. Xu, "Connected Roads of the Future: Use Cases, Requirements, and Design Considerations for Vehicle-to-Everything Communications," *IEEE Vehicular Technology Magazine*, vol. 13, no. 3, pp. 110–123, September 2018.

[15] Nokia, "5G deployment below 6 GHz. Ubiquitous coverage for critical communication and massive IoT," Available at: https://onestore.nokia.com/asset/201315, 2017, White paper.

[16] Qualcomm, "LTE Unmanned Aircraft Systems," Available at: https://www.qualcomm.com/media/documents/files/lte-unmanned-aircraft-systems-trial-report.pdf, 2017, Trial Report.

[17] A. A. Khuwaja, Y. Chen, N. Zhao, M. Alouini, and P. Dobbins, "A Survey of Channel Modeling for UAV Communications," *IEEE Communications Surveys Tutorials*, vol. 20, no. 4, pp. 2804–2821, 2018.

[18] B. V. Der Bergh, A. Chiumento, and S. Pollin, "LTE in the sky: trading off propagation benefits with interference costs for aerial nodes," *IEEE Communications Magazine*, vol. 54, no. 5, pp. 44–50, May 2016.

[19] M. Renner, N. Münzenberger, J. Hammerstein, S. Lins, and A. Sunyaev, "Challenges of vehicle-to-everything communication. interviews among industry experts," March 2020.

[20] S. A. Busari, M. Khan, K. Huq, S. Mumtaz, and J. Rodriguez, "Millimetre-wave massive MIMO for cellular vehicle-to-infrastructure communication," *IET Intelligent Transport Systems*, vol. 13, pp. 983–990, June 2019.

[21] M. Giordani, A. Zanella, and M. Zorzi, "Millimeter wave communication in vehicular networks: Challenges and opportunities," *2017 6th International Conference on Modern Circuits and Systems Technologies (MOCAST)*, pp. 1–6, 2017.

[22] M. Boban, A. Kousaridas, K. Manolakis, J. Eichinger, and W. Xu, "Use Cases, Requirements, and Design Considerations for 5G V2X," Available at: https://arxiv.org/abs/1712.01754, 2017.

[23] S. Sou and O. K. Tonguz, "Enhancing VANET Connectivity Through Roadside Units on Highways," *IEEE Transactions on Vehicular Technology*, vol. 60, no. 8, pp. 3586–3602, 2011.

[24] B. Aslam, F. Amjad, and C. C. Zou, "Optimal roadside units placement in urban areas for vehicular networks," *2012 IEEE Symposium on Computers and Communications (ISCC)*, pp. 423–429, 2012.

[25] F. Jimenez, *Intelligent Vehicles, Enabling Technologies and Future Developments*. Elsevier Inc, 2018.

[26] 3GPP, 3rd Generation Partnership Project, "Study on NR Vehicle-to-Everything (V2X)," Tech. Rep. TR 38.885 V16.0.0, March 2019.

[27] R. Molina-Masegosa and J. Gozalvez, "LTE-V for Sidelink 5G V2X Vehicular Communications: A New 5G Technology for Short-Range Vehicle-to-Everything Communications," *IEEE Vehicular Technology Magazine*, vol. 12, no. 4, pp. 30–39, 2017.

[28] G. Jornod, T. Nan, M. Schweins, A. E. Assaad, A. Kwoczek, and T. Kurner, "Sidelink Technologies Comparison for Highway High-Density Platoon Emergency Braking," *2018 16th International Conference on Intelligent Transportation Systems Telecommunications (ITST)*, pp. 1–7, 2018.

[29] Official Journal of the European Union, "Commission decision on the harmonised use of radio spectrum in the 5 875-5 905 MHz frequency band for safety-related applications of Intelligent Transport Systems (ITS)," Available at: https://www.ecodocdb.dk/download/03f9ec4f-27f0/2008671EC.PDF, 2008, 2008/671/EC.

[30] G. Geraci, A. Garcia-Rodriguez, L. G. Giordano, D. Lopez-Perez, and E. Bjornson, "Supporting UAV Cellular Communications through Massive MIMO," *2018 IEEE International Conference on Communications Workshops (ICC Workshops)*, pp. 1–6, May 2018.

[31] P. Chandhar, D. Danev, and E. G. Larsson, "Massive MIMO as enabler for communications with drone swarms," *2016 International Conference on Unmanned Aircraft Systems (ICUAS)*, pp. 347–354, 2016.

[32] C. D'Andrea, A. Garcia-Rodriguez, G. Geraci, L. G. Giordano, and S. Buzzi, "Analysis of UAV Communications in Cell-Free Massive MIMO Systems," *IEEE Open Journal of the Communications Society*, vol. 1, pp. 133–147, 2020.

[33] X. Lin, R. Wiren, S. Euler, A. Sadam, H. Määttänen, S. Muruganathan, S. Gao, Y. E. Wang, J. Kauppi, Z. Zou, and V. Yajnanarayana, "Mobile Network-Connected Drones: Field Trials, Simulations, and Design Insights," *IEEE Vehicular Technology Magazine*, vol. 14, no. 3, pp. 115–125, 2019.

[34] 3GPP, 3rd Generation Partnership Project, "Summary for WI Enhanced LTE Support for Aerial Vehicles," Tech. Rep. RP-181644, September 2018.

[35] A. Otto, N. Agatz, J. Campbell, B. Golden, and E. Pesch, "Optimization approaches for civil applications of unmanned aerial vehicles (UAVs) or aerial drones: A survey," *Networks, An International Journal*, vol. 72, no. 4, pp. 411–458, 2018.

[36] M. Mozaffari, W. Saad, M. Bennis, Y. Nam, and M. Debbah, "A Tutorial on UAVs for Wireless Networks: Applications, Challenges, and Open Problems," *IEEE Communications Surveys Tutorials*, vol. 21, no. 3, pp. 2334–2360, 2019.

[37] S. De Bast, E. Vinogradov, and S. Pollin, "Cellular Coverage-Aware Path Planning for UAVs," *2019 IEEE 20th International Workshop on Signal Processing Advances in Wireless Communications (SPAWC)*, pp. 1–5, 2019.

[38] D. Tse and P. Viswanath, *Fundamentals of Wireless Communication*. Cambridge University Press, 2005.

[39] J. Benesty, I. Cohen, and J. Chen, *Fundamentals of Signal Enhancement and Array Signal Processing*. John Wiley & Sons, 2017.

[40] T. Eng, N. Kong, and L. B. Milstein, "Comparison of diversity combining techniques for Rayleigh-fading channels," *IEEE Transactions on Communications*, vol. 44, no. 9, pp. 1117–1129, September 1996.

[41] J. Karlsson and J. Heinegard, "Interference rejection combining for GSM," *Proceedings of ICUPC - 5th International Conference on Universal Personal Communications*, vol. 1, pp. 433–437, October 1996.

[42] R. Amorim, H. Nguyen, P. Mogensen, I. Z. Kovács, J. Wigard, and T. B. Sørensen, "Radio Channel Modeling for UAV Communication Over Cellular Networks," *IEEE Wireless Communications Letters*, vol. 6, no. 4, pp. 514–517, August 2017.

Chapter 2

Downlink vehicular communication

This part of the thesis focuses on the performance of multi-antenna receivers to face the challenges of downlink ground and aerial vehicular communications, such as coverage and reliability improvements in the presence of strong downlink interference. Following, the practical design of beamforming system is discussed, focusing on direction acquisition techniques and the optimal antenna beamwidth. The experimental results presented in this chapter were obtained during two measurement campaigns: ground-level and aerial, both performed using the same multi-antenna testbed designed to record live LTE signals.

2.1 Motivation

Ground and Aerial vehicles will require reliable downlink connectivity everywhere on the ground and in the air [1]. VUEs and UAVs will observe a typical slow and fast fading channel. Besides, large interference increase due to high LoS probability in the A2G channels as well as cell densification may severely impact the observed SINR levels at the vehicles [2].

An increased number of antennas installed on a vehicle, provide extra degrees of freedom which can be used to counter the negative effects of the channel. Antenna diversity techniques are a well-known group of methods to combat fading [3]. Besides, beamforming has the promise to mitigate interference by placing antenna nulls towards their direction [4].

Although, multi-antenna techniques are known for decades, only very little attention has been placed on their applicability in downlink vehicular scenarios. The work in [5] studies the performance of MRC and beamforming

using Singular Value Decomposition (SVD) precoding and receiver for the C-V2X communication using system-level simulations. The authors show that the SVD receiver outperforms MRC at the expense of large signaling overhead. However, the authors study only one, very simple, straight-line highway scenario, with constant LoS link to the serving RSU. The work does not extend to any other, more challenging scenario as assumed in this thesis. Other works related to ground vehicular communications, usually focused on multi-antenna channel modeling for the V2V communication link (see for example [6,7]).

Multi-antenna receivers, used to improve the C2 link of the UAVs were acknowledged among others in two publications [8,9]. In both of them, authors praise the potential of these techniques, identifying practical implementation aspects as their biggest drawback. However, both works focus on simulation evaluation of massive MIMO techniques at the BS, assuming only a single-antenna UAV, with the benefits of using multi-antenna UAVs being only mentioned in the discussion section. Besides, authors in [10] study the potential of directional antennas in the UAV-to-UAV link using a stochastic geometry approach. However, up to the best of my knowledge, there is not a single complete work dedicated to the performance of multi-antenna receivers installed on a UAV. To fill this literature gap, the goal of this chapter is to study the performance of two such methods: MRC and receive beamforming in the vehicular scenarios using experimental methodology.

Expected performance of multi-antenna receivers

It is assumed that the performance of both techniques may depend on the measured environment and especially on the distribution of desired and interfering signals. MRC may outperform beamforming in rich multipath scenarios, where narrow beamwidth becomes a drawback since a large part of the signal's power would be received by paths located outside the main beam. On the other hand, in LoS-dominant scenarios, where most of the signal's power is received throughout a single path, beamforming may perform better than MRC due to interference filtering properties. To best capture the impact of interference on the performance of studied techniques, it was decided to design the measurement campaigns, such that they cover multiple scenarios, where different desired and interference patterns were expected.

The design of a measurement setup

In order to perform measurements as best as possible, it was decided to design a measurement setup receiving signals from live cellular networks. The main benefit of recording the cellular signals is their ubiquitous coverage. This is beneficiary in vehicular scenarios, where drive tests are usually assumed to perform measurements in different environments. When recording

cellular signals, only a moving receiver needs to be deployed as cellular coverage is available almost everywhere. Due to inherited inter-cell interference observed in cellular systems, their influence on the performance of multi-antenna techniques can also be studied.

The possibility of testing both receiver types on the same data set was one of the main constraints influencing the design of a measurement tool. Therefore it was decided to design a measurement system, capable of recording live cellular signals and storing them unprocessed for offline analysis. In this way, the same data set can be processed in multiple ways depending on the desired research activity.

Design of beamforming receiver

Designing an experiment that includes receive beamforming raises many practical concerns. When receiving the signal, the receiver needs to choose the beamforming direction. It can be done in multiple ways. A receiver may estimate the Angle of Arrival (AoA) of incoming signals using algorithms such as Space-Alternating Generalized Expectation-maximization (SAGE) [11] or Multiple Signal Classification (MUSIC) [12] and point the beam towards the direction where most of the energy is coming from. Besides, a beam sweeping technique can be used and afterwards the beam maximizing desired KPI is chosen as the final beam [4]. Finally the receiver may possess some knowledge about the environment (LoS probability, physical location of the BS), which can also influence the beamforming decision.

There is a performance-complexity trade-off between all these methods [13]. High computing power may be required for AoA estimation, while a long time may be needed to perform full beam sweep. Therefore, as a part of this thesis, it was decided to study different direction acquisition methods to test their performance in vehicular scenarios and better understand their potential practical application.

Another concern faced when designing the beamforming receiver is the HPBW of the main beam. There is a well-known trade-off between the beamwidth and the achievable antenna gain. The narrower the beam, the higher the antenna gain. On the other hand, as a rule of thumb, the beam should not be narrower than the Angular Spread (AS) of the signal [4]. Otherwise, a large part of the received energy may not be captured within the main beam, potentially harming receive SINR.

Intuitively, the AS in the ground-level channels is generally larger in the urban scenarios due to multipath propagation and lower in rural scenarios due to high LoS probability. However, in aerial channels such prediction is difficult. When UAVs fly at high altitudes (usually 40 m and higher), as shown in [14], the channel can be assumed as LoS with very low AS. In addition, UAVs will also fly at lower heights, below 40 m. During take-off, landing

or for example last-mile delivery services, UAVs will fly in-between or right above buildings, in a so-called obstructed-LoS zone [15], where low AS cannot be assumed. At the time of conducting this research, there were no A2G channel models characterizing the variations of AS with height. Therefore it was decided to attempt characterizing this important parameter influencing beamforming design.

Time-distance coherence of AoA

Both ground and aerial vehicles are constantly moving potentially at a high speed. When doing so, the beamforming direction has to be regularly adjusted. Otherwise, the beam may be pointing towards the wrong direction, harming the reliability and in the worst case, leading even to a radio link failure. Due to practical limitations, direction acquisition methods cannot be constantly performed. Therefore it is assumed, that the incoming AoA and thus optimal beamforming direction doesn't change in between two direction acquisition instances.

However, this can only be assumed if there is a so-called time-distance coherence of AoA - a smooth change of AoA over time and space. At the time of performing this work, 3GPP channel models used for system-level simulations [16] did not contain such a parameter, as AoA was drawn randomly and independently for each time slot. As a result, at every simulation step a direction acquisition would have to be performed.

In the real world, there is a certain AoA's coherence time [17]. Intuitively it should be larger in areas with high LoS probability and shorter in urban scenarios with a high amount of obstructions. Therefore, as part of Paper E, ground-level measurements were used to study the possibility to track the changes of AoA and investigate the impact of different beamwidths on the tracking distance.

2.2 Objectives

The objectives of this part of the thesis are the following:

- Design a multi-functional testbed, capable of receiving live LTE signals both on the ground and in the air using multiple antennas.
- Investigate the downlink performance of MRC and receive beamforming in ground and aerial scenarios, focusing on the differences between both environments and the impact of downlink interference.
- Study the factors influencing beamforming design: optimal antenna beamwidth and potential of direction acquisition techniques.

2.3 Included articles

Below, the list of articles that constitute the main body of this part of the thesis are listed:

Paper A: A USRP-based multi-antenna testbed for reception of multi-site cellular signals

Measurement tool's description. This article presents the design of a multi-antenna SDR measurement setup capable of measuring live LTE signals. The publication discusses motivation factors influencing the design, the hardware and software development as well as post-processing methodologies such as LTE decoding or SAGE processing. Finally, a preliminary validation campaign is reported and discussed. This setup was used in two measurement campaigns regarding ground and aerial downlink communications. The results reported in Papers B-E were obtained after analyzing data recorded using this tool.

Paper B: Experimental evaluation of multi-antenna receivers for UAV communication in live LTE networks

Downlink coverage of UAVs and Practical implementation of beamforming. This publication discusses the potential of multi-antenna techniques for downlink UAV communication. The performance of MRC and receive beamforming are compared based on the obtained SINR and outage metrics. Different beam sweeping techniques are compared and practical insights on the number of used antennas or optimal beamforming elevation angle are presented.

Paper C: Angular Distribution of Cellular Signals for UAVs in Urban and Rural Scenarios

Practical implementation of beamforming. The attempt to perform spatial channel characterization using SAGE on live LTE signals is presented in this publication. The stability of estimated azimuth AoA during landing/takeoff of a UAV is discussed to address the beamforming design during this crucial phase of flight. Besides, AS of received signals is computed to discuss the optimal beamwidth.

Paper D: Performance evaluation of multi-antenna receivers for vehicular communications in live LTE networks

Downlink coverage of VUEs. This publication discusses the potential of multi-antenna techniques in ground-level downlink vehicular communication. The performance of MRC and receive beamforming is compared based on the obtained SINR. Further, the observed interference measured using a radio scanner is correlated with multi-antenna gains, to understand the potential of both multi-antenna techniques under different interference conditions.

Paper E: On the potential of uplink beamforming in vehicular networks based on experimental measurements

Practical implementation of beamforming. Based on spatial channel characterization of LTE signals obtained during a ground-level measurement campaign, different beam direction's acquisition techniques: AoA estimation, naive beamforming and RSRP-based beam switching are discussed. Besides, two AoA tracking techniques are compared and the feasibility of signal tracking over time is argued depending on the antenna beamwidth.

2.4 Main findings

The benefits of multi-antenna receivers in vehicular scenarios

The results shown in Papers B and D confirm the superior performance of multi-antenna receivers over a single-antenna system. Using a sixteen antennas array leads to median 5-9 dB SINR gain over a single antenna receiver depending on the recorded scenario and used multi-antenna technique. The obtained results show the promise of using multiple antennas to extend downlink coverage and improve the reliability of vehicular systems, yet are lower than the theoretical gain computed using Equation (1.1). The reason for that is the inter-cell interference inherently measured in the cellular systems.

The inter-cell interference has a major impact on the relative performance of the two multi-antenna techniques. Average measured SINR levels when using MRC and receive beamforming are shown to be very similar in urban scenarios (such as route 3 in Paper D), where interference is spread along all directions. However, in high DIR scenarios or when interference is concentrated along certain directions, receive beamforming tends to outperform MRC. This is due to the ability to null the incoming source of interference, by positioning the main beam towards other direction. Results obtained in a low flight level zone in Paper B support this hypothesis. Figure B.6 indi-

cates that when flying at higher heights, or in other words, when channel (and interference) becomes more LoS-alike, the performance of beamforming increases with respect to flights at lower heights. The same trend is further observed in Paper D where high beamforming gains are correlated with high DIR scenarios.

When comparing the performance of multi-antenna systems based on the studied scenario, it is visible that all three receivers (multi and single antenna) perform better in the ground rather than the aerial scenario. The reason for this more than 5 dB difference in measured mean SINR values is the higher average interference level in the air due to LoS propagation. Similar results are expected to be seen in the future ground-level vehicular communications. It is expected, that the potential challenge of high downlink interference will not emerge until the first RSUs and autonomous vehicles are deployed.

Factors influencing beamforming design

The beamforming direction can be acquired in multiple ways. In this thesis AoA estimation, beam sweeping and naive beamforming towards the serving cell are studied. The performance of beam sweeping, when different metrics are used as a beam selectors is studied in Paper B. The obtained results indicate that depending on which metric is used as a KPI to select the beam, different performance results are observed. Not surprisingly, beamforming using metrics for beam selection that quantify both desired power and interference (such as RSRQ or SINR) leads to better downlink coverage outperforming beamforming using metrics based only on the desired power (RSRP or raw unprocessed power). This happens as when using more information, a beam maximizing a trade-off between the highest desired power and lowest interference can be chosen.

Moreover, as indicated in Paper E, beamforming using the RSRP-based beam sweeping, leads to higher SINR than if the signal is beamformed towards the estimated AoA of the main path estimated using SAGE algorithm. Further, in the measured suburban and rural scenarios, where high LoS probability is observed, the performance of beamforming when pointing the beam towards the estimated AoA is very similar to the performance of the naive algorithm in which the beam is pointed towards the direction of the serving cell, simply assuming that this path is not heavily attenuated.

All the results cast doubt on the practical use of AoA estimation. It is the most resource-consuming method among all studied. Results indicate that it is outperformed even by RSRP-based beam sweeping (although at the expense of the delay introduced by beam sweeping). Furthermore, naive beamforming requires only a percentile of computing power required for AoA estimation while similar performance is observed, assuming that the BS's location is known.

Choosing the optimal half-power beamwidth is a trade-off between multiple factors. During the first study, in Paper B, a narrow 22.5^{o} beamwidth was used to maximize the antenna gain. However by further analyzing the same data, in Paper C, it was found that the AS was larger and a minimum 50^{o} beamwidth would be needed to receive the most of the incoming signal's energy within the main beam.

Tracking of AoA in LoS-dominant scenarios

After analyzing the data recorded during ground-level measurements in rural and suburban scenarios, the feasibility of AoA tracking has been validated. Surprisingly, as shown in Paper E, the coherence distances may be very long and allow to keep tracking the AoA in a range of tenths of seconds. As expected, the larger the beamwidth, the longer is the possibility to maintain the connectivity to a given cell and track the signal without the need to perform latency and reliability-harming direction acquisition procedures.

Very interesting conclusions can be drawn from a similar study performed in Paper C, where the feasibility of tracking the azimuth AoA during the UAV landing procedure was studied. In some measurement locations the azimuth AoA remains approximately the same during the entire procedure, showing the promises for beam tracking. Unexpectedly, in other locations, serving cell tracked during the start of the procedure at 40 m was not decodable at lower heights. In practical systems, the network would be forced to perform a handover to a different cell. During such a crucial phase of flight as landing, handovers may potentially harm the reliability of the connection. Therefore, as further work, it is recommended to carefully study the mobility management during vertical flights of the UAV. Moreover, in all situations when a UAV is surrounded by buildings it is recommended to use omni-directional receivers and techniques like MRC instead of beamforming. By doing so, the effect of losing connection to the serving cell due to beam misalignment is reduced and reliability improved.

References

[1] M. Boban, K. Manolakis, M. Ibrahim, S. Bazzi, and W. Xu, "Design aspects for 5G V2X physical layer," in *2016 IEEE Conference on Standards for Communications and Networking (CSCN)*, 2016, pp. 1–7.

[2] V. Yajnanarayana, Y. Eric Wang, S. Gao, S. Muruganathan, and X. Lin Ericsson, "Interference Mitigation Methods for Unmanned Aerial Vehicles Served by Cellular Networks," in *2018 IEEE 5G World Forum (5GWF)*, 2018, pp. 118–122.

[3] J. Liu, W. Q. Malik, D. J. Edwards, and M. Ghavami, *Ultra-Wideband - Antenna Diversity Techniques*. John Wiley & Sons, Ltd, 2006, ch. 6, pp. 89–104. [Online]. Available: https://onlinelibrary.wiley.com/doi/abs/10.1002/0470056843.ch6

[4] B. Allen, *Ultra-Wideband - Beamforming*. John Wiley & Sons, Ltd, 2006, ch. 5, pp. 67–87. [Online]. Available: https://onlinelibrary.wiley.com/doi/abs/10.1002/0470056843.ch5

[5] I. Maskulainen, P. Luoto, P. Pirinen, M. Bennis, K. Horneman, and M. Latva-aho, "Performance evaluation of adaptive beamforming in 5G-V2X networks," in *2017 European Conference on Networks and Communications (EuCNC)*, 2017, pp. 1–5.

[6] T. Abbas, J. Nuckelt, T. Kürner, T. Zemen, C. F. Mecklenbräuker, and F. Tufvesson, "Simulation and Measurement-Based Vehicle-to-Vehicle Channel Characterization: Accuracy and Constraint Analysis," *IEEE Transactions on Antennas and Propagation*, vol. 63, no. 7, pp. 3208–3218, 2015.

[7] O. Renaudin, V. Kolmonen, P. Vainikainen, and C. Oestges, "Non-stationary narrowband MIMO inter-vehicle channel characterization in the 5-GHz band," *IEEE Transactions on Vehicular Technology*, vol. 59, no. 4, pp. 2007–2015, 2010.

[8] G. Geraci, A. Garcia-Rodriguez, L. Galati Giordano, D. López-Pérez, and E. Björnson, "Understanding UAV cellular communications: From existing networks to massive MIMO," *IEEE Access*, vol. 6, pp. 67 853–67 865, 2018.

[9] Y. Zeng, R. Zhang, and T. J. Lim, "Wireless communications with unmanned aerial vehicles: opportunities and challenges," *IEEE Communications Magazine*, vol. 54, no. 5, pp. 36–42, 2016.

[10] E. Chu, J. M. Kim, and B. C. Jung, "Interference Analysis of Directional UAV Networks: A Stochastic Geometry Approach," in *2019 Eleventh International Conference on Ubiquitous and Future Networks (ICUFN)*, 2019, pp. 9–12.

[11] B. H. Fleury, M. Tschudin, R. Heddergott, D. Dahlhaus, and K. Ingeman Pedersen, "Channel parameter estimation in mobile radio environments using the SAGE algorithm," *IEEE Journal on Selected Areas in Communications*, vol. 17, no. 3, pp. 434–450, 1999.

[12] P. Stoica and A. Nehorai, "MUSIC, maximum likelihood, and Cramer-Rao bound," *IEEE Transactions on Acoustics, Speech, and Signal Processing*, vol. 37, no. 5, pp. 720–741, 1989.

[13] T. E. Tuncer and B. Friedlander, *Classical and Modern Direction-of-Arrival Estimation*. Academic Press, 2009.

[14] Y. Wang, R. Zhang, B. Li, X. Tang, and D. Wang, "Angular Spread Analysis and Modeling of UAV Air-to-Ground Channels at 3.5 GHz," in *2019 11th International Conference on Wireless Communications and Signal Processing (WCSP)*, 2019, pp. 1–5.

[15] E. Vinogradov, H. Sallouha, S. D. Bast, M. M. Azari, and S. Pollin, "Tutorial on UAVs: A Blue Sky View on Wireless Communication," *Journal of Mobile Multimedia*, vol. 14, no. 4, p. 395–468, 2018.

[16] 3GPP, 3rd Generation Partnership Project, "Spatial channel model for Multiple Input Multiple Output (MIMO) simulations," Tech. Rep. TR 25.996, March 2011.

[17] F. Ademaj and S. Schwarz, "Spatial Consistency of Multipath Components in a Typical Urban Scenario," in *2019 13th European Conference on Antennas and Propagation (EuCAP)*, 2019, pp. 1–5.

Chapter 3

Uplink vehicular communication

This part of the thesis focuses on the performance of uplink beamforming in vehicular scenarios to extend coverage and deal with increased levels of vehicle-originated uplink interference. A new measurement setup was designed to perform the analysis included in this chapter. Benefiting from real-time connectivity to the network, the impact of using directional antenna patterns on the mobility management performance is also discussed.

3.1 Motivation

High uplink throughput is a necessary communication requirement needed to support autonomously driving VUEs and to meet the demands of UAV applications such as surveillance or search and rescue missions [1]. In cellular networks, high uplink throughput can be provided to the user only if two conditions are satisfied. First, serving cell needs to have enough available resources to schedule the demanding vehicle - the load of the cell cannot be a constraining factor. Second, the uplink SINR needs to be sufficiently high to enable high order modulation and coding scheme to be used.

However, as shown in [2], UAVs streaming video data will create a high amount of uplink interference effectively reducing the SINR observed by other users of the cellular network. Therefore as noted in [3], uplink interference mitigation is one of the biggest challenges imposed on UAV communications as it may be a limiting factor constraining the performance of not only other UAVs but also GdUEs.

As of today, ground vehicles do not face challenges at a similar scale as UAVs, due to a limited number of cellular-connected VUEs. Their uplink

throughput is mostly constrained in rural scenarios, due to a large distance to the serving cell. However, it is expected that, with a rapid increase of autonomous vehicles, the uplink interference may rise [4].

Vehicular performance improvements using uplink beamforming

Beamforming has the potential to cope with the challenges of uplink vehicular communication. The directional antenna gain is expected to increase the coverage by raising the uplink SINR thus leading to improved throughput. Meanwhile, the narrow beams are expected to spatially filter the transmitted signal and therefore limit the interference radiated in other directions, leading to more fair coexistence with other users in the network [5].

In the publications constituting this chapter, the performance of uplink beamforming is studied by analyzing the uplink throughput of the vehicular devices, the amount of interference radiated by them to the network as well as a correlation between vehicle-originated interference and the performance of all users in the network.

Mobility management when using beamforming

Any device attached to the cellular network, measures serving and neighbor cells' RSRP levels and report them back to the network. Based on the obtained measurements, if a neighbor signal power is sufficiently higher than the serving cell's power, the network may trigger a handover procedure to the neighbor cell [6].

Beamforming, due to the directional antenna pattern will affect the mobility management procedure. Unless the network is aware of the different antenna pattern of a device, depending on a beamforming direction, the measured power of some cells will be augmented while for others, located outside of the main beam of the antenna, RSRP will decrease. Such spatial selectivity may lead to a particular situation in which a device, when using beamforming, will connect to a different cell than the one it would be connected when using an omni-directional antenna and which was assumed by the network operator during cell planing.

Connection to different cells due to spatial selectivity may have both positive and negative effects on the vehicular device. As shown in [7] and [8], UAVs using an omni-directional antenna will observe an increased number of potentially latency and reliability-harming handovers compared to GdUEs, due to similar power of many cells in the air. It is expected that by using beamforming, the connection to the serving cell can be maintained longer, reducing the number of handovers. However, in such situation, other potentially better-suited neighbor cells, may be disregarded, harming the performance of the vehicular device. As a part of the study presented in this chap-

ter, mobility management is investigated, by comparing the number of successful handovers when the device is using beamforming or omni-directional antenna system.

Spatially controlled load balancing

Freedom of choosing beamforming direction has one more distinctive benefit. By pointing the beam in different directions, the device can potentially be connected to different cells, although being located in the same physical location. Beam steering may be beneficial if the cell load in these cells is uneven. Imagine a vehicle connected to a loaded cell, which is not able to meet the uplink throughput demands. In such a case, by redirecting the beam, a vehicle may try to find a different, potentially less loaded cell. In Paper H, this effect is studied, focusing on selfish uplink demands of the UAVs as well as the impact of spatial selectivity and beam steering on other users of cellular networks.

Measurement methodology

The work presented in this chapter is a result of measurements and system-level simulations. Similar to downlink studies presented in Chapter 2, it was decided to design measurements using live cellular networks, such that uplink signals transmitted from a single measurement device, will be received by multiple real BSs. However, the measurement testbed must maintain real-time connectivity to the serving cell. Only in this case, metrics like uplink throughput and uplink interference over thermal noise can be used as KPIs to assess the performance of uplink beamforming. The measurement tool described in Chapter 2 and Paper A, used during the downlink evaluation, was found not capable of maintaining real-time cellular connectivity, forcing the development of a new platform.

The new measurement testbed was inspired by [9], and contains a six directional antennas switching system, in which each antenna has 60^{o} HPBW and points in a different direction. Following the outcome of the downlink studies, it was decided to implement a so-called naive beamforming system, in which a vehicle points its beam towards the physical direction of a serving cell. An LTE modem is used to maintain a real-time connection to the network. Due to space and battery constraints, the measurement platforms used during ground and aerial studies slightly differ. Both are described in Papers F and H respectively.

Besides measurements, system-level simulations were performed to study the benefits of uplink beamforming in multi-UAV scenarios. Measurements performed in this chapter using a single UAV are an important source of knowledge reflecting the real-world performance of uplink beamforming in

vehicular scenarios. When complemented with system-level simulations, the observations can be extended to multi-UAV scenarios to show the scalability of proposed solutions.

3.2 Objectives

The objectives of this part of the thesis are the following:

- Study the potential of beamforming to improve uplink coverage in vehicular scenarios.
- Analyze the spatial interference mitigation properties of beamforming focusing on their impact to meet high uplink throughput demands of the UAVs and fair coexistence with GdUEs.
- Study the impact of antenna directionality and beam steering on mobility management procedures.

3.3 Included articles

Below, the articles that constitute the main body of this part of the thesis are listed:

Paper F: Enhancing vehicular link performance using directional antennas at the terminal

Uplink coverage of VUEs. This publication discusses the potential of using uplink beamforming on a VUE. The performance is analyzed based on recorded uplink throughput during a measurement campaign using an array of directional antennas and real-time connectivity to LTE networks. The potential of beamforming is compared with benchmark omni-directional antenna. Further, the effect of using beamforming on mobility management performance is studied by analyzing the numbers of successful handovers performed by the network.

Paper G: Experimental evaluation of beamforming on UAVs in cellular systems

Uplink coverage of UAVs. This is the first of two publications focusing on the potential of uplink beamforming in aerial scenarios. It describes the implementation details of a measurement testbed containing six directional

antennas switching system installed on a UAV. It is followed by the preliminary results from the measurement campaign focusing on achievable uplink throughput when using beamforming on board of a UAV. The mobility management aspects are also discussed.

Paper H: Achieving high UAV uplink throughput by using beamforming on board

Uplink coverage of UAVs and coexistence between UAVs and GdUEs. This journal article extends the studies form Paper G and analyzes the performance of uplink beamforming to meet high uplink throughput requirements of the UAVs in a multi-UAV scenario. It reports the outcome of system-level simulations followed by the results of two measurement campaigns. The article is focused on showing the potential of spatial filtering of interference to improve UAV's uplink throughput and ensure fair coexistence with GdUEs.

3.4 Main findings

Impact of beamforming on uplink throughput

Let us first consider a single-vehicle scenario - a scenario in which there is only one cellular-connected vehicle. The observed uplink throughput of this vehicle (VUE or UAV) is approximately the same regardless of the used antenna system. As reported in the measurements covered in Papers F and G, the directional gain is compensated by the uplink power control, limiting the benefit of beamforming just to uplink transmit power reduction. Cellular network, unaware of the beamforming system being used on a vehicle, misclassified the origin of this gain as due to a lower path loss, thus reducing the uplink transmit power of a device. Both measurements (aerial and ground-level) were performed in good coverage conditions. It is expected that, if a similar experiment is repeated in worse coverage, in which a vehicle using omni-directional antenna would have to use maximum uplink transmit power, the directional gains of beamforming would translate into uplink throughput gains.

Uplink throughput gains become visible in a multi-UAV scenario as presented in Paper H. When multiple UAVs in the network use beamforming (instead of the omni-directional antenna), their uplink throughput increases, as they cause less harm to each other due to spatial filtering of interference. Further, the results presented in the paper indicate that, when all UAVs use beamforming system, a cellular network is capable of serving approximately twice as many UAVs, comparing with the case in which all of them use omni-directional antennas. Beamforming can also be used to improve uplink

throughput when some cells in the network are highly loaded. The ability to steer the beam, using, for example, the proposed RSRQ-based beam switching increases the probability that the UAV connects to low loaded cells, capable of meeting high uplink throughput demands of the UAVs. Although a multi-VUE scenario was not studied in this thesis, it is assumed that with an increased number of vehicles, similar conclusions would be drawn.

Coexistence of UAVs and GdUEs

Spatial filtering of interference, presented in Paper H, has a positive influence on the performance of GdUEs. Beamforming mitigates the UAV-originated interference observed in the network, leading to increased uplink SINR levels of all the users.

However, beamforming may also have a negative impact on some GdUEs. Measurement results, validating the concept of load balancing, indicate that when a UAV redirects the beam and connects to a far located cell, it harms the performance of GdUEs located in the closest vicinity of the UAV. Typically, if an omni-directional antenna is used on board of the UAV, all of these users including UAV should be connected to the same cell. However, due to directional gain, the UAV is connected to a different cell, becoming an interferer to the GdUEs located in proximity, in spite of the fact that the main lobe is pointing towards a different direction than their serving cell. During the measurements, this interference translated into increased uplink transmit power of GdUEs and a lower than expected throughput.

Impact of beamforming on mobility management

The directional antenna pattern has a great influence on the number of performed handovers in the network. Beamforming, can be used to maintain the connectivity to the serving cell longer, than when an omni-directional antenna is used, thus reducing the number of observed handovers. The concerns raised in Section 3.2, regarding the possibility of overlooking better cell candidates due to uneven antenna pattern were not confirmed (yet are still plausible). Different handover decisions taken when using two antenna systems did not have any influence on the uplink throughput observed in the network.

The described behavior was observed in most of the ground and all aerial scenarios, reported in Papers F and G respectively. Only, when VUE drove in an urban scenario, the total number of handovers remained similar regardless of the antenna system used on a vehicle. This is related to the characteristics of an urban channel. Due to vast amount of obstructions, even when using beamforming, the connectivity to the same cell could not be maintained as the signals were potentially blocked and attenuated by buildings or other elements of infrastructure leading to frequent handovers.

Disclaimer

All the results presented in this chapter are valid in a situation when the network has no knowledge about the beamforming capabilities of a vehicular device. Possessing such a knowledge, may change the drawn conclusions as the network could optimize its service to cope with such transmitters. However it is expected that, in such a case, the potential benefits of beamforming would only increase. The network could potentially optimize the uplink power control procedure to cope with devices using beamforming transmission or optimize the mobility management performance. Finally as suggested in Paper H, the network may eventually overtake the control over the beamforming direction of a vehicle. The design of such control mechanisms can be considered as an optimization problem and are out of scope of this thesis.

References

[1] N. H. Motlagh, M. Bagaa, and T. Taleb, "UAV-Based IoT Platform: A Crowd Surveillance Use Case," *IEEE Communications Magazine*, vol. 55, no. 2, pp. 128–134, 2017.

[2] I. Kovacs, R. Amorim, H. C. Nguyen, J. Wigard, and P. Mogensen, "Interference Analysis for UAV Connectivity over LTE Using Aerial Radio Measurements," in *2017 IEEE 86th Vehicular Technology Conference (VTC-Fall)*, 2017, pp. 1–6.

[3] Y. Zeng, Q. Wu, and R. Zhang, "Accessing From the Sky: A Tutorial on UAV Communications for 5G and Beyond," *Proceedings of the IEEE*, vol. 107, no. 12, pp. 2327–2375, 2019.

[4] Analysis Mason, "Socio-economic benefits of cellular V2X," Available at: https://5gaa.org/wp-content/uploads/2017/12/Final-report-for-5GAA-on-cellular-V2X-socio-economic-benefits-051217_FINAL.pdf, December 2017, Final report for 5GAA.

[5] H. Trees, *Optimum Array Processing – Part IV of Detection, Estimation, and Modulation Therory*, May 2002.

[6] S. Sesia, I. Toufik, and M. Baker, *LTE - The UMTS Long Term Evolution: From Theory to Practice*, August 2011.

[7] A. Fakhreddine, C. Bettstetter, S. Hayat, R. Muzaffar, and D. Emini, "Handover challenges for cellular-connected drones," June 2019, pp. 9–14.

[8] S. Euler, H. Maattanen, X. Lin, Z. Zou, M. Bergström, and J. Sedin, "Mobility support for cellular connected unmanned aerial vehicles: Performance and analysis," in *2019 IEEE Wireless Communications and Networking Conference (WCNC)*, 2019, pp. 1–6.

[9] H. C. Nguyen, R. Amorim, J. Wigard, I. Z. Kovács, T. B. Sørensen, and P. E. Mogensen, "How to ensure reliable connectivity for aerial vehicles over cellular networks," *IEEE Access*, vol. 6, pp. 12 304–12 317, 2018.

Chapter 4

Conclusions

4.1 Summary

Vehicular communication is a key technology component to enable the development of autonomous vehicles and Beyond Visual Line of Sight (BVLOS) UAV flights. Cellular networks, such as LTE or 5G, due to their ubiquitous connectivity, are promising wireless communication technologies to meet the requirements of connected vehicles. Vehicular demands, such as high uplink and downlink throughput, increased coverage and reliability of the communication link impose new challenges on the design of cellular systems. Besides, predicted large concentration of vehicles, high LoS probability of the A2G channel and the ongoing trend of cell densification will result in major interference increase observed and generated by the vehicles.

Typically, throughput and reliability challenges are solved by introducing new network-side techniques, by investments into BS's hardware or by the acquisition of a new frequency spectrum. Such approaches are justified in large metropolitan areas, where expensive investments may fast become profitable due to a large number of users. However, vehicles demand ubiquitous connectivity everywhere - also in less populated areas, where investment in cellular infrastructure is usually not profitable.

Using multiple-antennas installed on vehicle terminals to combat vehicular communication challenges is an alternative approach. Benefiting from increased space and battery of the vehicles, multi-antenna techniques may be used to increase throughput and reliability of vehicular communication, due to extra available DoF. The additional benefit of these techniques is the lack of changes required in the network-side equipment.

This thesis focuses on the verification of multi-antenna techniques for vehicular communication. The performance of two techniques: beamforming and MRC is studied using an experimental methodology, to show the po-

tential of multi-antenna systems in real scenarios. Based on the assumption, that the performance will depend strongly on the interference observed in the network, a set of measurement campaigns was conducted in different environments using live cellular systems.

First, the potential of multi-antenna techniques to improve downlink vehicular connectivity is discussed in Chapter 2. Based on the measurements conducted in both ground and aerial scenarios, the performance of MRC and beamforming in different interference conditions was studied. In addition, different beamforming strategies such as direction acquisition techniques, optimal HPBW or the feasibility of AoA tracking were discussed, to better understand the practical implementation aspects of a beamforming system. The obtained results, confirm the great potential of both multi-antenna techniques. Depending on the measurement environment, and especially on the observed interference, the relative performance of both techniques differs, favoring beamforming techniques in high DIR scenarios.

In Chapter 3, the performance of uplink beamforming in vehicular scenarios was studied. First, measurements were used to showcase the potential of beamforming in a single-vehicle scenario. The results obtained during ground and aerial experiments indicate, that beamforming influences the mobility management procedure. However, due to uplink power control, the observed throughput was similar to an omni-directional antenna system. To showcase uplink throughput gains, system-level simulations extend the study by focusing on a multi-UAV scenario. High uplink throughput gains and improved coexistence with GdUEs were observed due to spatial mitigation of interference. Besides, load balancing due to beam switching can be a promising strategy to further increase the throughput of vehicular devices.

4.2 Research questions revisited

This thesis contains a set of diverse material, targeting various aspects of using multi-antenna techniques installed on vehicles. Based on the obtained results, it is worth reflecting on the hypotheses and research questions first presented in Chapter 1.4.

4.2.1 Performance of multi-antenna techniques

Hypothesis 1: Multi-antenna techniques such as MRC and receive beamforming can improve the performance of downlink vehicular communication by addressing downlink coverage and throughput challenges

- *RQ1: What is the performance of a multi-antenna vehicular receiver with respect to a single antenna system? Does the performance differ regarding the operational scenarios of the two vehicle types?*

Both studied multi-antenna techniques were shown to greatly outperform a single-antenna receiver. The average SINR gains of multi-antenna techniques, obtained using the 16-antennas measurement setup, were shown to be dependent on the type of a studied vehicle, being higher (up to 9.5 dB) in aerial scenarios and lower (up to 7 dB) in ground-level scenarios. This gain difference is a result of different interference patterns observed in both scenarios, as the interference is typically more concentrated along a certain direction in aerial channels and more widespread on the ground.

- *RQ2: Which multi-antenna technique yield the best performance improvements in downlink signal reception in terms of received SINR?*
  Both MRC and receive beamforming perform similarly in rich multipath scenarios. Beamforming is shown to outperform MRC by more than 2 dB in high LoS probability environments such as high altitude UAV flights in which the interfering signals are received with a low angular spread. Based on ground-level measurements, it was found that beamforming may also outperform MRC in high DIR scenarios, due to the ability to place antenna nulls in the direction of the interference.

- *RQ3: What is the best approach to choose beamforming direction and HPBW?*
  Beam sweeping using RSRQ or SINR as a beam selection metric has shown the best performance among all studied methods, as the knowledge of both desired and interfering signals is exploited. Beam sweeping outperforms other metrics such as AoA estimation or naive beamforming based on known location of a serving cell and can lead to even 4 dB better SINR. Load balancing using RSRQ-based beam switching has been shown to be an efficient metric to avoid connection to a loaded cell thus leading to increased throughput. As argued in this thesis, optimal beamwidth should be as narrow as possible to spatially mitigate the interference. However it should not be narrower than the angular spread of the received signal, such that most of the received energy is captured within the main beam. Based on angular spread estimation performed for the downlink A2G channels, it was decided to use a 60^{o} beamwidth during the uplink studies described in Chapter 3.

All in all, as assumed in the hypothesis, multi-antenna techniques studied in this thesis show potential to improve downlink vehicular connectivity. They can be used to improve downlink coverage and throughput rates by increasing the SINR, even under severe interference conditions.

Hypothesis 2: Transmit beamforming can improve uplink performance of vehicular systems

- *RQ1: Can beamforming be used to improve uplink throughput in a vehicular scenarios?*
  Beamforming is shown to increase the observed RSRP and SINR values, with the gains being comparable with a directional antenna gain used for the measurements. As of today, if there is only one cellular-connected vehicle (UAV or VUE), it may not observe any average throughput gains due to uplink power control misclassifying the directional gain as better path loss, thus reducing the vehicle's transmit power. Only if a vehicle is connected in very low RSRP conditions, in which the transmit power cannot be reduced due to large path loss, the directional gain will result in better throughput and coverage extension.

- *RQ2: Can beamforming techniques be used to meet UAV traffic requirements for payload communications while ensuring coexistence with GdUEs?*
  As shown in Paper G, provided the low-loaded network, if only a single UAV is present in a certain region, the observed uplink throughput usually exceeds the required 10 Mbps traffic requirement, even if an omni-directional antenna is used. Transmit beamforming is shown to spatially reduce generated uplink interference, leading to increased SINR observed at the BSs by more than 5 dB with respect to the case when an omni-directional antenna is used. When multiple UAVs using beamforming are flying over the same region, their performance improves since each of them steers the energy towards the direction of the serving base station, thus reducing the interference footprint. In such cases, a throughput increase (more than 5 Mbps) can be observed, meeting the traffic requirements for payload communications in the presence of a low-loaded network. Furthermore, in the presence of high-loaded cells, beam steering can be used for load balancing and connecting to a cell with a lower load, leading to increased data rates for the UAV. Reduced interference footprint of the UAVs has also a positive influence on the performance of GdUEs. When UAVs use beamforming, the average throughput of the GdUEs improves by more than 2 Mbps due to higher observed SINR at the BSs.

- *RQ3: What is the effect of using beamforming on the mobility management performance?*
  Directional antenna gain and beam steering were shown to be an efficient way to affect mobility management performance, provided the network is not aware of the beamforming capabilities of a vehicle. Beamforming can be used to prolong connectivity to the same serving cell, leading to a decreased number of handovers. Beam steering can be also

beneficial if it is used to connect to a low loaded cell, leading to increased throughput of the vehicle. However, using beamforming may also have a negative impact on the nearby located GdUEs. In the case in which a UAV uses beamforming to redirect the connection to a less-loaded cell, its signal might still affect GdUEs served by a closer cell, due to a high level of generated interference.

To sum up, transmit beamforming shows great potential to improve uplink performance of connected vehicles. Directional antenna gain, together with the beam steering capabilities, can be used to not only improve the reliability and uplink throughput of a given vehicle but can ensure more fair coexistence with other users of the network.

4.3 Recommendations

In addition to the conclusions presented in the previous sections, the following recommendations are worth consideration:

- Mobile network operators should consider issuing UAV-side beamforming as a recommended technique to be used by UAV vendors for all cellular-connected UAVs flying above a certain height threshold. As shown in this work, beamforming can improve connectivity for all the incumbents of cellular systems with respect to omni-directional antennas. If all UAVs use beamforming, mobile network operators can incorporate more UAVs at the same time/region while ensuring coexistence with GdUEs. The height threshold, can depend on the average building height in a country or a certain geographical area, such that UAVs flying higher than the threshold are assumed to observe high LoS probability.

- The designer of UAV communication systems should consider using an omni-directional antenna pattern for connectivity during crucial procedures like landing, takeoff or in-between building flying. This recommendation is complementary to the previous one. To improve reliability when flying in regions where dominant LoS path cannot be assumed and a high average level of multipath is expected, it is recommended that the UAVs should use an omni-directional antenna pattern or multi-antenna combining techniques to improve signal's SINR and therefore reliability.

- The designer of VUE communication systems should consider using beamforming for ground-level vehicular communication in rural areas to strengthen the observed SINR and therefore improve coverage. This relatively straightforward solution can give a car manufacturer a competitive advantage over other carmakers that are using only a single

omni-directional antenna and are counting on 5G coverage to be sufficient in all places. Using beamforming can only help to improve the coverage and data rates, leading to more reliable connectivity, increased safety during automated driving as well as better services offered to the passengers of the vehicle.

- The 3GPP standardization committee members should consider adding new, standardized network signaling, to alleviate practical concerns of using beamforming on board of a (ground or aerial) vehicle. User Equipment (UE)-side beamforming signaling without distinction among GdUEs and vehicles is already available as a part of the 5G standard. However further amendments should be considered. As an example, if a network signals the physical location of all the cells in the vicinity, the vehicle may proactively use this information to better align the beam or choose the direction such that for example the number of handovers is minimized. Moreover, the creation of new UE classes should be considered, in which a vehicle can report the type of antenna system it is using. As an example the number of beams, the front-to-back ratio, or the HPBW may be signaled. This information can be used by the network operator to optimize the beamforming direction of such a vehicle.

4.4 Future work

This work presents a comprehensive yet not exhaustive analysis on the potential of using multi-antenna techniques installed on a vehicle terminal. In the remainder of this section, some potential research directions which can be considered as a future work are presented.

Impact of beam steering on cellular systems

The impact of beam steering on mobility management performance as well as its effect on other users have found only little to no attention in the literature. As stated in this thesis, by using beamforming, a device can connect to the cells which were not available due to higher path loss than the serving cell when using an omni-directional antenna. By doing so, the vehicular device may improve the uplink throughput due to connectivity to a low-loaded cell or prolong connectivity to the same BS, thus reducing the number of observed handovers. On the other hand, the device may become a strong source of interference to the users connected to nearby cells. As of today, most of the works focusing on cellular networks, assume all users operating using omni-directional antennas. As a potential future work, it is recommended to study the impact of using directional antennas by some (e.g. vehicular) devices on

the cellular network protocols such as mobility management. Furthermore, the potential effects of beamforming on cell planning should be considered.

Network-assisted beamforming

In this work, it was assumed that the beamforming decisions are made independently at each vehicle without assistance from the network. If the cellular system possesses information of all vehicular devices equipped with beamforming systems, their capabilities and antenna patterns, a network can potentially assist or even overtake the control of beamforming decisions from the vehicle. Given the discussed vehicular challenges, such as mutual interference with other vehicles and GdUEs, as well as different requirements imposed by GdUEs and vehicles, network-assisted beamforming can potentially be used to optimize the system performance. Therefore it is recommended to study, how can the network-assisted beamforming be used most efficiently. The impact of multiple factors such as cell load, distance to the cell or position of users on the decision strategy should be considered. Further, the optimal range of cells involved in the decision-making process may also be studied.

Use of 5G new radio for vehicular communications

5G provides a new opportunity for vehicular communications. It contains the UE-side beamforming procedures. It is recommended, to repeat some of the experimental studies performed in this thesis using a 5G network and device (when available), to better understand the applicability of this technology for vehicular communications. Before such devices (and fully deployed networks) are available, system-level simulations studies should be considered in which a vehicle uses 5G-compliant beamforming procedures.

Part II

Publications

Paper A

A USRP-based multi-antenna testbed for reception of multi-site cellular signals

Tomasz Izydorczyk, Fernando M.L. Tavares, Gilberto Berardinelli and Preben Mogensen

The paper has been published in the
IEEE Access, 2019.

The layout has been revised.

Abstract

This paper presents a design of a Software Defined Radio (SDR) multi-antenna testbed able to record live cellular signals from multiple sites. This measurement setup, based on Universal Software Radio Peripheral (USRP) boards, is used to record live Long Term Evolution (LTE) signals in sub-6 GHz frequency bands. Due to recording of raw I&Q samples, this fully digital testbed is suitable for variety of research activities spanning channel characterization and beamforming performance evaluation. We propose a phase calibration method based on transmission of a single out of band tone to overcome the uncertainty introduced by the USRP's lack of phase alignment. We demonstrate two use cases where the proposed testbed can be used, and we validate its performance during two measurement campaigns with self-generated and real cellular signals.

A.1 Introduction

Multiple antenna systems are well known to increase capacity and reliability of the communication links. For many years, theoretical and simulation works have shown the achievable gains when large antenna arrays are used [1]. Such studies rely on the channel models existing in the literature derived from measurement campaigns. Moreover, field trials using wireless platforms and testbeds are conducted to provide the algorithms' performance evaluation in real deployment scenarios. New use cases including Industry 4.0 [2], Vehicle-to-Everything (V2X) [3] or Unmanned Aerial Vehicle (UAV) [4] communications open up new scenarios which may not be properly characterized by existing models. Therefore, there is an even greater need for further experimental channel modeling, as well as empirical studies of multi-antenna algorithms in the mentioned scenarios.

Building large testbeds with multiple antennas is not a trivial task. Although typical requirements of a measurement system are operating frequency, bandwidth and the number of antennas, the design is usually influenced by multiple other factors. One of them is the actual use case which determines what type of transmitted signal should be used. Very often multi-antenna testbeds are complemented with a self-made transmitter (single or multi-antenna) radiating self-generated excitation signal. By using such an approach, different measurements can be conducted in controlled scenarios with exact control of the transmitter (TX) and receiver (RX) positions, the type of radiated signal and the synchronization between nodes [5].

However, there are certain situations in which using a self-made transmitter can be impractical and pose unnecessary constraints on the designed experiment. Studies on algorithms as beamforming or Interference Rejection Combining (IRC) receivers require gathering samples in the presence of in-

terference. In these situations, multiple transmitting nodes imitating WiFi access points or cellular base stations are required to be deployed relatively far from each other in order to emulate the target and interfering signals. Very often they would need to be placed in hardly accessible places like roofs of the buildings or lamp posts. Although such a measurement system using self-made transmitters can be deployed, scalability may become cumbersome. To obtain reliable results, numerous deployment scenarios need to be tested, requiring time consuming redeployments of the transmitting nodes.

Similar problems may occur if the studied use-case demands measuring over a large geographical area. V2X or UAV communications are some exemplary studies that require gathering numerous samples in different scenarios. Several redeployments of the self-made transmitter might be required to efficiently cover large areas; this might render the measurement campaign unfeasible.

One of the potential alternatives is to measure signals directly from live cellular networks. In this case, the redeployment time is shortened as only the receiver needs to be repositioned. Moreover, obtained results are more reliable since they are taken from a real network deployment. Another benefit of using live cellular networks is the possibility of concurrent recording of signals incoming from multiple visible cells. As each of the cell has its own identifier - Cell ID, multiple cells can potentially be decoded from the same data snapshot, leading to expansion of the recorded data set. Multiple visible cells recorded during the same data snapshot can also be seen as interference with respect to a target cellular signal. The ability to differentiate among them can be beneficiary when studying the performance of interference rejection or receive beamforming algorithms.

Although, as shown in Section A.2, many multi-antenna testbeds are reported in the literature, none of them operates using live cellular signals as for example Long Term Evolution (LTE). The measurements of live cellular signals impose several constraints on a measurement system. Due to lack of control of the transmitter, the TX-RX synchronization would only be achieved if real-time signal decoding is performed. Moreover, the increased receiver complexity with respect to a self-generated excitation signal can discourage its possible usage. However, many research activities do not require any real time processing and their target research objectives can be achieved offline, by recording raw I&Q data samples and processing them later using software. Works in [6] and [7] are some example use cases where offline processing is used.

This work describes a novel measurement methodology, in which a large multi-antenna testbed is used to record live cellular signals transmitted from multiple base stations. The testbed was built for a wide range of studies related to V2X and UAV communications including spatial channel characterization and beamforming performance evaluation. The major focus is placed

on the flexibility of the measurement system as this fully digital design is based on Universal Software Radio Peripheral (USRP) boards and can operate with any cellular signals. The proposed methodology and hardware design are complemented by the practical description of the offline post-processing methods covering LTE signal reception using Matlab's LTE toolbox [8] and channel characterization using Space Alternating Generalized Expectation-Maximization (SAGE) algorithm [9]. Up to the best of the author's knowledge, this is the first testbed with a large antenna array capable of working with live cellular systems presented in the literature.

The rest of this article is structured as follows. An extensive literature survey on the existing testbeds is presented in Section A.2. Section A.3 discusses the general system design requirements. It is followed by Section A.4, focusing on the system implementation in both hardware and software. As a part of the hardware description in Section A.4.2, the problem of establishing phase synchronization between boards is described. Later in Section A.5 two examples of post-processing methodology are presented. Section A.6 presents the validation of the overall concept in real environments. Finally, Section A.7 discusses the potential use cases in which the proposed testbed is a suitable choice. The work is concluded in Section A.8.

A.2 Literature survey

Many research activities use large multi-antenna testbeds. Unfortunately, very frequently these articles are focused only on the results obtained using them, leaving only a small part of an article for the actual testbed description. However, the testbed design in both hardware and signal processing steps is a non-trivial task. Usually, measurement setups can be divided in three distinct categories: switched antenna testbeds, fully digital custom-built testbeds (based on Application-Specific Integrated Circuits (ASICs), Digital Signal Processors (DSPs) or Field-Programmable Gate Arrays (FPGAs)) and one's built based on Software Defined Radios (SDRs). All types of a measurement system have their distinctive features. If a real time, high throughput capability is necessary, a dedicated ASIC-based testbed with algorithms being developed on FPGA chips is the most common design choice. If fast prototyping and high reconfigurability are desired, SDR-based testbeds are the best option.

In the remaining of this section, a literature survey presenting multi-antenna testbeds is presented. Please note that the proposed literature list is by any means not exhaustive, but is rather a subjective list of works where, in the author's opinion, the used testbeds were sufficiently described.

The literature on channel sounders built based on the switching antenna systems is broad. The descriptions of multiple developed channel sounders

can be found in the deliverables of some large international projects like WINNER [5] or TSUNAMI [10]. Also, many smaller research activities use the switched antenna systems. In [3], the 16-elements switched antenna system was used to study the vehicle-to-vehicle (V2V) cluster-based propagation channel. Similar work is presented in [11] where a real-time channel sounder for V2V propagation studies at 5.9 GHz is presented with the focus on spatial channel characterization. This article together with [12] are examples of testbeds where a switched array is used in conjunction with a single USRP board providing the Radio Frequency (RF) chain.

A comprehensive survey on different types of a fully digital custom-built testbeds with large antenna arrays is presented in [13]. This work contains three examples of testbeds built based on ASIC, FPGA and DSP components. Their potential use cases are also discussed. Work in [14] presents a custom-built testbed with a large 12-elements circular array used to study the potential mismatches in the beamforming directions between Downlink (DL) and Uplink (UL). Another large testbed using dedicated hardware is presented in [15]. It is a 16x16 multi-user MIMO system operating using indoor Wi-Fi to study the effects of the increased number of users on a transmission bit rate. Interesting work on interference alignment techniques using a multi-user MIMO testbed is presented in [16]. In this work, authors use a customized testbed working in a 5 GHz band to measure and exploit the interference channels caused by multiple users. Finally, authors in [7] focus on receive beamforming using a testbed with a 4-element antenna array in the 2 GHz frequency band and [17] focuses on beamforming with side lobe level reduction where beams are created using a testbed built with a dedicated hardware and 8-element array.

There are many multi-antenna testbeds built based on SDRs reported in the literature confirming the ongoing trends. Authors in [18] use a self-built SDR setup to study the impact of imperfections in hardware and channel estimation inaccuracies using a 4x4 multi-user multi-antenna setup. A four antennas system to study the DoA estimation and digital beamforming for jamming signal avoidance in satellite communication is described in [19]. The authors use a single dual-port USRP equipped with an additional daughterboard installed as RF-port extension. By using such, they are able to accommodate all four antennas within a single USRP omitting the burden of providing phase calibration between different boards as it would be required if two dual-port USRPs are used.

Multi-antenna testbeds built by connecting multiple USRP boards in sub-6 GHz bands are also available in the literature. The researchers from Lund university developed a 100-antennas testbed for real time massive MIMO evaluation [20] and together with Bristol University even larger 128-antennas setup presented in [21]. However, their usage was still constrained to receive self-generated cellular signal and was not extended to operate with live sig-

nals. Works in [22] and [23] focus on adaptive beamformers using a 4 and 3 elements antenna arrays respectively, where each antenna is connected to a different USRP board. In [24] and [25] the antenna arrays (up to 8 antennas in the latter case!) are used for DoA estimation. Finally, a USRP-system containing 4 synchronized nodes is used for the localization purposes in [26].

Although, as presented in this section, there are many multi-antenna testbeds available in the literature, none of the acknowledged works use them for reception of live cellular signals. Therefore, this article presents a setup extendable to operate with arbitrary number of antennas; thoroughly explaining the process of recording, decoding and utilizing the multi-site transmitted cellular signals for various research purposes.

A.3 System design

System requirements

While designing the proposed measurement testbed, multiple different factors were considered. Although the first research directions to be targeted using the designed testbed were already defined at the design phase (channel characterization for the cellular V2X communication), it was assumed that in the future the proposed testbed will be used for some activities which at this stage had not yet been defined. The ideal envisioned setup should therefore provide flexibility of usage for various research activities including spatial channel characterization or beamforming evaluation, possibly in different frequency bands up to 6 GHz.

To satisfy the envisioned use cases, the designed testbed is required to concurrently measure signals from multiple transmitters using multiple antennas. For the reasons explained in the introduction, it was decided to measure live LTE signals. This requirement imposes the use of fully digital system where each antenna port has its own RF chain. The use of switching antenna system, although theoretically possible, would be cumbersome to implement due to channel non-stationarity and challenging transmitter-receiver synchronization. As some research activities may impose special demands on an antenna array, including different number of antennas or a specific antenna configuration, the designed testbed should be adaptable and allow to accommodate different number of antennas with only little changes to the overall hardware architecture.

General design

To address flexibility demands, it was determined that the designed platform should be based on SDRs and be capable of recording and storing data

snapshots containing raw I&Q samples with no real-time processing. By using SDR boards, one can benefit from their high reconfigurability, usual high range of operating frequencies and recorded signal bandwidths. By recording raw, unprocessed data samples, there is no risk that the real-time processing would reduce or prevent certain future activities in post-processing. As some of the potential use-cases may require precise location information, the Global Positioning System (GPS) antenna need to complement the design.

In the described testbed we decided to use the NI USRP 2953R boards as an SDR platform. The operating frequency range from 1.2 GHz to 6 GHz is deemed to be sufficient to assure the flexibility demands. Each board contains two RF chains, therefore multiple boards are required to build a large multi-antenna testbed. The boards can record up to 40 MHz real time bandwidth, which is sufficient to record live LTE signal (with maximum 20 MHz bandwidth). By using additional National Instruments (NI) equipment, further described in the next section, the remaining design requirements can be fulfilled. A PXI chassis and its embedded controller allow to control multiple boards, while a timing module is used to distribute a common synchronization signal via Octoclocks, enabling coherent measurements across all boards. In extreme situations, when desired array size (and therefore number of USRP boards) is larger than the amount of slots available within a PXI chassis, these can be combined to create a multi-chassis acquisition system.

Although, the proposed system architecture matches the design requirements, for some use cases it is not sufficient. Beamforming applications or DoA estimation algorithms require, a tight phase synchronization over all antennas in order to exploit small phase differences in their signal processing algorithms. The multi-USRP platform designed as proposed would not support these applications as it is known that the USRP boards are not phase-coherent [24]. Therefore, an extra phase calibration procedure needs to be implemented. Its details are described later in Section A.4.2.

A.4 System implementation

A.4.1 Measurement system

The presented measurement system is composed of a multi-antenna receiver, as well as additional hardware used for transmission of the calibration signal needed to phase-align all USRP boards, as will be described in Section A.4.2. Figure A.1 presents the block diagram of the setup with calibration part highlighted by a green dashed line. Besides, Table A.1 summarizes the general and implementation-specific configurations of the designed testbed. For the envisioned use cases, 1.845 GHz operating carrier frequency was chosen. This particular carrier frequency is the middle of LTE band 3 occupied by two

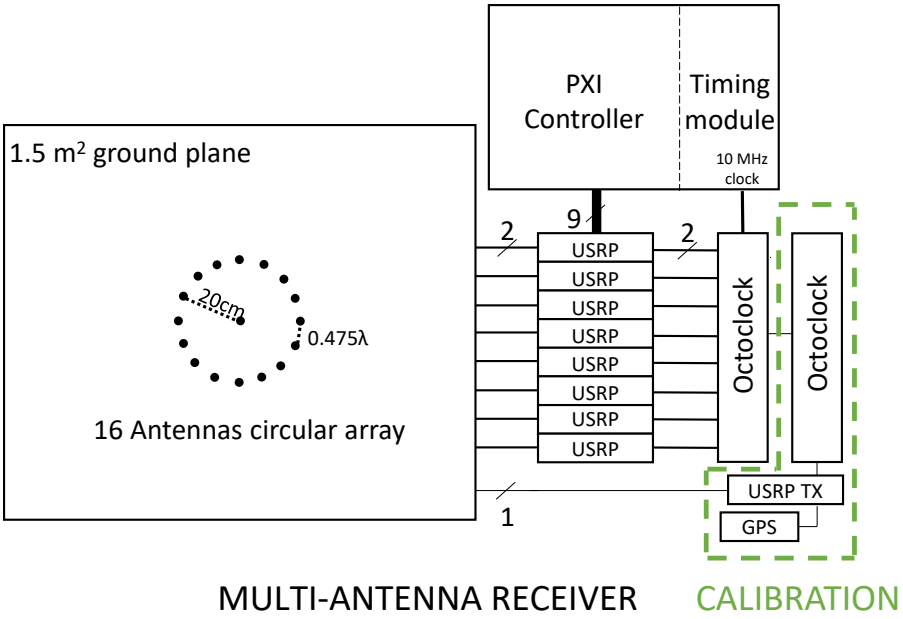

Fig. A.1: Measurement system schematic

Danish telecom operators with more than 50 base stations deployed per operator. Such choice allows to double the potential measurements using the same testbed and antenna configuration.

The receiver features a 16-antennas Uniform Circular Array (UCA), which has been manufactured on an aluminum ground plane. The reason for using UCA rather than a linear array, is its ability to scan the incoming signals in all 360^o without ambiguity. The number of antennas was selected as a good trade-off between setup complexity and achievable system resolution. Antennas are connected to 8 USRP 2953R boards, each providing two separate RF chains. All boards are connected to an embedded controller using Peripheral Component Interconnect (PCI) bus. The synchronization signal is generated by an Oven Controlled Crystal Oscillator (OCXO) and distributed to all USRPs using an Octoclock.

The receiving part is complemented with an additional ninth USRP board (and antenna located in the center of the array), used for generation of the calibration signal. The board is connected to the same embedded controller and synchronized to the same synchronization signal using a second Octoclock. In the remaining of this Section, each hardware element is described.

Table A.1: Reference configuration of a proposed multi-antenna testbed

Parameter	**General Design**	**Proposed Implementation**
Type of recording platform	Any USRP-type boards	USRP 2953R
Type of recorded signal	Any signal with power above the receiver's sensitivity	live LTE incoming concurrently from multiple base stations
Number of USRP boards	Flexible (For large number of boards, the multi-PXI system would be required)	8 RX and 1 TX board
Number of antennas	Flexible (Depends on the amount of the USRP boards)	16 RX and 1 TX
Array configuration	Flexible (although the calibration procedure might need to be adjusted)	UCA
Carrier frequencies	1.2 - 6 GHz	1.845 GHz
Signal bandwidth	Depends on a use case (up to 40 MHz)	40 MHz
Sampling rate	Up to 200 MS/s	40 MS/s
Length of the recorded signal	Flexible (depends on a sampling rate and signal bandwidth)	100 ms
Frequency accuracy	Up to 5 ppb with GPS-locked OCXO signal	25 ppb
Phase accuracy	Depends on an implemented calibration procedure	$\leq 1^o$
Receiver sensitivity	Depends on signal bandwidth and minimum SINR	~ -114 dBm assuming 1.08 GHz bandwidth of MIB, minimum SINR of -5 dB and USRP receiver window reference level set to -25 dB

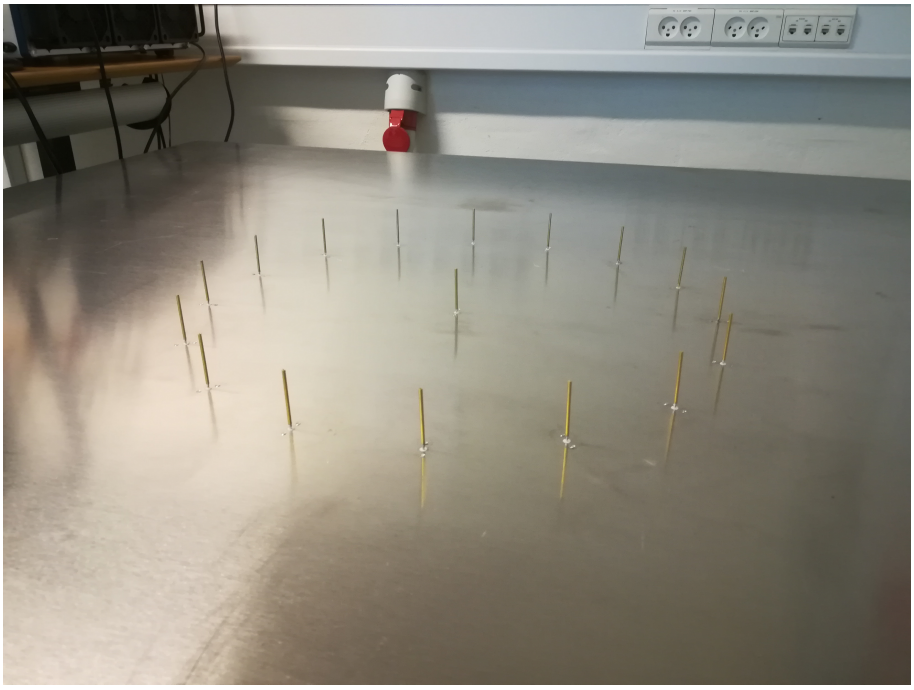

Fig. A.2: Antenna array used in the setup

Uniform Circular Array design

The UCA is composed of 16 monopoles placed on a 1.5 m $\times$ 1.5 m aluminum ground plane. The ground plane has been manufactured with bent edges to reduce border effects arising due to its finite length and therefore limit the potential up-tilt of the antenna radiation pattern. The array has been designed to work in the downlink part of LTE Band 3 (center frequency of 1.845 GHz), which corresponds to a circular radius of 20 cm, wavelength $\lambda = 0.1625$ m and antenna spacing 0.475λ. Proposed design was simulated in CST Studio - a software, among others, used for antenna design and simulation. Results showed that array's far-field radiation pattern can be very well approximated by an omni-directional pattern in the azimuth domain. Antenna array is meant to be installed on the roof of a vehicle, to facilitate drive tests. To minimize the risks of possible short circuit between antennas and ground plane in case of rain and to prevent any physical damage, a Styrofoam radome of 25 cm radius covers the monopoles on the ground plane. Figure A.2 presents the complete antenna array design before the radome installation.

NI USRP 2953R

Eight USRP boards have been used as RF chains. Each board is equipped with two separate RF chains, which are configurable using NI LabView Communications software. An additional ninth USRP was used as a transmitter for the calibration signal. As already mentioned, this model of the USRP operates in the frequency range from 1.2 GHz to 6 GHz, with up to 40 MHz real time bandwidth, which is sufficient to record live LTE signal (that can occupy up to 20 MHz bandwidth).

The USRP boards perform digital down conversion and stream the I&Q samples via fast PCI bus to the controller. The described setup is able to record the "raw" radio signals. The processing of the LTE signal, including frame alignment, cell search, demodulation of the reference signals, etc. is done offline using, for example, Matlab LTE toolbox.

NI PXIe-1085 and NI PXIe-8135

NI PXIe-8135 is a powerful embedded controller for PXI Express systems, which can be used to control the measurement setup using LabView Communications software as described later in Section A.4.3. The controller is installed within the PXIe-1085 chassis, which also contains sixteen hybrid slots with up to 24 GB/s connection speed and 1 PXIe timing slot. Nine slots are used as extension boards to connect all USRPs and Timing module (OCXO board) is used in the timing slot. By using the chassis, there is a possibility to use even more antenna elements as remaining empty slots can be used to accommodate more receiving USRP boards and extend the system to larger antenna arrays.

Octoclocks CDA-2990 and NI PXIe-6674T

Even though each USRP board is equipped with its own local oscillator, coherent data detection requires data to be collected with time and frequency synchronized system, while beamforming or DoA estimation algorithms require even tighter phase alignment between all antennas. Frequency synchronization between different boards can be achieved by providing an external 10 MHz reference clock. Also, a Pulse Per Second (PPS) trigger, in this case generated by one of the USRP boards, must be distributed to all of the boards, so that its rising edge initializes the reception on all boards.

The NI PXIe-6674T Timing Module provides a 25 parts per billion (ppb) precision 10 MHz clock, which is installed as an extension board within the PXI chassis. The 10 MHz clock is then distributed to two eight ports Ettus Octoclocks CDA-2990 which further distribute it coherently to all nine USRP boards. To avoid any ambiguities in delays and due to limited number of ports per Octoclock, all eight receiving USRP boards are connected to the

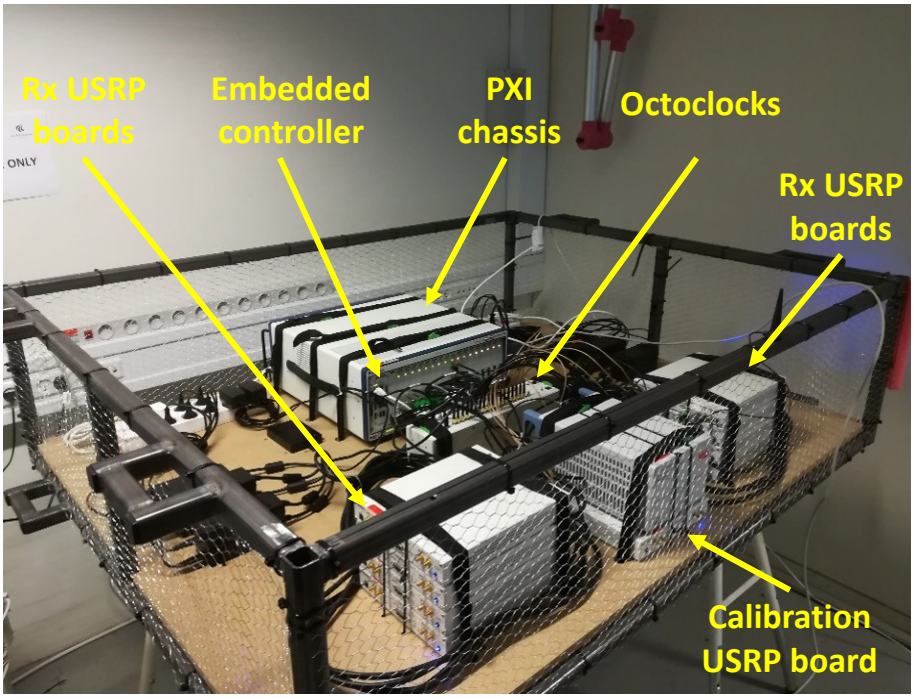

Fig. A.3: Assembled setup

single Octoclock (as shown on Figure A.1), while the USRP used for calibration purpose is connected to the second one.

Figure A.3 presents the assembled measurement setup before its connection with the antennas using 3-meter-long RG233 cables. It is worth to note that although the proposed measurement system was designed (and is further described) as a multi-antenna receiver, it can potentially be used as a multi-antenna transmitter, nonetheless some changes to the overall design methodology would be required. First, the receiver's software as described in Section A.4.3 would need to be upgraded to incorporate the transmitter. Second, if the phase alignment between all transmitting antennas is required, the proposed calibration would become insufficient and would need to be redesigned to occur in real-time rather than in post-processing.

A.4.2 Calibration procedure

Time and frequency synchronization, as explained in previous section, is not sufficient if signals recorded by the proposed testbed are to be used for beamforming or DoA estimation where phase differences are important. Even though all USRP boards are phase coherent, they are not phase aligned (each

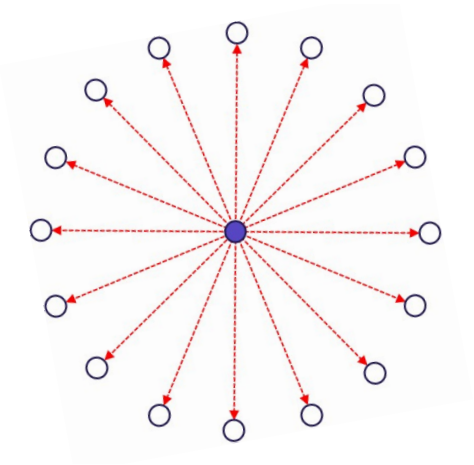

Fig. A.4: Principle of calibration tone transmission

board starts receiving with a different unknown phase offset) and therefore a calibration method is required to compensate this misalignment.

Different methods for calibration are proposed in the literature. All of them are however related to the same principle - generation of the known calibration signal and its redistribution to all USRPs. Authors in [24] and [26] use an additional USRP board to generate the signal. By using a RF power divider, the signal is distributed using antenna cables of the same length to all boards. The drawback of this method is the eventual loss of one transceiver chain in each receiving USRP just for calibration.

Over the air calibration is proposed in [22] and [25]. In both works the calibration signal is transmitted wirelessly to the receiving array. In post-processing the signal is filtered and phase-difference between boards is computed assuming that it was only caused by the initial USRP phase difference. As both works use linear array, the systematic phase difference occurring due to unequal signal's travel distance from the reference antenna to each antenna element can be calculated beforehand and corrected.

In this project, a low power Out-of-Band (OoB) calibration signal is transmitted from the additional antenna placed in the center of the array. In this case, given the array symmetry, all antennas will receive the signal with equal delay, power and phase as illustrated on Figure A.4. Therefore, no additional phase shift between antenna elements is observed as if a linear array would be used.

The calibration signal is a single tone transmitted approximately 5 MHz away from the edge of the target LTE band with -50 dBm transmit power. Such low power prevents significant interference to other systems potentially transmitting in this band. OoB transmission is also beneficial as it does not

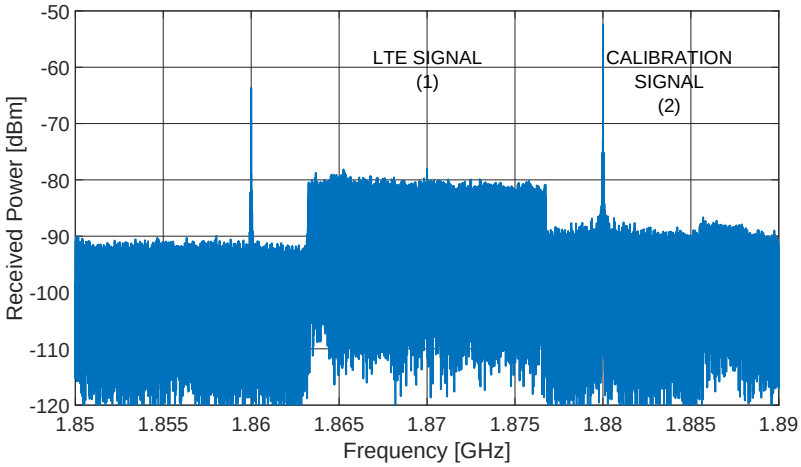

Fig. A.5: Received signal spectrum

interfere with the received LTE signal. Before the final decision on frequency used to transmit the calibration tone, frequency spectrum is scanned with a spectrum analyzer in order to avoid the choice of frequencies that are occupied by another system, potentially interfering with the calibration tone. Figure A.5 presents a sample recorded signal in 1.8 GHz band with LTE (1) and Calibration signals (2).

After samples are recorded, the first step before any array processing is the system calibration. Calibration tone is separated from the received signal by means of digital filtering in frequency domain. Then the frequency position of its actual peak is found based on maximum energy detector for all the receiving antennas. Assuming the received phase of the signal on one of the antennas as a reference, the phase difference can be computed for all remaining ones. Finally, the entire received sequence is phase shifted for the remaining fifteen data streams according to the computed difference. The proposed calibration method effectively reduces the phase offset down to less than 1^{o}, which is sufficient for accurate beamforming and DoA estimation as presented later in Sections A.6 and A.7.

A.4.3 Measurement software design

Measurements are conducted using LabView Communications software installed on the PXI embedded controller. The setup has been designed in a flexible way, such that the duration of a measurement snapshot can be adjusted up to 350 ms of continuous recording. Limitation of recording time is the result of limited size of Direct Memory Access (DMA) buffer of the

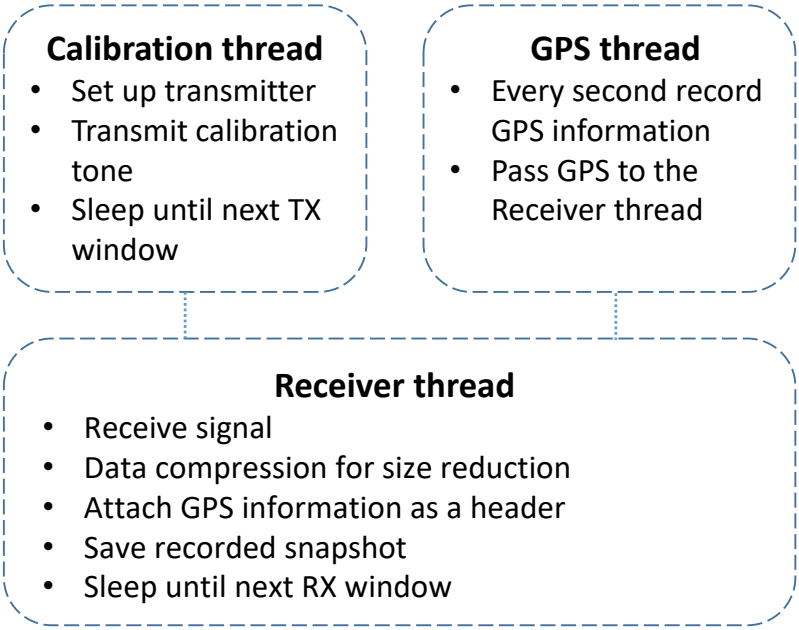

Fig. A.6: Block diagram of the measurement software

USRP board. Besides snapshot duration, the recording periodicity can also be adjusted. Its minimum value is limited by the time required to store all the data on a hard drive. Therefore, the designed software offers a flexibility to record short snapshots at higher frequency or longer ones with a larger measurement gap between them. This flexibility is especially valuable in case of the drive tests or other use cases in which the receiver changes its position with time.

Designed software is composed of three main threads as presented on Figure A.6. First thread is responsible for generation of the calibration signal and its transmission during the receiving time window. When the recorded data is being processed and saved, the transmitter is inactive, to reduce the potential interference caused to the other systems. Second thread is used for periodic acquisition of the GPS information recorded using NI-compatible magnetic mount GPS antenna, connected to one of the USRP boards. Finally, the third thread receives the signal. Later it performs simple data compression to reduce the size of the data (which speeds up the saving process), adds header information where GPS information is included and saves each snapshot independently on the hard drive. Finally, all three threads wait until the new recording cycle begins according to the desired periodicity.

A.5 Examples of post-processing methodology

In this Section, two different examples of post-processing are presented to indicate possible use cases of proposed testbed. First the LTE signal demodulation is presented, followed by channel estimation using SAGE algorithm. The described post-processing is used in the upcoming sections during the validation measurements to showcase the capabilities of the proposed setup. Although data processing is usually use case dependent, the post-processing presented in this section is very generic and can be used as a building block for many diverse, more advanced, research applications.

A.5.1 LTE demodulation and beamforming

Received signal can be processed to demodulate LTE signals in order to extract common cell information (available in the Master Information Block (MIB) and System Information Block 1 (SIB1)) or to estimate received channel and use it as an input for SAGE processing. The demodulation can be done twofold. One way is to program the entire LTE receive processing by writing code based on relevant 3GPP standards, as done for example in [27], where the code for correlation-based network synchronization or channel estimation was self-written. An interesting alternative is to use Matlab LTE toolbox. It contains all the relevant functions for signal demodulation. Although this toolbox is primarily used for the simulation-based evaluation of LTE system, as shown in this work, it can also be used for demodulation of the live cellular signals recorded with USRPs.

In the remaining of this section, the potential of using the LTE toolbox is discussed by describing the receive beamforming processing. Although this section is focused only on the receiving beamforming, other multi-antenna combining techniques including Maximum Ratio Combiner (MRC) or even single antenna processing can be achieved by replacing the beamforming block with the desired antenna processing as described in [28].

Figure A.7 presents the flowchart of the data processing. Received signals impinging on the multiple antennas are first phase-calibrated and then beamformed towards the desired angle as below:

$$\mathbf{y} = \left(e^{-2\pi j \frac{r}{\lambda}\cos(\varphi)\cos(\theta-\boldsymbol{\theta})}\right)^{H} \cdot \mathbf{S} \tag{A.1}$$

where $\mathbf{S}$ is the phase-calibrated input data stream, θ and φ refer to the azimuth and elevation angle for a given beam, r is the radius of the antenna array, λ is the wavelength and $\boldsymbol{\theta}$ is the antenna position-dependent column vector of angles of size $[N_{RX} \times 1]$ where N_{RX} denotes number of receiving antennas. $(\cdot)^H$ denotes the hermitian operator.

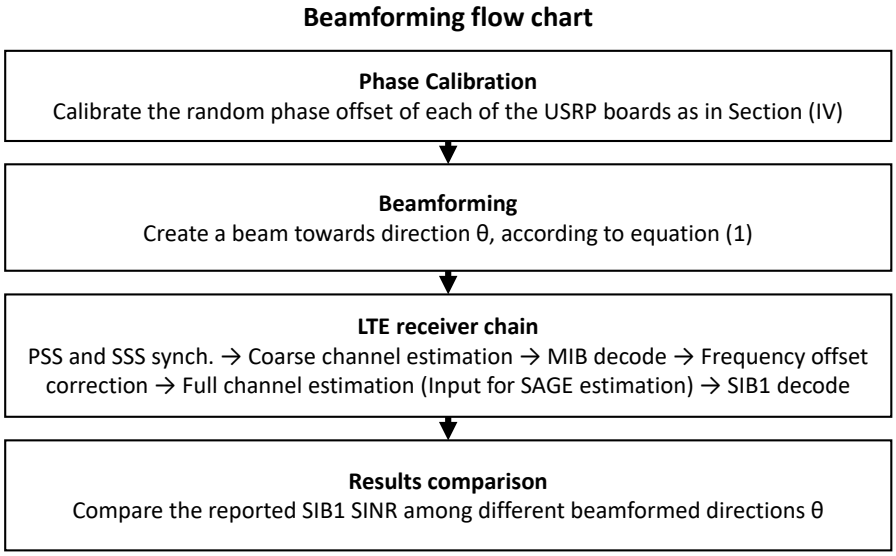

Fig. A.7: Post-processing flowchart for beamforming evaluation

After beamforming, the resulting data vector $\mathbf{y}$ is obtained and processed by the LTE receiver, where using Matlab's framework, first an LTE synchronization procedure is performed based on LTE synchronization signals (PSS and SSS). In the next steps, there is a frequency and time offset estimation and correction followed by MIB decoding for selected (one or more) Cell-IDs. In this way, all the necessary information required for channel Cell-specific Reference Signal (CRS) extraction are obtained.

After down-sampling to the sampling rate corresponding to the bandwidth of received LTE signal, channel reconstruction based on LTE CRSs can be performed. Moreover, if the entire process is repeated for different Cell-IDs, potential number of transmitting LTE base stations can be deduced. Finally, provided sufficient signal quality, SIB1 can be decoded. If successful, the Error Vector Magnitude (EVM) and Signal to Interference plus Noise Ratio (SINR) of this control channel are computed.

A.5.2 Channel parameters estimation using SAGE

SAGE algorithm is a well-known, powerful tool to estimate the number of signal taps, their gains, delays, DoAs and doppler shifts. Readers are referred to [9] for details on the algorithm.

Only few examples in the literature can be found where SAGE was used to estimate parameters of the live LTE signal. Even fewer works can be found presenting the insights of its usage such as algorithm's initialization. One

example of such work is [27] where authors used continuous chunks of 50 ms of recorded LTE signal (only the CRS grid) for SAGE estimation. At first, they pre-initialize their algorithm to pre-estimate 30 multipath components. After some SAGE iterations, the potential number of multipath components is estimated and the results are refined by running additional 15 iterations of SAGE only for the predicted number of paths.

In this work, similar to [27], the CRS signals are used for SAGE estimation. The main reason for choosing CRS over any other common signals available in LTE is the fact that CRS are equally spread over the entire frequency band and they are always transmitted using the same deterministic pattern, which can be learned from the MIB. Usage of the entire recorded LTE signal would not be feasible as it contains unknown user-specific data transmissions. The transmitted CRS pattern, used in SAGE as a blueprint for channel estimation, is again re-created at the receiver using Matlab LTE toolbox based on information from the MIB.

Contrary to the cited work, our SAGE implementation can work with a flexible length of CRS sequence from 30 ms up to 300 ms. Such range is a consequence of the flexible recording duration as explained in Section A.4.3. Algorithm is initialized to estimate 50 paths. However, after initial five iterations, all the taps with a path gain minimum 40 dB lower than a maximum path gain are discarded as they are deemed to represent noise. Later another ten iterations of SAGE are run for the remaining, limited number of taps. In the upcoming section, the presented approach and algorithm's implementation are validated using both self-generated and live LTE signals.

A.6 System Verification

First step after the design of a measurement testbed is its verification in a known environment. This Section describes two measurement campaigns used for testbed's validation. In the first one, the proper recording, calibration and implementation of a post-processing software (beamforming algorithm and SAGE processing) are validated. By using self-generated LTE signal in a Line of Sight (LoS) scenario, the expected DoA can be inferred from the position of the receiving array and confronted with the estimated one. Second validation campaign is used to test if the proposed testbed can correctly operate with a live LTE signal with presence of interference.

A.6.1 Measurements using self-generated LTE signal

In the first measurement, the proposed testbed, its calibration and post-processing methodology were tested in controlled scenario. The target of this measurement was to estimate DoA of the transmitted self-generated LTE

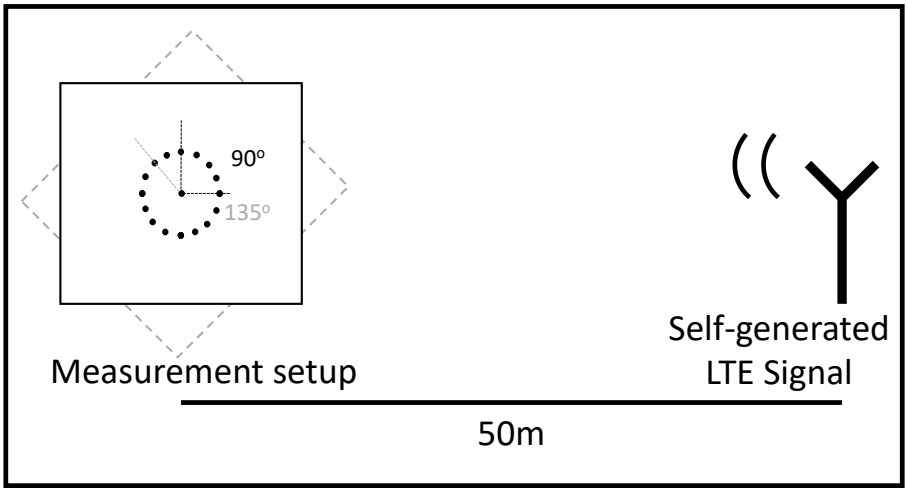

Fig. A.8: Concept of the first validation campaign

signal by using two different methodologies - beam sweeping and SAGE estimation. By using an additional USRP board, the self-generated LTE signal was transmitted with 0 dBm transmit power as shown on Figure A.8. The multi-antenna testbed was placed approximately 50 m away in a clear LoS condition with respect to the transmitter. Two 100 ms snapshots of the LTE signal were recorded and the antenna array was carefully positioned in two orientations, such that approximately 90^o DoA in orientation 1 and 135^o DoA in orientation 2 are expected. If estimation is correct, all building blocks (hardware and software) of the proposed testbed will be validated.

First way of DoA estimation is beam sweeping. It uses the beamforming methodology explained in Section A.5.1. Recorded signals for both orientations are in the post-processing beamformed towards 360 different directions in the azimuth domain with a step of 1^o. 0^o elevation angle is assumed. For each beamformed angle, the whole LTE demodulation processing is made and provided successful decoding, SINR of SIB1 is computed.

Figure A.9 presents the computed SINR distribution for different beamformed angles. As expected, the maximum SINR values are obtained for the angles close to 90^o and 135^o respectively, corresponding to the situations when beam was pointed in the direction of the transmitter. The missing SINR values for some angles are related to the angles where SIB1 was not decodable due to insufficient SINR.

The same recorded snapshot was also used to estimate DoA based on SAGE as explained in Section A.5.2. The estimated channel matrix using LTE toolbox was used as an input for SAGE estimator set to estimate 50 paths. Figure A.10 presents the azimuth DoA versus gain for each estimated

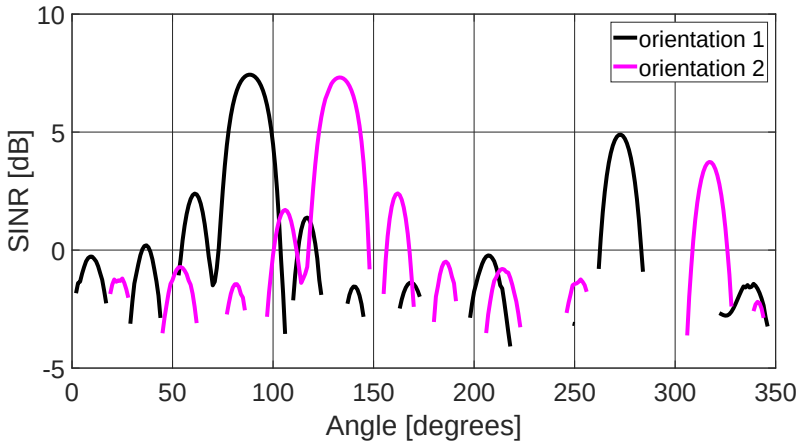

Fig. A.9: Angular distribution of SINR for self-generated signal

path. As expected, paths with the highest gain have their corresponding DoA located at approximately 90^o for orientation 1 and 135^o for orientation 2. The remaining paths have much lower power and are assumed as noise.

Results presented in this section validate the correct performance of the proposed testbed, as both methods indicate the expected DoA. This preliminary measurement was an important step to show the proper operation of the proposed calibration system and assures that the post-processing methodology can be used with over-the-air transmitted signals. However in this test, only the self-generated LTE signal was used. Therefore, a second measurement campaign was performed in which the live LTE signals were recorded.

A.6.2 Measurements using live LTE network

After measurements using self-generated LTE signal, the target of the second campaign was to validate the performance of the measurement testbed and post-processing using live LTE signals, with inherited interference from other cells. The measurement equipment was put inside a university van and transported to rural location as shown on Figure A.11.

In this location the same set of tests as explained in the previous section were performed. 100 ms snapshots were recorded twice. In between two recordings, the antenna array was turned by 180^o. The array was again placed in the LoS conditions with respect to the base station located approximately 1.5 km away. Based on GPS coordinates of the van and the serving Base Station, it was determined that the expected angles are approximately 230^o for the first orientation of the array and 50^o in its second position. During the post-processing, the decoded serving Cell ID was carefully checked to belong

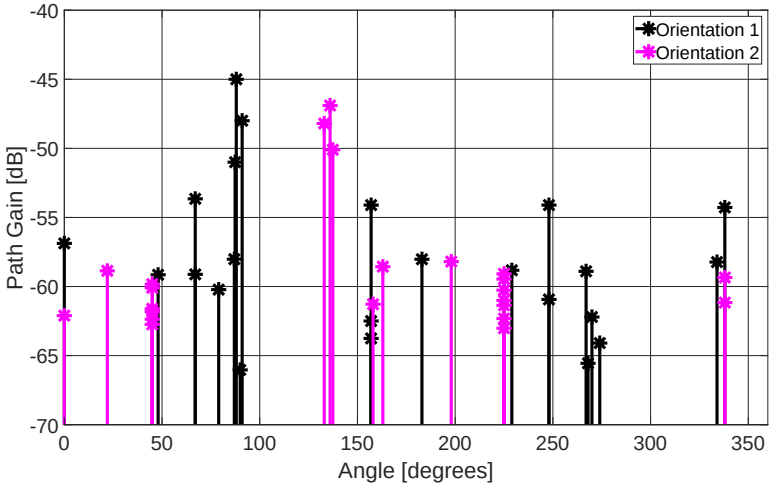

Fig. A.10: Estimated DoA of self-generated signal using SAGE

to the expected Base Station.

Figures A.12 and A.13 present the obtained results using beam sweep and SAGE respectively. Using both methods and for two considered orientations of the array the maximum SINR and path gain correspond to the expected angle. It is worth to notice that the computed SINR is much higher than in the first test using self-generated signal. Even though the distance from the receiver to the base station was much longer with respect to the first tests, the considerable increase of transmit power (real base stations transmit with power above 40 dBm while our transmitter was set only to 0 dBm) contributes to the increased SINR values. Contrary to the self-generated signal, as shown on Figure A.12, the SINR difference between its peak values at the expected DoAs and the values for other angles is much lower than in case of the self-generated signal. It is an expected behavior as even in a LoS scenario, due to distance between the transmitter and the receiver the level of multipath is higher than in the first experiment where a low power self-generated signal was transmitted only from 50 m distance.

Results obtained in this section show, that the proposed testbed and post-processing methodology can reliably be used for various research activities. First, they validate the correct reception and demodulation of real LTE signals, a fundamental step required before any further research activity can be conducted. The correct DoA estimation shows the robustness of the setup even in the presence of interfering signals coming from different cells further expanding the potential of the proposed testbed.

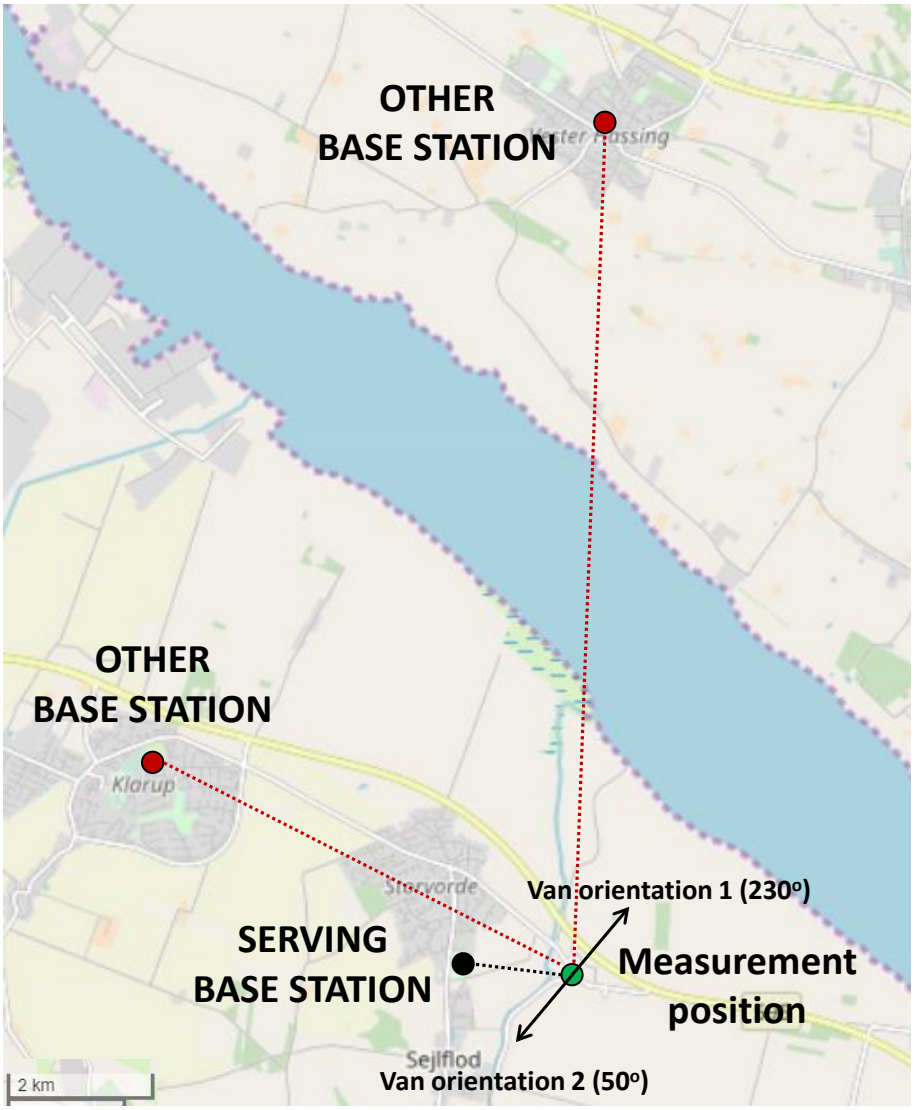

Fig. A.11: Location of the measurement campaign with real LTE signals

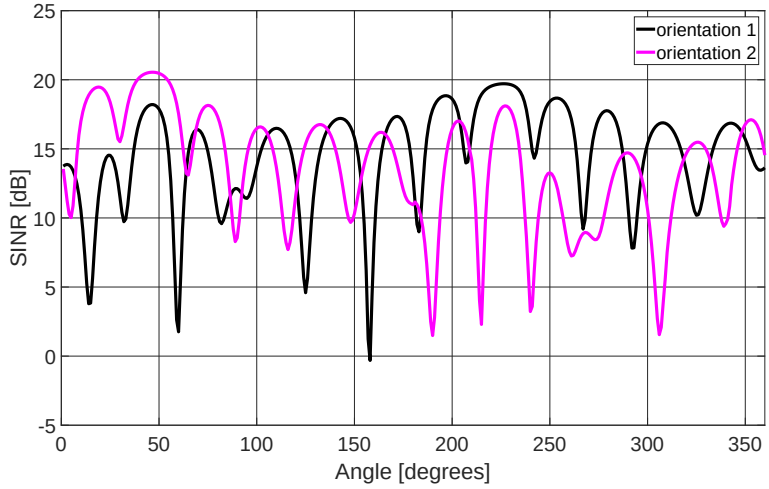

Fig. A.12: Angular distribution of SINR for real LTE signal

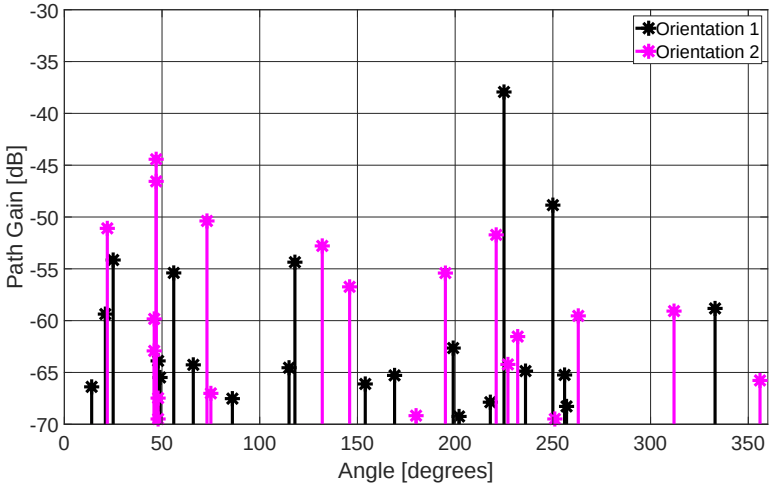

Fig. A.13: Estimated DoA of real LTE signal using SAGE

A.7 Potential applications of the measurement testbed

In this Section a set of possible options for testbed usage is discussed. Some of the applications are related to the already conducted research activities, while others are planned as a future work or are foreseen as new potential projects. The objective of this section is to give the reader a perspective on how the testbed can be used and to encourage a reflection on its other possible applications.

A.7.1 Conducted measurement campaigns

At the time of writing this article, the proposed testbed was already used by the authors in two different measurement campaigns. In the first campaign, related to studies of Vehicle-to-Network (V2N) communications, the described testbed was placed inside a car with the antenna array installed on its roof and multiple drive tests were performed in which more than 6000 snapshots were recorded in different environments. The recorded data was used for different research purposes.

First, for validating the performance of multi-antenna receivers: beamforming and MRC are studied in [29]. The study focuses on the downlink interference observed by a vehicle and its impact on beamforming and MRC performance. It is observed that, on average, the performance of both receivers is comparable. However, in the situations where there is one single dominant interferer coming from a specific direction, the use of receive beamforming can help mitigating this interference by steering the beam in the different direction and leads to an average 3 dB SINR improvement over the MRC receiver that performs diversity combining. Moreover, in post-processing by taking the signal from only one antenna stream and removing the remaining ones, the single antenna receiver is emulated and used in comparison with multi-antenna receivers to showcase the expected antenna processing gains.

The same dataset was processed using SAGE in [30]. The focus of this work is on experimental assessment of uplink beamforming on the vehicle terminal. In the first part, three different direction acquisition methodologies: beam sweeping, DoA estimation and naive beamforming towards the direct path to the serving cell are compared to understand the trade-off between their complexity and accuracy. It was determined that the beamforming direction obtained using beam sweeping methodology tends to lead to higher overall SINR than by using DoA estimation. Not surprisingly, in clear LoS scenarios, the DoA estimation leads to comparable SINR as naive beamforming towards the direct path to the serving cell.

In the second part of this study, after DoA estimation of each snapshot using SAGE, two different direction tracking algorithms are studied to understand their possible use to alleviate the frequency of time-consuming direction acquisition. By comparing the estimated DoA using SAGE with the prediction of the tracking algorithm, it was determined that in rural and suburban scenarios, the directions of incoming signals can be predicted without the need for performing any direction acquisition even for distances exceeding 1 km. Finally, the impact of 3-dB beamwidth of the antenna beam on the tracking algorithm's performance is studied.

The second measurement campaign conducted using the proposed setup was targeted to better understand propagation characteristics of the Air-to-Ground (A2G) channel between a cellular-connected UAV and a base station. As can be seen on Figure A.14, the proposed setup was placed inside a cage and lifted with a crane in order to record cellular signals in the air up to 40 m.

The work in [31] is related to spatial channel characterization of the A2G channel and targets the changes in the main path's DoA during the vertical flight of a UAV. Snapshots recorded at different heights are used as an input for SAGE to estimate DoAs of incoming signals. Moreover, by computing the Angular Spread (AS) of the incoming signals for different heights and measured environments, the authors study from which height one can assume that only the dominant LoS path between a Base Station and a UAV exists and the impact of multipath components can be neglected. Surprisingly, the results show that even 20 m above the roofs of the buildings, the multipath components still contribute to the overall received signal power and cannot be neglected.

Finally, in [28], similar to the previously described application, the very same snapshots recorded in the air were used to compare the performance of multi-antenna receivers in UAV scenarios. In contrast to the results obtained during the vehicular campaign, in the air the beamforming constantly outperforms MRC receiver. It is related to the fact that, comparing with ground, more often there is a dominant strong LoS path from the transmitter. When beamformed towards this direction, the MRC receiver can be outperformed.

A.7.2 Future work and other testbed applications

In the future work, the same recorded data snapshots can be further post-processed. So far only the conventional beamforming, pointing towards the estimated DoA was studied. Different beamforming algorithms, as for example, null-steering or side lobe level reduction techniques can be implemented to study their potential to mitigate the strongest interferers and therefore further improve the received SINR. Up to this point, the performed channel characterization for the A2G channel focused only on the spatial properties of the incoming signals. Contrary to the work in [27] other parameters in-

Fig. A.14: Designed testbed lifted in the air during measurement campaign focusing on a UAV A2G channel characterization

cluding Path Loss or delay spread were not yet examined and can be a part of a future work.

The proposed testbed and the described measurement activities are expected to be easily adjustable when the new 5^{th} Generation (5G) networks becomes widely available. As already described in the introduction, 5G with its new use cases will open the possibility for more studies on various channel and system-level functionalities. It is presumed that the proposed general design would remain valid and only the implementation specific parameters such as operating frequency (and therefore antenna array) or recorded bandwidth would have to be adjusted. In order to cope with large 5G bandwidths (up to 100 MHz), it may be necessary to replace the currently-used USRP boards with a model allowing to record larger bandwidths. In case the proposed post-processing method, based on the LTE toolbox, the complimentary 5G toolbox is already available and could potentially be used as a replacement.

Although the presented testbed was designed to receive the LTE signals (both self-generated and live from deployed customer networks), it may also be used to receive any kind of excitation signal provided the operating frequency and bandwidth are within the limits of the USRP boards and that the used antennas are suitable to receive signals from the target frequency band. This paves the way for a new variety of use cases. One example can be the experimental validation of channel charting algorithms [32]. The main concept of channel charting can be summarized as a user localization technique performed by the network, based only on the received estimated UL channel. If the signals are recorded with a multi-antenna system, the slowly changing features such as DoA can be estimated. Provided that many samples from different locations are recorded (and therefore multiple copies of estimated UL channel are obtained) several machine learning algorithms are used to map these slowly changing channel features into the precise estimation of user's position. By deploying an extra transmitter with a self-generated signal, the proposed multi-antenna testbed can be used to record these signals. Later in the post-processing the charting algorithms can be validated.

A.8 Conclusions

In this work a large multi-antenna measurement setup used to record multi-site cellular signals such as LTE is presented. It can be used for various research activities including multi-antenna channel characterization in the emerging use cases such as V2X or UAV communications. After hardware description, a calibration method required for phase alignment of USRPs is proposed and validated during measurement campaigns with self-generated LTE signals. Two post-processing methods were discussed using Matlab LTE

testbed for beamforming evaluation and SAGE for channel parameter estimation. Finally, results from measurement campaigns are discussed, where live LTE signals were recorded and used for DoA estimation using both SAGE and beam sweeping methodologies. The setup is shown to be a versatile tool, perfectly suitable to record signals incoming concurrently from multiple transmitters in situations where the same recorded raw I&Q samples can be used for many diverse research activities.

References

[1] A. Goldsmith, S. A. Jafar, N. Jindal, and S. Vishwanath, "Capacity limits of MIMO channels," *IEEE Journal on Selected Areas in Communications*, vol. 21, no. 5, pp. 684–702, June 2003.

[2] W. Wang, S. L. Capitaneanu, D. Marinca, and E. Lohan, "Comparative analysis of channel models for industrial IoT wireless communication," *IEEE Access*, vol. 7, pp. 91 627–91 640, 2019.

[3] M. Yang, B. Ai, R. He, L. Chen, X. Li, J. Li, B. Zhang, C. Huang, and Z. Zhong, "A cluster-based three-dimensional channel model for vehicle-to-vehicle communications," *IEEE Transactions on Vehicular Technology*, vol. 68, no. 6, pp. 5208–5220, June 2019.

[4] B. V. Der Bergh, A. Chiumento, and S. Pollin, "LTE in the sky: trading off propagation benefits with interference costs for aerial nodes," *IEEE Communications Magazine*, vol. 54, no. 5, pp. 44–50, May 2016.

[5] *"WINNER II Channel Models"*, September 2007, iST-4-027756 WINNER II D1.1.2 V1.2.

[6] D. A. Wassie, I. Rodriguez, G. Berardinelli, F. M. L. Tavares, T. B. Sørensen, T. L. Hansen, and P. Mogensen, "An agile multi-node multi-antenna wireless channel sounding system," *IEEE Access*, vol. 7, pp. 17 503–17 516, 2019.

[7] G. G. Joshi, C. B. Dietrich, and W. L. Stutzman, "Adaptive beamforming measurements using four-element portable and mobile arrays," *IEEE Transactions on Antennas and Propagation*, vol. 53, no. 12, pp. 4065–4072, December 2005.

[8] "Matlab LTE system toolbox reference page," https://ch.mathworks.com/products/lte-system.html, 2017.

[9] B. H. Fleury, D. Dahlhaus, R. Heddergott, and M. Tschudin, "Wideband angle of arrival estimation using the SAGE algorithm," in *IEEE 4th International Symposium on Spread Spectrum Techniques and Applications Proceedings*, vol. 1, September 1996, pp. 79–85.

[10] C. M. Simmonds and M. A. Beach, "Downlink calibration requirements for the TSUNAMI (II) adaptive antenna testbed," in *Ninth IEEE International Symposium on Personal, Indoor and Mobile Radio Communications*, vol. 3, September 1998, pp. 1260–1264.

[11] R. Wang, C. U. Bas, O. Renaudin, S. Sangodoyin, U. T. Virk, and A. F. Molisch, "A real-time MIMO channel sounder for vehicle-to-vehicle propagation channel at 5.9 GHz," in *2017 IEEE International Conference on Communications (ICC)*, May 2017, pp. 1–6.

[12] C. Scarborough, K. Venugopal, A. Alkhateeb, and R. W. Heath, "Beamforming in millimeter wave systems: Prototyping and measurement results," in *2018 IEEE 88th Vehicular Technology Conference (VTC-Fall)*, August 2018, pp. 1–5.

[13] R. M. Rao, Wiejun Zhu, S. Lang, C. Oberli, D. Browne, J. Bhatia, J. Frigon, Jingming Wang, P. Gupta, Heechoon Lee, D. N. Liu, S. G. Wong, M. Fitz, B. Daneshrad, and O. Takeshita, "Multi-antenna testbeds for research and education in wireless communications," *IEEE Communications Magazine*, vol. 42, no. 12, pp. 72–81, December 2004.

[14] Y. Amano, T. Inoue, and H. Shinonaga, "Performances of beamforming in downlink with smart antenna testbed," in *Proceedings IEEE 56th Vehicular Technology Conference*, vol. 1, September 2002, pp. 77–81.

[15] K. Nishimori, R. Kudo, N. Honma, Y. Takatori, O. Atsushi, and K. Okada, "Experimental evaluation using 16 x 16 multiuser MIMO testbed in an actual indoor scenario," in *2008 IEEE Antennas and Propagation Society International Symposium*, July 2008, pp. 1–4.

[16] Ó. Gonzalez, D. Ramírez, I. Santamaria, J. A. García-Naya, and L. Castedo, "Experimental validation of interference alignment techniques using a multiuser MIMO testbed," in *2011 International ITG Workshop on Smart Antennas*, February 2011, pp. 1–8.

[17] R. Weinmann, M. Tangemann, S. Fritsch, and C. Hoek, "Beamforming performance measurements in a DCS 1800 smart antenna testbed," in *VTC '98. 48th IEEE Vehicular Technology Conference. Pathway to Global Wireless Revolution (Cat. No.98CH36151)*, vol. 2, May 1998, pp. 1024–1028.

[18] J. M. V. Burgos, E. Gago-Cerezal, V. A. Gracia, and L. M. C. Cervera, "DEMIURGO, an SDR testbed for distributed MIMO," in *2006 3rd International Symposium on Wireless Communication Systems*, September 2006, pp. 210–213.

[19] W. Xiong, J. Lu, X. Tian, G. Chen, K. Pham, and E. Blasch, "Cognitive radio testbed for digital beamforming of satellite communication," in *2017 Cognitive Communications for Aerospace Applications Workshop (CCAA)*, June 2017, pp. 1–5.

[20] J. Vieira, S. Malkowsky, K. Nieman, Z. Miers, N. Kundargi, L. Liu, I. Wong, V. Öwall, O. Edfors, and F. Tufvesson, "A flexible 100-antenna testbed for massive MIMO," in *2014 IEEE Globecom Workshops (GC Wkshps)*, December 2014, pp. 287–293.

[21] P. Harris, W. B. Hasan, S. Malkowsky, J. Vieira, S. Zhang, M. Beach, L. Liu, E. Mellios, A. Nix, S. Armour, A. Doufexi, K. Nieman, and N. Kundargi, "Serving 22 users in real-time with a 128-antenna massive MIMO testbed," in *2016 IEEE International Workshop on Signal Processing Systems (SiPS)*, October 2016, pp. 266–272.

[22] D. Gaydos, P. Nayeri, and R. Haupt, "Experimental demonstration of a software-defined-radio adaptive beamformer," in *2018 48th European Microwave Conference (EuMC)*, September 2018, pp. 1581–1584.

[23] P. Nayeri and R. L. Haupt, "A testbed for adaptive beamforming with software defined radio arrays," in *2016 IEEE/ACES International Conference on Wireless Information Technology and Systems (ICWITS) and Applied Computational Electromagnetics (ACES)*, March 2016, pp. 1–2.

[24] N. Tayem, M. Omer, and A. A. Hussain, "Hardware implementation of MUSIC and ESPRIT on NI-PXI platform," in *2014 IEEE Military Communications Conference*, October 2014, pp. 329–332.

[25] B. Rares, C. Codau, A. Pastrav, T. Palade, H. Hedesiu, B. Balauta, and E. Puschita, "Experimental evaluation of AoA algorithms using NI USRP software defined radios," in *2018 17th RoEduNet Conference: Networking in Education and Research (RoEduNet)*, September 2018, pp. 1–6.

[26] M. Willerton, D. Yates, V. Goverdovsky, and C. Papavassiliou, "Experimental characterization of a large aperture array localization technique using an SDR testbench," in *Wireless Innovation Forum Conference on Communications Technologies and Software Defined Radio (SDR?11-WInnComm)*, 2011.

[27] X. Cai, J. Rodríguez-Piñeiro, X. Yin, N. Wang, B. Ai, G. F. Pedersen, and A. P. Yuste, "An empirical air-to-ground channel model based on passive measurements in LTE," *IEEE Transactions on Vehicular Technology*, vol. 68, no. 2, pp. 1140–1154, February 2019.

[28] T. Izydorczyk, M. Bucur, F. M. L. Tavares, G. Berardinelli, and P. Mogensen, "Experimental evaluation of multi-antenna receivers for UAV Communication in Live LTE networks," in *2018 IEEE Globecom Workshops (GC Wkshps)*, December 2018, pp. 1–6.

[29] T. Izydorczyk, F. M. L. Tavares, G. Berardinelli, M. Bucur, and P. Mogensen, "Performance evaluation of multi-antenna receivers for vehicular communications in live LTE networks," in *2019 IEEE 89th Vehicular Technology Conference (VTC2019-Spring)*, April 2019, pp. 1–6.

[30] T. Izydorczyk, G. Berardinelli, F. M. L. Tavares, M. Bucur, and P. Mogensen, "On the potential of uplink beamforming in vehicular networks based on experimental measurements," in *2019 IEEE 90th Vehicular Technology Conference (VTC2019-Fall)*, September 2019, pp. 1–5.

[31] T. Izydorczyk, F. M. L. Tavares, G. Berardinelli, M. Bucur, and P. Mogensen, "Angular distribution of cellular signals for UAVs in urban and rural scenarios," in *2019 13th European Conference on Antennas and Propagation (EuCAP)*, March 2019, pp. 1–5.

[32] C. Studer, S. Medjkouh, E. Gönültas, T. Goldstein, and O. Tirkkonen, "Channel charting: Locating users within the radio environment using channel state information," *IEEE Access*, vol. 6, pp. 47 682–47 698, 2018.

Paper B

Experimental evaluation of multi-antenna receivers for UAV communication in live LTE networks

Tomasz Izydorczyk, Mădălina Bucur, Fernando M. L. Tavares,
Gilberto Berardinelli and Preben Mogensen

The paper has been published in the
IEEE GLOBECOM workshops proceedings, 2018.

The layout has been revised.

Abstract

Unmanned Aerial Vehicle (UAV) communication is known to suffer from significant interference due to the clearance of the radio paths with ground base stations. Multi-antenna receive combining has the promise of alleviating the impact of interference, translating to improved connectivity performance. In this paper, we evaluate the performance of Conventional Beamforming (CB) and Maximum Ratio Combining (MRC) receivers for UAV communication based on live Long Term Evolution (LTE) networks. Our measurement setup consists of nine Universal Software Radio Peripheral (USRP) boards and a circular antenna array with sixteen elements. The LTE signals are recorded at different UAV flight heights in urban environments, and processed offline. Results show similar Signal-to-Interference-plus-Noise Ratio (SINR) performance by MRC and CB, with CB slightly outperforming MRC provided knowledge of LTE signal structure is used for the beam selection. No significant dependency from the flight height has been observed. The outage probability analysis further emphasizes the benefits of using CB in the studied scenarios.

B.1 Introduction

The use of Unmanned Aerial Vehicles (UAV), commonly referred to as 'drones', is expected to grow rapidly in the next few years, fueled by multiple new use cases. In [1], the authors indicate different data traffic patterns which characterize UAV-ground communication links. Many surveillance applications will require extra uplink capacity to transmit video feeds from cameras installed on a UAV [2]. On the other hand, ground-to-UAV communication, traditionally referred as downlink, will be largely dominated by Communication and Control (C2) messages, which can be characterized as a low-throughput messages containing commands for UAV flight path alternation.

Cellular networks such as Long Term Evolution (LTE) are considered a promising solution for future UAV communication, due to their widespread coverage and instantaneous availability. The potential of LTE in the context of UAV communication was recognized by the Third Generation Partnership Project (3GPP) and a study item [3] was created. However, cellular networks are optimized for terrestrial communications. Relevant parameters such as antenna down-tilt or power control settings are set with the aim of maximizing the performance of ground-level communications.

Since it is not provisioned to change cell-wide settings, research activity focused on assessing the quality of UAV communication over existing cellular networks. In [4] and [5], the radio channel characterization based on experimental measurement campaigns was studied with particular focus on path loss modeling. It has been observed that at sufficiently high UAV flight altitudes, the propagation becomes more similar to free-space. This is due to

the more probable Line-of-Sight (LOS) link between Base Station (BS) and the UAV. However, as shown in [6], the Signal-to-Interference-plus-Noise Ratio (SINR) observed by UAVs is significantly lower in comparison to the terrestrial User Equipment (UE) given the LOS conditions on the vast majority of interfering links. This problem was further addressed in [7] and [8] where analytical models for interference and coverage were developed.

Multiple research activities have focused on interference mitigation schemes for UAVs. Physical layer techniques, such as beamforming and multi-antenna received signal combining, are expected to improve the SINR levels experienced by UAVs. In [9], the authors show promising simulation results of interference mitigation using different multi-antenna techniques including narrow beam antenna selection and Interference Rejection Combining (IRC).

As multiple analytical attempts to quantify and combat the interference impact were made, only a few experimental studies were performed. Studies based on real network measurements can help mitigate the simulation bias and assess the problem in real propagation conditions. Very often they allow to detect previously unforeseen problems and effects overlooked in simulation assumptions. In [10], authors discuss the impact of non-ideal antenna pattern and time-variant UAV orientation on UAV connectivity using IEEE 802.11 network. In [11], authors experimentally quantify the uplink interference introduced to the network by the UAV. Based on the input from the network operator, they estimate the interference caused by their UAVs constantly transmitting the uplink data to the network. Those interference levels were later used in [12] to simulate the performance of interference cancellation schemes using an ideal IRC receiver.

Even though these studies showed the potential of the multi-antenna techniques, the methodology used within cannot fully reflect their performance in a real network. In the existing literature, the experimental input is indeed limited to the interference power levels, and receiver performance is still evaluated by assuming ideal knowledge of the radio channel responses of the received signals. This may severely bias the estimated outcome of the studied receivers. A workaround to this problem is to test the multi-antenna techniques directly on recorded live network signals to quantify their actual benefits.

In this work, we experimentally evaluate the performance of multi-antenna techniques at UAV flight heights, based on live Long Term Evolution (LTE) cellular signals. In view of recorded I/Q samples from live cellular networks, the link performance of Maximum Ratio Combining (MRC) and Conventional Beamforming (CB) techniques is compared with single antenna UAV links. By using Universal Software Radio Peripheral (USRP)-based setup and offline signal processing, we measure the average SINR of different LTE control channels and use it as a metric to compare single antenna links to MRC and CB using multiple beam selection strategies. Further, we also study the

performance in low-SINR regime, by discussing the applicability of multi-antenna techniques for ensuring uninterrupted connectivity.

The rest of the paper has the following structure. In Section B.2 the measurement methodology is described. This is followed by the description of the post-processing method in Section B.3. Section B.4.1 discusses the levels of interference experienced at the UAV. This section is followed by Section B.4.2, where the performance of multi-antenna techniques is studied. The work is concluded with Section B.5.

B.2 Measurement Methodology

B.2.1 Hardware setup

The measurement setup consists of a sixteen-antennas uniform circular array, which is connected with eight fully synchronized and calibrated USRP boards. Each of the boards is equipped with two receiver (RX) chains. The boards are then connected to a PXI-8820 controller using a PXIe-1085 chassis which acts as a data hub. On Figure B.1, the block diagram of the setup is presented. The main advantage of using USRPs and the PXI controller is the possibility to record a large amount of data without any real-time processing. UAV-based setups are usually power-limited and due to payload limitations their usage is reduced to the simple scanner-like measurements. By using our setup, measured samples can later be used as input in a wide range of activities ranging from channel propagation studies to advanced transceiver design.

Antenna array

Sixteen monopole antennas disposed in an uniform circular array were manufactured to record signals from the downlink (DL) part of LTE Band 3 used by two Danish network operators (center frequencies of 1.815 GHz and 1.87 GHz). They are installed on an aluminum ground plane and are connected to the USRP boards using three-meter-long RG233 cables.

Although it is highly unlikely that first autonomous UAVs will be equipped with many antennas, by using this amount one can set the focus on the comparison among different receiver techniques in their upper-bound performance limits. It is worth mentioning that due to raw signal recordings, in Section B.4.2 the performance of MRC with reduced number of antennas is also studied by simply discarding the data recorded by some of the antennas.

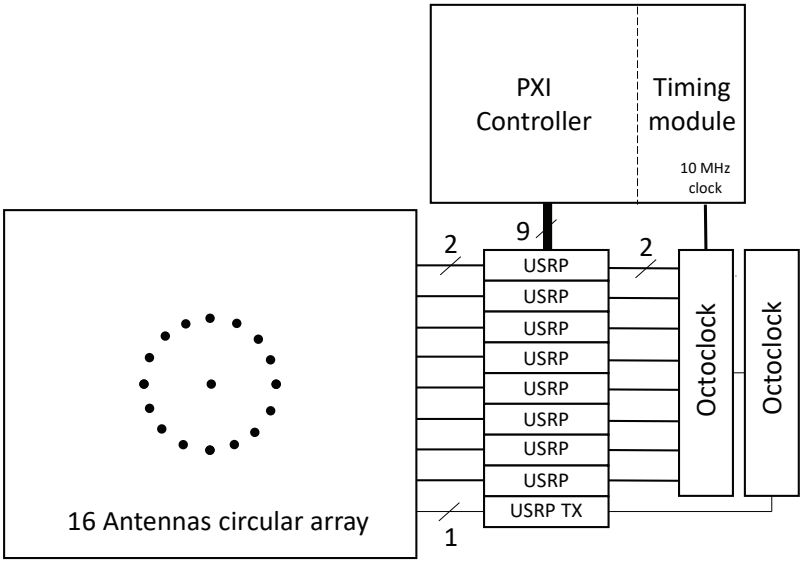

Fig. B.1: Measurement setup schematic

USRP and PXI controller

Eight USRP 2953R boards are used to record the LTE DL Band 3 signals at 40 MS/s. They perform digital down conversion and stream the I/Q samples via fast Peripheral Component Interconnect (PCI) bus to the PXI controller. To ensure the perfect time/frequency alignment among the eight boards, the external 10 MHz clock is generated by the timing module NI PXIe-6674T and redistributed to all boards by two Octoclocks CDA-2990.

Since digital beamforming algorithms require alignment in both frequency and phase, a calibration procedure for the receiving USRPs is required. Another USRP board is used for transmission of a single-tone out-of-band signal from the antenna placed at the center of the array. Given the omni-directional radiation pattern, all sixteen antennas receive the calibration tone at the same time and with the same phase. By using one of the antennas as a reference, the random phase offset of each USRP can be compensated.

Assembled setup

The described setup was assembled in a metal structure and was safely lifted using a crane as presented in Figure B.2. The antenna array was attached to the structure and covered by a hemisphere radome to prevent any short-circuit in case of rain. The radome was tested to be transparent for the radio waves at the measured frequency.

B.2.2 Measurement campaign

Seven different locations in Aalborg, Denmark were selected for the measurements: three in the city center (surrounded by tall buildings with average height 20 m and multiple BS), one in the suburbs (surrounded by houses and limited number of BS), one in a rural area (with limited coverage and interference levels) while the remaining two in the industrial part of the city. Combined altogether, they provide a set of diverse propagation environments observed by flying UAV.

In each location, the designed setup was lifted using the crane up to a 40 m height. Starting from the ground, 100 ms snapshots of LTE signals were taken every 5 m. On average, eight snapshots were recorded for each of the two network operators at each height. To avoid the possible signal blockage due to the existence of the metal cage and the ground plane, half of the measurements were taken with the antenna array pointing downwards (as can be seen at the right side of Figure B.2) while another half with the array pointing upwards. There were on average 156 snapshots taken per location.

Fig. B.2: Assembled setup lifted to 40 meters high by a crane (left) and zoomed (right)

B.3 Post-processing

The performance of CB and MRC is studied in the post-processing. The case of a UAV equipped with a single antenna receiver processing is also included as a benchmark. Other techniques, such as IRC and advanced beamforming (with for example multiple beams or null-steering), are left for future work. The total number of 1069 snapshots are independently processed as

presented in Figure B.3. The signal received by each antenna is phase shifted to compensate for the random phase offset introduced by each USRP board. Further processing depends on the receiver technique and is described in the next subsections.

The following notation is used. The received and phase-calibrated N_{RX} input data streams are collected in a matrix $\mathbf{S}$ of size $[N_{RX} \times N_{samp}]$, where $N_{samp} = 4 \cdot 10^6$ corresponds to the number of recorded samples. $\mathbf{y}_i$ is the resulting vector of size $[1 \times N_{samp}]$ after beamforming operation on signal $\mathbf{S}$ and r is the single complex number after equalization of various LTE physical channels.

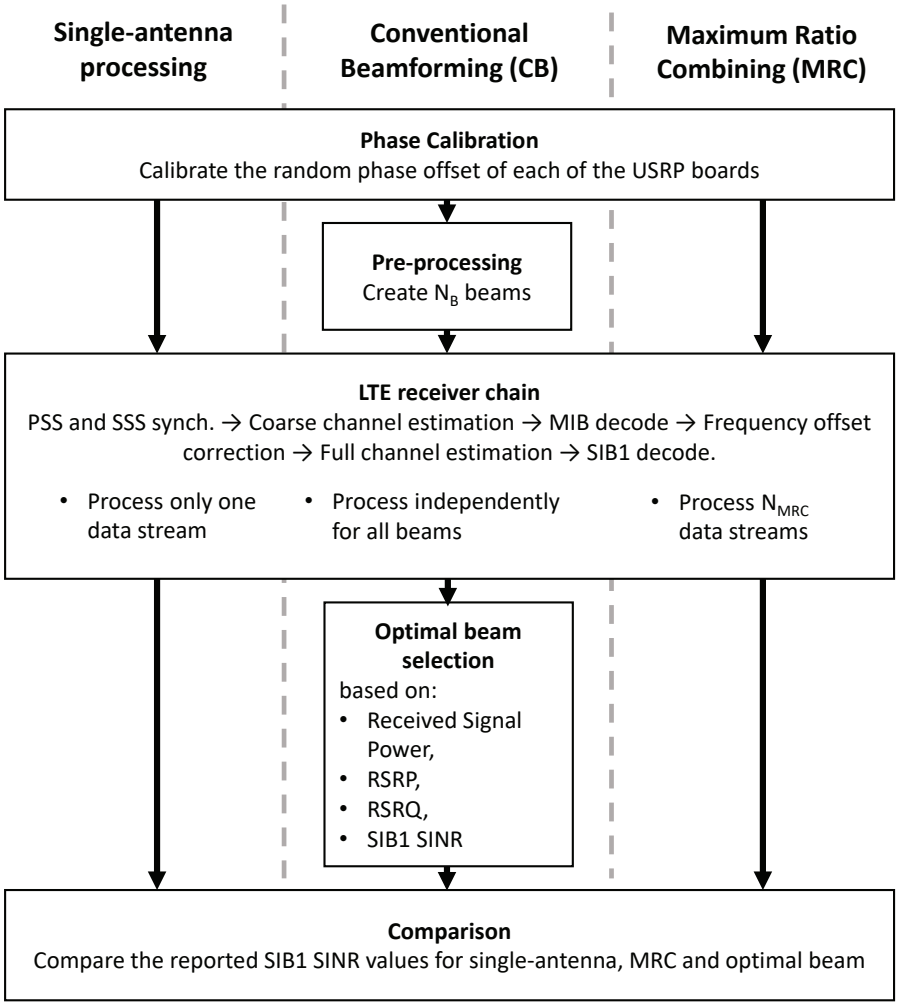

Fig. B.3: Post-processing flow chart

B.3.1 Single-antenna receiver

After phase calibration, only the first row ($N_{RX} = 1$) of the recorded data matrix $\mathbf{S}$ is processed by the LTE receiver which is designed based on the Matlab LTE toolbox. The reception methodology follows the procedure implemented in a typical LTE UE. First, the received signal is downsampled to 1.92 MHz and synchronization to the network is performed based on the LTE Primary and Secondary Synchronization Signals (PSS and SSS). The correlation between all 504 Physical Cell Identities (PCIs) and received signal is computed. After frame offset correction, attachment is made to the cell with the strongest power at the output of the correlator.

In the next step, after synchronization and coarse channel estimation based on the synchronization signals, Physical Broadcast Channel (PBCH) containing Master Information Block (MIB) is equalized using a matched filter. After MIB decoding information on the bandwidth of the LTE signal is retrieved. This information is used to resample the signal to the sampling rate matching the given bandwidth. Later, the frequency offset is estimated and corrected, which is followed by the estimation of the channel matrix over the entire operational bandwidth based on the Cell-specific Reference Signals (CRS). From the estimated channel matrix the Reference Signal Received Power (RSRP) and the Reference Signal Received Quality (RSRQ) are computed following the 3GPP specifications [13].

Finally, provided sufficient signal quality, the LTE receiver attempts to decode the System Information Block 1 (SIB1) using as before a matched filter for the detection of Physical Downlink Shared Channel (PDSCH). If successful, the Error Vector Magnitude (EVM) and SINR of this control channel are computed. Due to the length of the recorded snapshot, there are on average five instances of SIB1 message in each of them. The computed SINR values are averaged and a single value per snapshot is reported. Due to the averaging and different SIB1 locations in the time-frequency grid among different cells, the effect of the different cell loads of the network can be captured.

B.3.2 Conventional beamforming receiver

To evaluate the performance of beamforming, in pre-processing, $N_b = \{16, 360\}$ beams pointing towards different azimuth and elevation angles are created and the received signal impinging the array is weighted by each of these beams. The resulting signals $\mathbf{y}_i$ are independently decoded at the receiver for each created beam $i \leq N_b$. Later, after the receiving process is done for all of the beams, the optimal one is selected, while others are discarded. CB is used to create a beam with the half-power beamwidth equal to 22.5^o.

The received and phase-calibrated input data streams $\mathbf{S}$ are weighted as below:

$$\mathbf{y}_i = \left(e^{-2\pi j \frac{r}{\lambda}\cos(\varphi_i)\cos(\theta_i - \boldsymbol{\theta})}\right)^H \cdot \mathbf{S} \tag{B.1}$$

where θ_i and φ_i refer to the azimuth and elevation angle for a given beam i, r is the radius of the antenna array equal 20 cm, λ is the wavelength equal to 0.1652 m or 0.1603 m for two network operators and $\boldsymbol{\theta}$ is the antenna position-dependent column vector of angles of size $[N_{RX} \times 1]$. $(\cdot)^H$ denotes the hermitian operator.

After beamforming, all the $\mathbf{y}_i$ beams are processed identically by the LTE receiver as a single-antenna stream. The next step is to decide which of the created beams should be used by the receiver for further processing of the data channels. The so-called *optimal beam* is the beam which maximizes the UE performance quantified by one of the various metrics. Given the near real-time requirements and UAV power constraints, the following metrics for selecting the optimal beam, varying with receiver complexity are investigated:

- **Received signal power:** This is the simplest and least computationally-heavy metric proposed. The receiver computes the power level M_i of the beamsteered input signal before the LTE receiver for each of the beams i, based on the given formula:

$$M_i = 10 \cdot \log_{10}\left(|\mathbf{y}_i|^2\right) \tag{B.2}$$

- **RSRP**: After the channel estimation for all of the beams, their respective RSRP is computed. Since this metric is constantly measured by the ground-level UE to assess the quality of the signal from the attached and neighbor cells (for the handover procedure), its use does not require any additional processing. The metric can be written as: $M_i = RSRP_i$.

- **RSRQ**: The optimal beam is the beam which maximizes the RSRQ metric. The difference between using RSRP and RSRQ metrics lies in the fact that RSRQ accounts for the existence of interference while RSRP does not. The metric is therefore: $M_i = RSRQ_i$.

- **SIB1 SINR**: This is the most computationally-heavy method requiring long LTE Receiver processing to estimate the SIB1 SINR: $M_i = SINR_i$.

The optimal beam B_{opt} is the beam which maximizes the given metric as below:

$$B_{opt} = argmax_{i=1:N_b} M_i \tag{B.3}$$

After selection of the optimal beam, processing is ultimated and other beams are discarded.

B.3.3 MRC receiver

After phase calibration, a subset of signals received from N_{MRC} antennas (with $2 \leq N_{MRC} \leq 16$) is processed. Upon time and frequency offsets estimation, the receive combining is performed as follows:

$$r = (\mathbf{h}^H \mathbf{h})^{-1} \mathbf{h}^H \mathbf{x} \tag{B.4}$$

where $\mathbf{x}$ denotes the $[N_{MRC} \times 1]$ vector of a received resource element over the N_{MRC} antennas, $\mathbf{h}$ is the corresponding estimated channel vector, and r is the resultant estimated data symbol. Note that (B.4) is applied for both MIB and SIB detection. The remaining operations follow the steps of the single antenna receive processing.

B.4 Performance analysis

B.4.1 Single antenna performance from a UAV's perspective

Before the evaluation of multi-antenna techniques, the performance of a single antenna receiver is analyzed to show the signal degradation experienced by the UAV as it takes off to the air. The analysis is performed over all the recorded snapshots.

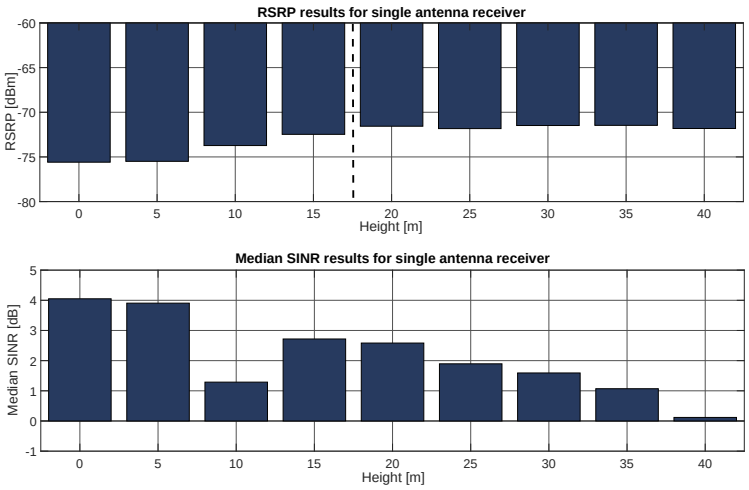

Fig. B.4: Median RSRP and SINR values of a single antenna receiver against height

Figure B.4 depicts the reported median RSRP and SINR values considering all the recorded locations for the single antenna receiver. As expected, as the height increases, the received signal becomes strongly affected by interference resulting in a SINR drop from 4 dB at the ground level up to 0 dB

at 40 m. The sudden SINR drop was observed at about 10 m. This may be due to the UAV leaving the BS's main beam, which is pointed downwards towards the ground. At higher heights, with increased radio clearance, this issue is mitigated by reception of signal from a different BS.

RSRP results allow to notice a distinct behavior. It can be observed that there is a separation of the results, based on height. From ground level to approximately 15 m, the RSRP values vary and increase with height from -76 to -72 dBm. After reaching 20 m - the average height of buildings in Aalborg, the reported RSRP stabilizes at around -72 dBm. This behavior was used to split the recorded snapshots into two groups, indicated by the dashed line on the figure: *take-off zone* with limited interference (0 - 15 m) and *low flight level zone* with increased interference levels (20 - 40 m).

B.4.2 Performance evaluation of multi-antenna receivers

All the results presented next are based on measurements collected from all locations for the aforementioned sets of heights. There was no significant difference in the observed receiver performance depending on the recorded location. Implicitly, the same data set was used for all the receiver types considered in this paper. The usage of SINR gains as a metric for the comparison is therefore feasible.

MRC with 2, 4, 8 and 16 antennas array

First, the gain of the MRC considering the different number of antenna elements with respect to the single antenna case is analyzed. As already mentioned, the processing is performed over subsets of the received signals.

Figure B.5 shows a clear improvement in the receiver's performance as the number of elements is increased. In the take-off zone, by adding only a second antenna a gain of 2.5 dB is observed, while the sixteen-antennas array provides a gain of 7.1 dB. However by adding more antenna elements, the additional gain decreases rapidly to only 1.1 dB. The observed array gains are also significantly lower with respect to the theoretical ones computed as $G_{array} = 10 \cdot \log_{10}(N_{RX})$. As an example, theoretical array gain G for $N_{RX} = 16$ number of elements is 12 dB and is 4.9 dB higher than the measured one. Both phenomena are the result of the observed interference on the CRS which affects the quality of the channel estimation. With an increased number of received antennas, the estimation error becomes more significant resulting in a lower-than-expected gain. It is expected that by replacing the least square channel estimator with a more advanced method, the performance gain can be slightly improved.

Very little difference was noted while comparing the SINR gains for the take-off and low level flight zones. Even with increased interference levels

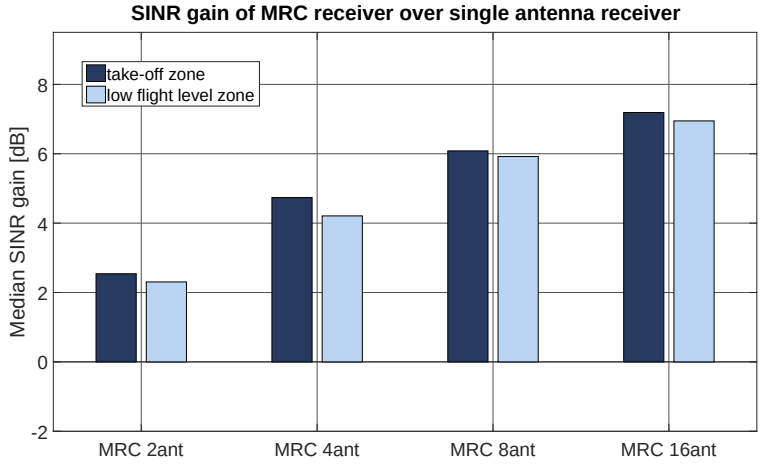

Fig. B.5: Comparison of median SINR gains of MRC over a single antenna receiver

at the higher heights, the overall performance drop of MRC was comparable with the respective performance drop of a single antenna receiver resulting in a comparable gain. In the worst case, for the four-antenna receiver a drop of 0.5 dB was observed.

Conventional beamforming

Second study considered the performance gains of using the CB for UAV communications. The simple strategy, where $N_b = 360$ beams are uniformly spaced only in the azimuth plane assuming $\varphi = 0^o$ elevation angle was studied. Figure B.6 shows the obtained performance gains with respect to a single antenna receiver, considering the beam selection criteria as described in Section B.3.2. The gain of MRC with sixteen antennas was added as a reference. In an upper-bound case of a beam-selector using an optimal SINR method, gains of 9.46 dB over a single antenna receiver and 2.52 dB over MRC were observed.

Surprising results were observed by looking at the performance of different beam-selectors. Using the received signal power as selection criterion provides the smallest gain among the considered cases. This gain is relatively similar to the one using RSRP as a beam selector, even though the latter exploits the structure of the LTE signal. Only if metrics with knowledge of interference are exploited (RSRQ or SINR), the observable gains are higher than the MRC ones. Lastly, it can be observed that the performance gains are higher for low flight level zone than the gains that can be attained at the take-off zone. CB technique appears to benefit in scenarios where the LOS

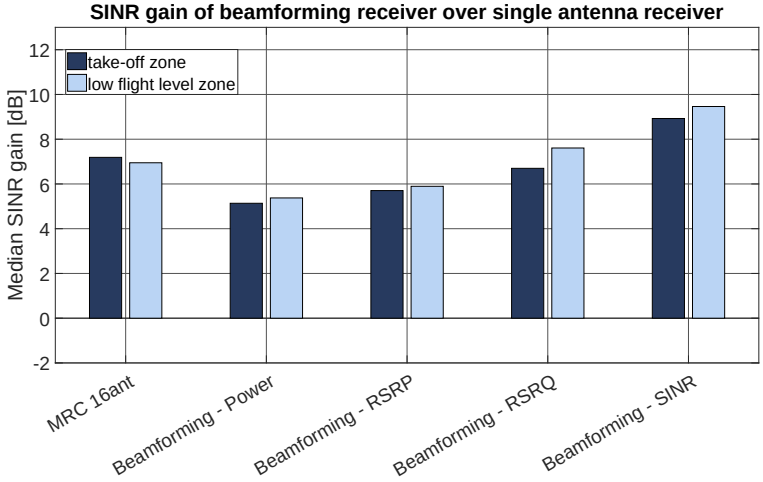

Fig. B.6: Comparison of beamforming gains over a single antenna receiver

path exists regardless of increased interference levels.

Other beam steering strategies were also considered. A performance gain of less than 0.1 dB was observed if beamforming was done considering different elevation angles φ (at a below 1^o resolution). An average performance drop of approximately 12% was observed if the number of possible beams N_b was reduced to sixteen, although the similar trends between different selectors as on Figure B.6 were observed. This was expected as the subspace covered by the beams was reduced. However, it can be argued that the performance loss is negligible comparing with the reduced complexity of the beamformer.

From a receiver perspective, the reported values for RSRP and RSRQ are already available and their use as beam selection criteria is straightforward. Even better performance can be achieved by using SIB1 SINR reported values, but this information is not as easily accessible to the receiver, as are the RSRP and RSRQ measurements. It requires the receiver to perform decoding of additional physical channels to attain it, which requires considerable processing time.

To complement this study, Figure B.7 presents how the optimal elevation angle changes with the height. As expected, in the take-off zone the optimal elevation angles are significantly higher than above the rooftops where signals are usually coming with low elevation angle. These findings can potentially justify the beam-steering only within an azimuth plane, thus reducing receiver complexity.

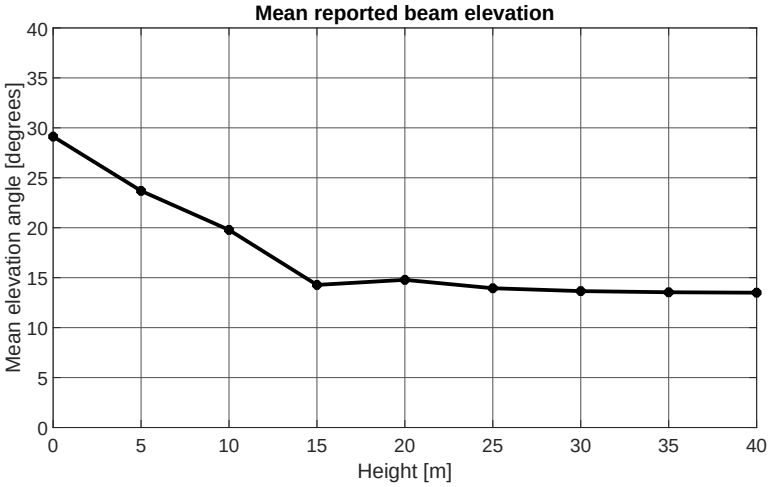

Fig. B.7: Measured optimal elevation angle

Outage comparison

One of the most important aspects of UAV connectivity is its reliability. In case of very low SINR, there may be no connection between BS and UAV, referred later as an *outage*, which can result in a life-threatening accident. In this work, a snapshot is defined to be in outage, if none of the SIB1 messages was decoded correctly. Implicitly, outage also occurs in all cases when MIB decoding failed.

In all previous studies, snapshots detected to be in outage were assigned a fixed low SINR value, such that their effect was captured in the median calculation. Figure B.8 presents the percentage of snapshots being in outage regardless of the measured height. The 6.4% (68 out of 1069) of snapshots processed using a single antenna were not decoded correctly. By using any of the multi-antenna techniques, this value can be greatly decreased. Surprisingly, beamforming techniques can help to further reduce the outage percentage compared to MRC. As beamforming is being done before any LTE processing, by co-phasing the received signal, the robustness of PSS/SSS synchronization is improved and number of outages further reduced. There were no outages reported for CB case with SINR used as a beam selector. This indicates that for all snapshots, there is at minimum one beam ensuring network connectivity and the observed outage is not related to limited received signal strength.

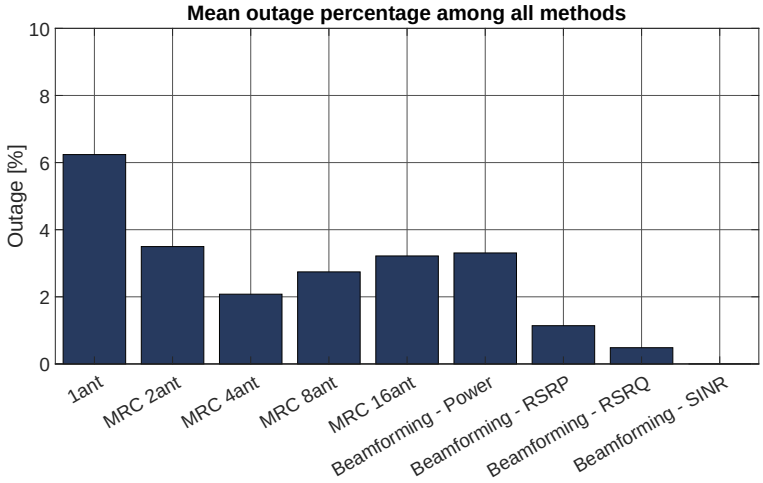

Fig. B.8: Percentage of outage calculated for all methods

B.5 Conclusions

In this work, the performance of multi-antenna receiver techniques for UAV communications was studied. Due to the interference resulting in imperfect channel estimation, the observed gains of MRC were lower than theoretical and saturated with increased number of antennas. Beamforming methods are promising alternatives to the MRC. They outperform MRC if LTE channel knowledge is exploited and provide similar gain also when a limited number of beams is considered. Surprisingly, height dependency has a very little impact on the observed performance, with similar results observed at both take-off and low height flying zones. It is expected that the observed changes can become more significant at an increased flight height.

Acknowledgment

This work has been supported by the cooperative project VIRTUOSO, partially funded by Innovationsfonden Denmark.

References

[1] S. Hayat, E. Yanmaz, and R. Muzaffar, "Survey on unmanned aerial vehicle networks for civil applications: A communications viewpoint," *IEEE Communications Surveys Tutorials*, vol. 18, no. 4, pp. 2624–2661, 2016.

[2] S. Qazi, A. S. Siddiqui, and A. I. Wagan, "UAV based real time video surveillance over 4G LTE," in *2015 International Conference on Open Source Systems Technologies (ICOSST)*, Dec 2015, pp. 141–145.

[3] "Study on enhanced LTE support for aerial vehicles (release 15)," 3GPP, Tech. Rep. TR 36.777 V0.4.0, November 2017.

[4] A. Al-Hourani and K. Gomez, "Modeling cellular-to-UAV path-loss for suburban environments," *IEEE Wireless Communications Letters*, vol. 7, no. 1, pp. 82–85, Feb 2018.

[5] R. Amorim, H. Nguyen, P. Mogensen, I. Z. Kovács, J. Wigard, and T. B. Sørensen, "Radio channel modeling for UAV communication over cellular networks," *IEEE Wireless Communications Letters*, vol. 6, no. 4, pp. 514–517, Aug 2017.

[6] B. V. D. Bergh, A. Chiumento, and S. Pollin, "LTE in the sky: trading off propagation benefits with interference costs for aerial nodes," *IEEE Communications Magazine*, vol. 54, no. 5, pp. 44–50, May 2016.

[7] M. Mozaffari, W. Saad, M. Bennis, and M. Debbah, "Unmanned aerial vehicle with underlaid device-to-device communications: Performance and tradeoffs," *IEEE Transactions on Wireless Communications*, vol. 15, no. 6, pp. 3949–3963, June 2016.

[8] M. M. Azari, F. Rosas, A. Chiumento, and S. Pollin, "Coexistence of terrestrial and aerial users in cellular networks," in *2017 IEEE Globecom Workshops (GC Wkshps)*, Dec 2017, pp. 1–6.

[9] H. C. Nguyen, R. Amorim, J. Wigard, I. Z. Kovács, T. B. Sørensen, and P. E. Mogensen, "How to ensure reliable connectivity for aerial vehicles over cellular networks," *IEEE Access*, vol. 6, pp. 12 304–12 317, 2018.

[10] E. Yanmaz, R. Kuschnig, and C. Bettstetter, "Achieving air-ground communications in 802.11 networks with three-dimensional aerial mobility," in *2013 Proceedings IEEE INFOCOM*, April 2013, pp. 120–124.

[11] I. Z. Kovács, R. Amorim, H. C. Nguyen, J. Wigard, and P. Mogensen, "Interference analysis for UAV connectivity over LTE using aerial radio measurements," in *2017 IEEE 86th Vehicular Technology Conference (VTC-Fall)*, Sept 2017, pp. 1–6.

[12] H. C. Nguyen, R. Amorim, J. Wigard, I. Z. Kovács, and P. Mogensen, "Using LTE networks for UAV command and control link: A rural-area coverage analysis," in *2017 IEEE 86th Vehicular Technology Conference (VTC-Fall)*, Sept 2017, pp. 1–6.

[13] "Evolved universal terrestrial radio access (E-UTRA) physical layer measurements," ETSI, Tech. Rep. TS 136 214, 2011.

Paper C

Angular Distribution of Cellular Signals for UAVs in Urban and Rural Scenarios

Tomasz Izydorczyk, Fernando M. L. Tavares, Gilberto Berardinelli, Mădălina Bucur and Preben Mogensen

The paper has been published in the
The 13th European Conference on Antennas and Propagation (EUCAP), 2019.

The layout has been revised.

Abstract

Spatial channel characterization of a cellular Unmanned Aerial Vehicle (UAV) Air-to-Ground (AG) communication link is a vital step to understand the potential of beamforming in the take-off zone, when a UAV flies in the vicinity of other objects. In this paper, we evaluate the variation of mean Angle of Arrival (AoA) and Angular Spread (AS) with height based on the experimental measurements using live Long Term Evolution (LTE) networks. The LTE signals are recorded at different heights from a ground level up to 40 m in rural and urban environments. Space-Alternating Generalized Expectation-Maximization (SAGE) algorithm is used for the estimation of the angular parameters. Results show similar mean AoA at different heights, with less than 55 degrees deviation in urban environment and no more than 20 degrees change in rural scenarios. Observed AS is reduced to less than 30 degrees at increasing heights as the Line of Sight (LoS) propagation becomes dominant. However the comparison between urban and rural environments clearly indicates the presence of relevant multipath components in the urban scenarios even 20 m above the rooftops level.

C.1 Introduction

Reliable connectivity is vital to ensure foregoing development of Unmanned Aerial Vehicles (UAVs) as low altitude platforms in safety, security or delivery applications. Nowadays, most of the commercially available UAVs use proprietary communication systems working in the Industrial, Scientific and Medical (ISM) bands for Air-to-Ground (AG) communication. These communication methods are not easily adaptable when UAVs are to be reliably controlled over large distances in beyond visual Line of Sight (LoS) scenarios. Existing cellular networks are an encouraging solution given their worldwide deployment [1]. Their major drawback lies in their design principle to provide ubiquitous connectivity for ground users.

It is important to characterize the radio channel to understand the limitations of cellular connectivity for UAVs. Widely-used terrestrial channel models [2–4] were created for ground-level communications and as shown for example in [5], are not extendable for flying UAVs. The study in [6] presents a comprehensive survey over research activities on UAV channel characterization. Empirical research focusing on a cellular bands, as presented in this work, is mostly related to large-scale fading statistics for AG channel or its small-scale fading distribution. Deterministic and stochastic radio channel characterization focus also on a LoS probability estimation based on the environment and UAV's flight height.

Authors in [7] report that at sufficient heights, path loss on the AG link approaches the free space model due to a high LoS probability. This leads

to increased interference levels as more signals from strongly interfering cells are received [8]. Network [1] and receiver side [9,10] beamforming were identified as possible solutions to mitigate this interference, as transmit/receive energy can be focused in a desired direction. Their applicability is thus strongly dependent on the common LoS assumption of the AG link at the UAV's flying heights.

Even though, in most applications the UAV is expected to fly at the higher heights, in some scenarios ('last-mile' delivery services, disaster recovery) and during take-off or landing procedures it will be surrounded by infrastructure where LoS propagation assumption can be violated. The potential of using beamforming in these scenarios depends on spatial channel characteristics. In [10], a fixed-beam solution was proposed and evaluated with system-level simulations, in which different number (2, 4 or 6) of fixed beams (with 90^o or 50^o beamwidth) were used to quantify the UAV performance. Even though the presented results are promising, Angle of Arrival (AoA) and Angular Spread (AS) characteristics at different flying heights need to be better studied, in order to investigate the potential of beamforming solutions. Only by measuring the AS of incoming signals and its AoA stability, the optimal beamwidth can be found and the design questions on, for example, periodicity of beam selection be addressed. To the best of the authors knowledge, there were no experimental studies focused on spatial signal characterization at the so-called *take-off heights* - spanning from the ground level up to the heights where only LoS propagation can be assumed. Understanding the propagation characteristics in the take-off zone is indeed important for addressing the possibility of maintaining a reliable connection in this intermittent flying phase.

In this paper we empirically study the small-scale spatial characteristics of a UAV channel at the take-off heights based on measured live cellular signals. Multi-antenna Universal Software Radio Peripheral (USRP)-based setup and Space-Alternating Generalized Expectation-Maximization (SAGE) algorithm are used for Long Term Evolution (LTE) signal measurements and AoA and AS estimation from the ground-level up to 40 m in different propagation environments. These two aspects are presented as a part of a research project focused on a complete UAV channel characterization based on large scale measurement campaigns using live LTE networks.

The rest of the paper has the following structure. In Section C.2 the measurement procedure is described. The description of the post-processing, from signal decoding up to the AS computation is presented in Section C.3. Section C.4 discusses the obtained small-scale spatial channel characteristics. The work is concluded with Section C.5.

C.2 Measurement Methodology

C.2.1 Hardware setup

The block diagram of the measurement setup, previously described in [9], is shown on Figure C.1. A sixteen antennas Uniform Circular Array (UCA), connected with eight dual-port USRP 2953R boards is used to record the cellular signals. The boards are connected with a data hub PXI-8820 controller using a PXIe-1085 chassis.

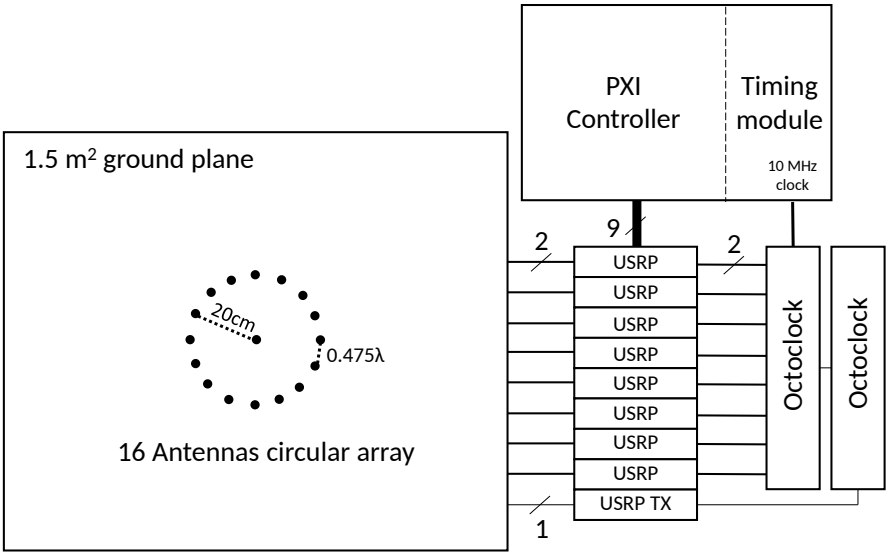

Fig. C.1: Measurement setup schematic

Since the main target of this study is to evaluate the spatial channel characteristics, it is inevitable to use a large antenna array to achieve good spatial resolution. The concept of using an actual UAV was quickly ruled out due to the payload limitations, as each of the antennas require its own receive (RX) chain. In addition, advanced channel estimation algorithms including SAGE are usually time consuming and not suitable for the real-time flights using a battery-limited UAV. The main advantage of using our setup is the possibility to record a large amount of data without any real-time processing. One of the unforeseen benefit is the fact that recorded samples can later be used as input in a wide range of activities ranging from channel propagation studies to advanced transceiver design.

Antenna array

An UCA composed of sixteen monopole antennas was manufactured to record signals from the Downlink (DL) part of LTE Band 3 used by two Danish mobile operators (center frequencies of 1.815 GHz and 1.87 GHz). The circular radius is 20 cm, which corresponds to a wavelength $\lambda = 0.1625$ m and antenna spacing 0.475λ. The reason for using an UCA rather than a linear array, is its ability to scan the incoming signals in all 360^o without ambiguity. The number of antennas was selected as a trade-off between setup complexity and achievable minimal detection resolution of 22.5^o. The UCA is installed on an aluminum ground plane and is connected to the USRP boards using three meter-long RG233 cables.

USRPs and PXI controller

Eight USRP 2953R boards record the cellular LTE signals at 40 MS/s and stream the I/Q samples to the PXI controller. Spatial channel estimation studies require perfect time/frequency/phase alignment among all antenna elements. Time and frequency synchronization was achieved by generating the external 10 MHz clock by the timing module NI PXIe-6674T and redistributing it to all boards by two Octoclocks CDA-2990. To achieve a tight phase synchronization between all USRP boards, a method inspired by [11] is introduced. An additional USRP board is used for transmission of a single-tone out-of-band signal from the omni-directional antenna placed at the center of the array. Assuming perfect antenna patterns, all sixteen antennas receive the calibration tone at the same time and with the same phase. By using one of the antennas as a reference, the random phase offset of each USRP board can be compensated. The described procedure was shown to lead to a phase offset error below 3^o.

Assembled setup

The described setup was assembled in a metal structure and was safely lifted using a crane as can be seen on Figure C.2. The ground plane with the installed antenna array was attached to the external of the structure. The antenna array was additionally covered by a hemisphere radome to prevent any short-circuit in case of rain. The radome was tested to be transparent for the radio waves at the measured frequency.

C.2.2 Measurement campaign

Measurements were conducted during a two-day campaign in Aalborg, Denmark. Seven different measurement locations, shown in Figure C.3, were selected. Two of the measurement locations were in a rural area with limited

building density, but still within the coverage area of two Base Stations (BS) located in a close proximity. The remaining five locations were distributed in the urban part of Aalborg in residential and industrial areas. Such choice allows us to sample various propagation environments where a UAV may fly in and compare their spatial channel characteristics. The average transmitter height in Aalborg, of the BS towers operating at the recorded frequency is 26.3 m and the average antenna downtilt is 5.3^{o}. The Inter-Site Distance (ISD) is only 580 m, leading to the measurement equipment being surrounded by BS in all urban locations. A reader is referred to the Section II in [12] for detailed description of the measured environment.

Fig. C.2: Assembled setup (top-right) lifted in various environments

In each location, the designed setup was lifted using the crane from the ground level up to a 40 m height. 100 ms snapshots of two LTE networks in a 1.8 GHz band were taken at every 5 m step starting from the ground. At each height the measurement equipment was stabilized using robes to avoid unintended turning due to the weather conditions, which could affect the AoA estimation. For each of the network operators, an average of eight snapshots were recorded at each height. To avoid signal blockage and self-shadowing due to the location of the antennas and the metal cage, measurements were repeated in two different antenna orientations - upwards and downwards as can be seen on Figure C.2. On average 156 snapshots were taken per location.

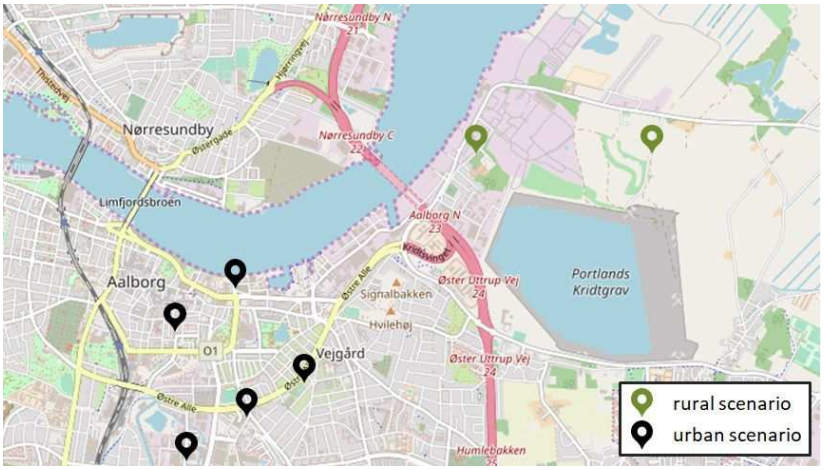

Fig. C.3: Map of measured locations in Aalborg, Northern Denmark

C.3 Post-processing

In this section the entire post-processing is described starting from the raw acquired data up to angular spread calculation. The method is analogous to the approach presented in [13]. The received and phase calibrated sixteen data streams are used to decode LTE signals in order to obtain Cell-Reference Signals (CRS). Then the original CRS pattern is reconstructed based on received Master Information Block (MIB) and subtracted from the received CRS such that only the received channel information is used by SAGE [14] algorithm to estimate the received signal parameters. Finally, AS can be calculated based on results obtained from multiple snapshots. In the next subsections a description of each step is provided.

LTE receiver

Data recorded independently for each snapshot is provided as an input to a Matlab software that runs the LTE receiver processing. The first step is the initial synchronization to the cell with highest correlation measured over synchronization signals. Next, after time/frequency offset correction, the MIB is decoded using the Maximum Ratio Combiner (MRC) equalizer. Based on the information encapsulated in a MIB payload, received signal is downsampled to the correct sampling rate and the CRS grid is recovered. To avoid estimation uncertainty, a Signal to Interference and Noise Ratio (SINR) of System Information Block 1 (SIB1) is computed. An empirically-found threshold is imposed and all the snapshots with SINR lower than 0 dB are discarded.

SAGE algorithm

SAGE is an Expectation-Maximization (EM) type of algorithm capable of accurate estimation of complex gain α_i, delay τ_i, azimuth AoA φ_i and doppler ν_i for each estimated propagation path i. Path's gain and respective AoA are of particular interest in this study. For each recorded snapshot, SAGE is initialized to estimate a large number of paths. We set $N_{\text{paths}} = 50$ paths in this study. Received, noisy CRS grid is provided as an input to the SAGE algorithm together with regenerated 'true' transmitted CRS pattern based on information recovered from the MIB. After ten iterations of the algorithm, from the estimated gain-AoA pairs, these with the path gain minimum 15 dB below the strongest path are excluded and treated as noise. Imposed number of iterations and cutoff threshold, come from a sensitivity study based on a preliminary simulation analysis.

When SAGE processing is complete for all the snapshots recorded at the given height, the AS can be estimated. To avoid the signal wrap-up around 0^{o}, estimates for all snapshots are angle-shifted such that the angle of the strongest path is 180^{o}. Figure C.4 depicts two example sets of SAGE results that reflect different propagation conditions: LoS (left) and multipath (right). The presented results show the combined SAGE estimates from all the snapshots recorded at the same height (40 m and 30 m respectively) in an urban environment. The presented example of multipath propagation will be further commented later, when obtained results are discussed.

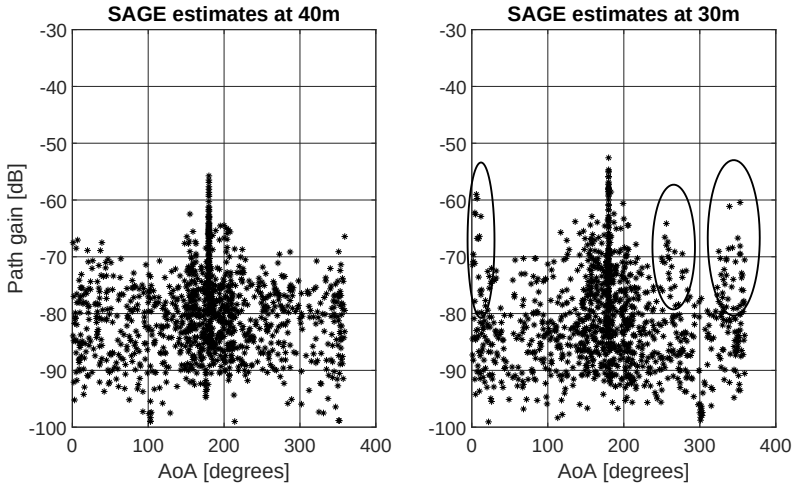

Fig. C.4: Typical set of SAGE results with dominant LoS (left), and multipath propagation (right)

Angular Spread estimation

In this work, the method proposed by [15] and used among others in [16,17] is applied. Angular spread AS is computed as below:

$$AS = \sqrt{\frac{\sum_{k=1}^{N_{\text{snapshots}}} \sum_{i=1}^{N_{\text{paths}}} \left|\varphi_{k,i} - \bar{\varphi}_k\right|^2 \left|\alpha_{k,i}\right|^2}{\sum_{k=1}^{N_{\text{snapshots}}} \sum_{i=1}^{N_{\text{paths}}} \left|\alpha_{k,i}\right|^2}} \tag{C.1}$$

where $N_{\text{snapshots}}$ is a number of snapshots recorded at the given height, $\alpha_{k,i}$ and $\varphi_{k,i}$ are the estimated gain and azimuth AoA for each path i and snapshot k. $\bar{\varphi}_k$ is the mean Angular Power Spectrum (APS) for snapshot k calculated as:

$$\bar{\varphi}_k = \frac{\sum_{i=1}^{N_{\text{paths}}} \varphi_{k,i} \left|\alpha_{k,i}\right|^2}{\sum_{i=1}^{N_{\text{paths}}} \left|\alpha_{k,i}\right|^2} \tag{C.2}$$

C.4 Spatial channel characterization

C.4.1 Estimation of mean Angular Power Spectrum

The mean direction of the APS is one of the key parameters in beamforming operation, as this is the direction towards which the beam should be pointed to capture the most of the incoming signal energy. Its height dependency provides an input on the required beamwidth such that selected direction can remain constant during vertical movement of a UAV provided that mean APS fluctuations are smaller than the selected beamwidth. On the other hand, if the fluctuations are large and the mean direction of the APS encounters major changes with height, a UAV would require to perform frequent beam selection, which may be infeasible in the practical systems and would compromise the reliability of the communication link.

Figure C.5 presents the geometrical representation of the mean deviation of APS (Δ_{APS}), defined as the difference in a mean azimuth direction of the incoming signal recorded at the 40 m and a given height. Mean APS at the 40 m is averaged over all snapshots and used as a reference value since it most likely represents the LoS direction towards the serving cell. Then for all remaining heights, their mean APS and Δ_{APS} can be computed. This study requires the same signal to be decoded at each height, as signals coming from different BS would have a different mean direction.

Figure C.6 presents the variations of the mean APS with respect to the height. There are two locations with a gap in the curves (15 to 20 m and 40 m in Urban 3 and 25 m in Urban 1) meaning that the signal from the target cell was not decoded at these heights due to the high level of interference from

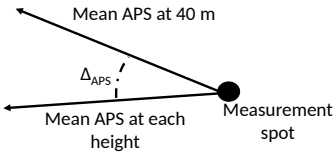

Fig. C.5: Geometrical representation of mean APS deviation

surrounding BSs. Apart from the measurements taken in the Urban 2 spot (which coincide to be the most-dense location surrounded by tall buildings), the observed deviation is small at the higher heights and only increase at the lower heights (below 15 m) when surrounded by the infrastructure. In all locations, the mean signal direction did not change more than 60º. In rural areas the observed change was even smaller and did not exceed 22º. In a real development, this would indicate, that unless surrounded by the tall buildings, the target beam direction found at the flying heights can be kept constant throughout the UAV's descend and the beam scan procedure does not need to be performed very frequently. On the other hand, the strategy of using a fixed beam with large beamwidth (as 60º) can negatively affect the receiver performance as more interfering signals can potentially be received, thus reducing the SINR.

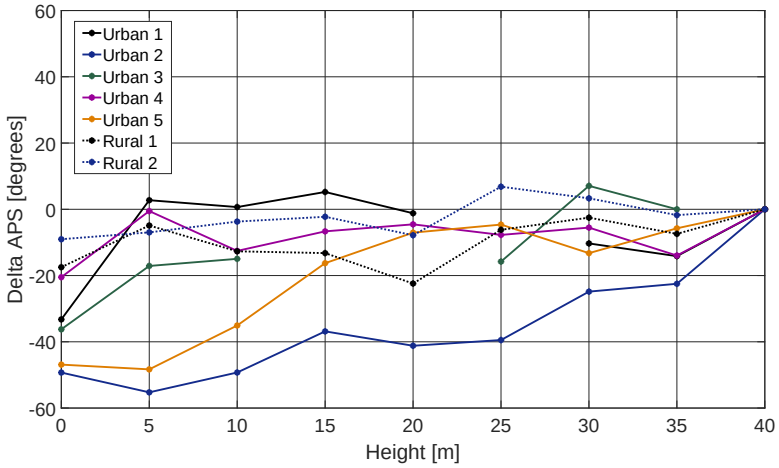

Fig. C.6: Measured mean Angular Power Spectrum deviation at different heights

C.4.2 Estimation of Angular Spread

AS is the metric which is used to characterize the energy spread of the incoming signal in the spatial domain around its mean direction. It is one of

the metrics, which can provide an input on the required beamwidth, sufficient to capture most of the incoming signal power. Its height dependency can be helpful to understand what is the required clearance over the rooftops when LoS propagation becomes dominant, or in other words, down to which height a landing UAV can rely on LoS links and beamforming before entering a rich multipath scenario.

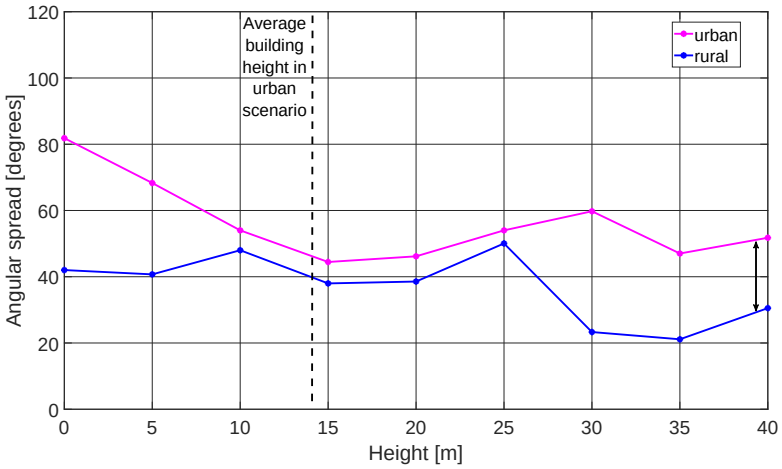

Fig. C.7: Measured angular spread at different heights

Figure C.7 presents the overall AS, estimated at different heights, for the different environments. In urban scenario, there is a clear descending trend as the UAV flies higher. At the ground level (0 to 10 m) there were multiple snapshots with multipath signal propagation coming from widely separated angles, contributing to the fairly high values of the AS. It is worth to mention, that the overall AS computed for these heights was 69^{o}, which well corresponds to the 68^{o} - the mean AS value proposed in 3GPP channel model [2]. As the UAV flies higher than the rooftops (15 m and higher) the LoS propagation becomes dominant as AS decreases.

A small increase in AS is observed at 30 m in the urban locations. SAGE estimates obtained from snapshots recorded in this scenario at 30 m are shown at the right side of Figure C.4. Three multipath clusters, marked in the figure, can be visually identified based on the quantity of estimates and their path gains. They are most probably caused by reflections from the rooftops. These multipaths contribute to the larger estimated AS. Analysis for larger heights (see one example on the left side of Figure C.4) does not reveal the identifiable multipath clusters.

Angular spread measured in the rural scenarios is generally lower than the one estimated from the urban locations, and does not depend on the

height. As expected, in the rural area, due to the absence of scatters in the vicinity of the measurement equipment, estimated AS is low even at the lower heights and there is only a slight decrease observed at the highest measurement positions. While comparing the AS estimated at 40 m for both scenarios (as indicated by the arrow on Figure C.7), there is more than a ten degrees difference, with the rural AS being narrower. It clearly indicates, that even a 20 m clearance over the rooftops is not sufficient to assume only LoS propagation as obtained results clearly show the presence of some multipath components. In case a so-called pencil beam is used, this can lead to a vast amount of power being left outside of the main beam region.

The low (22.5^o) resolution of our measurement equipment becomes a limiting factor for our study, as in general, the computed AS values for higher heights are larger than expected. However, over 15 m, they are constantly lower than 60^o, which can give an indication that this beamwidth is sufficient to capture most of the incoming signal energy.

C.5 Conclusions and future work

In this paper the spatial channel characteristics for cellular UAV air to ground link were analyzed. Mean angular power spectrum was found to not deviate more than 60^o between the ground and a 40 m height in scenarios when signals from the same cell were decodable at each height. The deviation was even smaller and did not exceed 22^o in rural scenarios. Angular spread was found to be height and location dependent. In urban scenarios angular spread decreases with height as fewer multipath components can be observed, while in rural scenarios the observed decrease is significantly smaller since AS is low also at the lower heights due to limited number of obstructions. The computed angular spread does not exceed 60^o at the heights above the rooftops. This further confirms the assumption that communication is dominated by LoS links and in case beamforming is used, gives an indication on the optimal beamwidth. Due to the resolution limitation of our equipment, in the further steps, similar study should be performed with more precise equipment in different measurement environments. The dense-urban 'metropolitan' scenario with skyscrapers should be considered as one of the most challenging environments for UAVs. In addition, the impact of the UAV's fuselage on incoming AS should be investigated.

Acknowledgment

This work has been supported by the cooperative project VIRTUOSO, partially funded by Innovationsfonden Denmark.

References

[1] Y. Zeng, J. Lyu, and R. Zhang, "Cellular-connected UAV: Potential, challenges and promising technologies," *IEEE Wireless Communications*, pp. 1–8, 2018.

[2] *"Spatial Channel Model for Multiple Input Multiple Output (MIMO) simulations (Rel. 13)"*, January 2016, 3GPP TR 125.996.

[3] *"WINNER II Channel Models"*, Sept 2007, iST-4-027756 WINNER II D1.1.2 V1.2.

[4] *"METIS Channel Models"*, Feb 2015, iCT-317669 METIS, Deliverable D1.4.

[5] K. Daniel, M. Putzke, B. Dusza, and C. Wietfeld, "Three dimensional channel characterization for low altitude aerial vehicles," in *2010 7th International Symposium on Wireless Communication Systems*, Sept 2010, pp. 756–760.

[6] A. A. Khuwaja, Y. Chen, N. Zhao, M. Alouini, and P. Dobbins, "A survey of channel modeling for UAV communications," *IEEE Communications Surveys Tutorials*, 2018.

[7] A. Al-Hourani and K. Gomez, "Modeling cellular-to-UAV path-loss for suburban environments," *IEEE Wireless Communications Letters*, vol. 7, no. 1, pp. 82–85, Feb 2018.

[8] B. V. D. Bergh, A. Chiumento, and S. Pollin, "LTE in the sky: trading off propagation benefits with interference costs for aerial nodes," *IEEE Communications Magazine*, vol. 54, no. 5, pp. 44–50, May 2016.

[9] T. Izydorczyk, M. Bucur, F. M. L. Tavares, G. Berardinelli, and P. Mogensen, "Experimental evaluation of multi-antenna receivers for UAV communication in live LTE networks," *Accepted at Globecom workshops*, Dec 2018.

[10] H. C. Nguyen, R. Amorim, J. Wigard, I. Z. Kovács, T. B. Sørensen, and P. E. Mogensen, "How to ensure reliable connectivity for aerial vehicles over cellular networks," *IEEE Access*, vol. 6, pp. 12 304–12 317, 2018.

[11] M. Willerton, D. Yates, V. Goverdovsky, and C. Papavassiliou, "Experimental characterization of a large aperture array localization technique using an SDR testbench," in *Wireless Innovation Forum Conference on Communications Technologies and Software Defined Radio (SDR'11-WInnComm)*, 2011.

[12] R. Amorim, H. Nguyen, J. Wigard, I. Z. Kovács, T. B. Sørensen, and P. Mogensen, "LTE radio measurements above urban rooftops for aerial communications," in *2018 IEEE Wireless Communications and Networking Conference*, April 2018, pp. 1–6.

[13] X. Cai, A. Gonzalez-Plaza, D. Alonso, L. Zhang, C. B. Rodríguez, A. P. Yuste, and X. Yin, "Low altitude UAV propagation channel modelling," in *2017 11th European Conference on Antennas and Propagation (EUCAP)*, March 2017, pp. 1443–1447.

[14] B. H. Fleury, D. Dahlhaus, R. Heddergott, and M. Tschudin, "Wideband angle of arrival estimation using the SAGE algorithm," in *IEEE 4th International Symposium on Spread Spectrum Techniques and Applications Proceedings*, vol. 1, Sep 1996, pp. 79–85.

[15] B. H. Fleury, "First- and second-order characterization of direction dispersion and space selectivity in the radio channel," *IEEE Transactions on Information Theory*, vol. 46, no. 6, pp. 2027–2044, Sept 2000.

[16] Czink, Bonek, X. Yin, and Fleury, "Cluster angular spreads in a MIMO indoor propagation environment," in *2005 IEEE 16th International Symposium on Personal, Indoor and Mobile Radio Communications*, Sept 2005, pp. 664–668.

[17] R. Zhang, X. Lu, J. Zhao, L. Cai, and J. Wang, "Measurement and modeling of angular spreads of three-dimensional urban street radio channels," *IEEE Transactions on Vehicular Technology*, vol. 66, no. 5, pp. 3555–3570, May 2017.

Paper D

Performance evaluation of multi-antenna receivers for vehicular communications in live LTE networks

Tomasz Izydorczyk, Fernando M. L. Tavares, Gilberto Berardinelli, Mădălina Bucur and Preben Mogensen

The paper has been published in the
IEEE 89th Vehicular Technology Conference (VTC2019-Spring), 2019.

The layout has been revised.

Abstract

Cellular Vehicle to Everything (C-V2X) communications with its safety and infotainment services will require a high performance receivers to cope with challenging throughput, latency and reliability requirements. With increasing levels of interference due to cell densification and introduction of the roadside units, single antenna receivers may not be able to provide the required quality of service. In this work we experimentally study the performance of multi antenna receivers based on more than 150 km of data recorded during experiments using a customized software defined radio testbed. The performance of sixteen antennas Maximum Ratio Combiner (MRC) is compared with the receive beamforming technique for the live cellular signals in the 1.8 GHz band. This study is followed by an analysis of the impact of interference and measurement environment on the receiver's performance. The results show that receive beamforming can outperform MRC in low-interfered scenarios with high Line of Sight (LoS) probability, like highways or rural areas, while ensuring comparable performance even in dense urban scenarios where LoS communication cannot be guaranteed.

D.1 Introduction

Cellular Vehicle to Everything (C-V2X) communications will enable new variety of services leading to safer vehicle transportation. It is usually composed of two different communication modes. Vehicle to Vehicle (V2V) communications will provide the driver with the sensor information available in the surrounding vehicles enhancing the road awareness and leading to faster reaction in unexpected situations. On the other hand, Vehicle to Infrastructure (V2I) communications will be used to provide high bit rate infotainment content as well as sensor information from distant vehicles. According to [1], connected vehicles will create up to 700 Mbps average downlink throughput per single vehicle.

Cellular networks (especially Long Term Evolution (LTE) and upcoming 5^{th} Generation (5G)) are expected to cope with challenging throughput, latency and reliability requirements [2] and ensure C-V2X connectivity. The current standardization work [3,4] focuses mostly on the sidelink (V2V) aspects (especially the out of coverage scenarios) as it is assumed that 5G with techniques like Network Slicing, Edge Computing and Content Caching [5] will provide the expected data rates and meet the latency requirements imposed on the V2I communications.

However the scalability of the V2I communications is still an open issue. With the amount of cars on today's roads, the network load can become a potential bottleneck of vehicular communications. Cell densification by means of small cells or Roadside Units (RSU) are expected to serve the in-

creased number of vehicles at the expense of increased interference levels and latency-harming handovers.

From the vehicle manufacturers perspective, ensuring the best possible connectivity for the newly produced vehicles is a main objective. As noted in [6], the increased number of antennas installed on a vehicle should lead to higher Signal to Noise and Interference Ratio (SINR) and therefore higher throughput and lower number of retransmissions. In this way car vendors can compete among themselves to provide better quality of services or add new features due to enhanced throughput and reduced latency.

Nowadays C-V2X tests are usually conducted using vehicles equipped with a LTE modem capable of 2x2 Multiple Input Multiple Output (MIMO) transmission [7]. The authors in [8], discuss the challenges of mounting larger antenna arrays on the vehicles. However, their objectives are mostly referred towards V2V communications disregarding V2I mode as similar to a typical User Equipment (UE). It is expected that certain types of cars (trucks, buses or large industrial vehicles) are less space constrained and therefore installation of large antenna arrays will become possible.

In this work we investigate the potential of using a large antenna array on the vehicle terminal based on experimental measurements from live LTE networks using a Software Defined Radio (SDR) measurement system. We study the performance of receive beamforming and Maximum Ratio Combining (MRC) techniques for SINR improvement over a single antenna receiver in the real scenarios, as the vehicle would experience in a currently deployed networks. Rural, suburban, dense urban and highway scenarios are of interest in this study. We further investigate the impact of the measuring environment (interference distribution and characteristics of the measured scenario) on the performance of both receiver types. For the best of our knowledge, it is the first experimental study related to the benefits of using multiple antenna techniques for the V2I communications, as previous works focus either on experimental vehicular channel characterization [9,10] or simulation assessment of receive beamforming [11] or combining [6] techniques.

The rest of the paper is structured as follows: Section D.2 describes the measurement equipment and conducted campaign. It is followed by the description of post-processing methods presented in Section D.3. Starting from Section D.4.1 first the performance of multiple antenna techniques in different scenarios is studied followed by a more detailed analysis of the impact of interference on the observed performance in Section D.4.2. The work is concluded in Section D.5.

D.2 Measurement Methodology

D.2.1 Measurement equipment

In this work we use the measurement setup thoroughly described in [12] or [13] and shown on Figure D.1. It is composed of sixteen antennas uniform circular array manufactured for 1.8 GHz LTE band 3 and connected to the measurement system built based on Universal Software Radio Peripheral (USRP) boards. In total eight boards are used as each board contains two independent transceiver ports. Additional ninth board is used for calibration procedure. Synchronization signal is distributed by Timing Module via Octoclocks to all boards such that after offline calibration there is a tight synchronization between all boards. The setup is used to record raw I and Q samples of LTE signal. In this way, different receiver types can be evaluated with the same portions of data during an offline processing as described later.

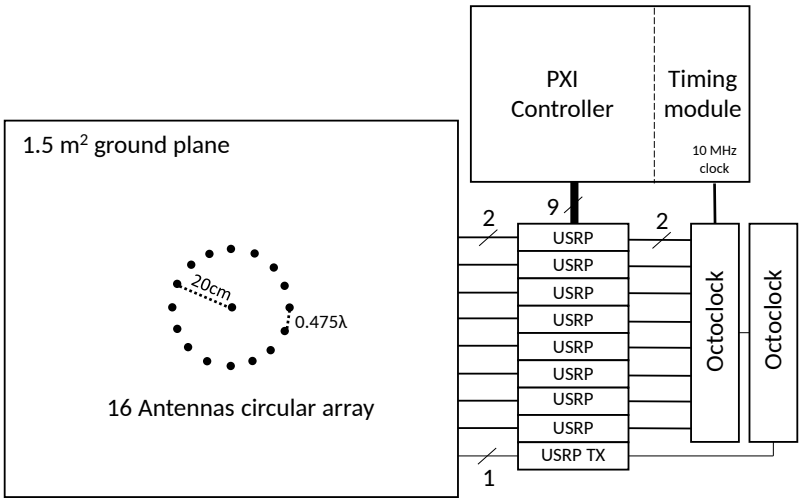

Fig. D.1: Schematic of the measurement setup

The assembled setup was placed inside a van, while antennas (sixteen monopoles) were manufactured on a 1.5 m^2 ground plane installed on top of the van as shown on Figure D.2. In order to enhance the measurement capabilities, network scanner TSMW from Rohde & Schwarz capable of recording up to 32 cells operating within the set band was used together with the measurement setup. Both measurement equipment and the scanner contain a Global Positioning System (GPS) receiver such that the data recorded by both systems can be correlated.

Fig. D.2: A van with measurement equipment (inside) and antenna array mounted on a ground plane (roof)

D.2.2 Measurement campaign

Measurement campaign was conducted in a vicinity of Aalborg in northern Denmark. While driving, measurement setup was used to record 100 ms snapshots of LTE signal every 5 s and store them for offline post-processing. In parallel, network scanner recorded the network information with approximately 100 ms granularity. Four routes were chosen for the experiment representing different propagation environments and are summarized in Table D.1. Each route was driven twice, each time recording the carrier frequency of a different network operator operating within the LTE band 3. In total more than 150 km were driven and more than 6000 snapshots were recorded. Please note that the speed of the vehicle varied from stationary (while waiting at the red lights) up to 100 km/h on a highway.

Figure D.3 presents the three driven routes. Route 4 although not shown here due to space constraints is also used for the analysis of the interference as described later.

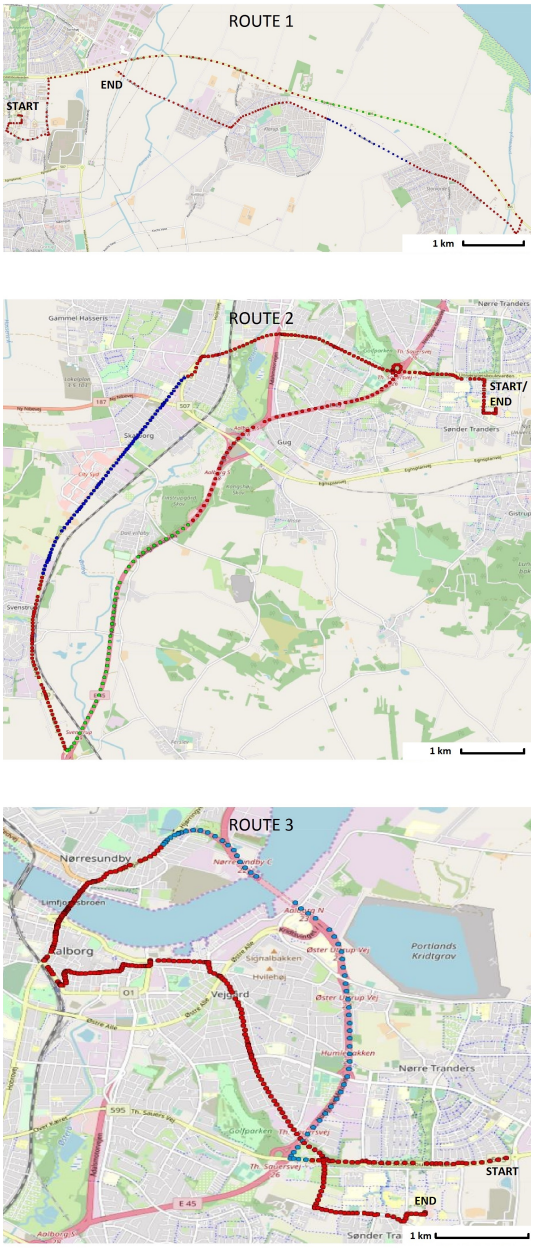

Fig. D.3: Three driven routes

Table D.1: Characteristics of the measured environment

Route index	Measurement environment	Short description
Route 1	Dominant rural and suburban	Small houses and meadows, seldom deployed Base Stations (BS)
Route 2	Highway and urban	Blocks up to the 3rd floor in the urban part, medium density of BS
Route 3	Highway and dense urban	Blocks up to the 6rd floor, high density of BS
Route 4	Suburban	University buildings, high density of BS

D.3 Post-processing

In this section post-processing of the recorded data is described, for both measurement setup and the scanner. Each of the data snapshot is processed independently using Matlab in order to compare the performance of different receiver types: a single antenna receiver, MRC and receive beamforming. Scanner information is processed in order to better understand the level of interference in all measured points. The entire process was thoroughly explained in [12], therefore in the next subsection only the summary of processing is outlined.

D.3.1 Receiving techniques

To study a single antenna receiver, one of the sixteen recorded data streams is used, while others are discarded. The signals recorded by the selected antenna are processed in the receiver built based on the Matlab LTE toolbox. In the receiver, synchronization based on the synchronization signals, channel and frequency offset estimations are performed. Two LTE control channels - Master Information Block (MIB) and System Information Block 1 (SIB1) are decoded and the SINR of the latter is computed and used as a metric for comparison among different receivers. Post processing using MRC is very similar to the single antenna receiver but the processed signal is obtained by combining the sixteen recorded data streams. We refer to [12] for further details on the receiver processing.

In order to assess the performance of the receive beamforming technique, one need to know the optimal direction where the beam should be pointed.

As in this work we focus on the ideal performance of the technique (and assume no Angle of Arrival (AoA) information available), for each snapshot 360 beams pointing towards different directions (in both elevation and azimuth planes) using conventional beamformer with 3 dB beamwidth of 22.5^o are created. By performing the entire processing for each of the beams, the optimal one can be found as the beam which results in the highest SIB1 SINR. This beam is used for comparison with other receiving techniques, while others are discarded.

D.3.2 Scanner processing

Scanner recordings were processed in order to characterize interference in the vicinity of the receiver. For each of the snapshots, scanner records the information of up to 32 different cells providing among others the Cell ID and Reference Signals Received Power (RSRP) of each decodable cell. Knowing the Cell ID of the serving cell (based on the information decoded from the MIB), this entry can be excluded from the scanner data. In this way, it will only contain the list of interfering BS with respective RSRPs. In this work two different metrics on how to quantify interference are used. First, the Dominant Interference Ratio (DIR) is computed as below:

$$\mathrm{DIR} = 10\log_{10}\frac{max(\mathrm{RSRP})}{\sum_{k=1}^{K}\mathrm{RSRP}(k) - max(\mathrm{RSRP}) + n} \tag{D.1}$$

where RSRP is a vector of K interfering RSRPs and n is the thermal noise power computed as:

$$n = -174 + 10\log_{10}(b) \tag{D.2}$$

where b is the bandwidth of the decoded LTE network in Hz (15 or 20 MHz). Computed DIR can reveal if there is a strong dominant interferer potentially harming the performance of the receiver.

As a second metric to describe the interference, the sum of interferers is computed as a total number of interferers with reported RSRP higher than an arbitrary value of -100 dBm. Imposed threshold is used to exclude the cells which due to the low RSRP are only sporadicly reported by the scanner. Since in most cases each interfering signal comes with different AoA, it is worth to study its impact on the performance of the receive beamforming. It is worth to notice that there were some special case snapshots for which scanner reported only one cell (a serving cell), meaning that in a given measurement position interfering signals were too weak to be decoded.

D.4 Performance analysis

D.4.1 Performance evaluation of multi-antenna receivers

First, the instantaneous SINR reported for each snapshot and receiver type is plotted against the covered distance for three different routes on Figure D.4. As can be noted, the SINR values vary rapidly with distance, due to large and small scale fading. It is worth to indicate that as each of the snapshots is treated independently, each receiver is always connected to the best serving cell without any handover-related considerations.

Two general trends are visible. As expected the single antenna receiver (blue line) generally results in the lowest reported SINR value. The performance of MRC (black line) and receive beamforming (magenta line) is roughly comparable, but some parts of the route where beamforming provides substantial gain over MRC can be visually identified and are marked with dashed rectangles on the figure. After recovering the GPS information for the identified snapshots and plotting them on the map (green and blue points on Figure D.3) one can notice that the regions where beamforming performs better than MRC are highway and rural parts where a higher probability of Line of Sight (LoS) link to the BS is expected.

The Empirical Cumulative Distribution Functions (ECDFs) of computed SINR are presented on Figure D.5 for three studied routes to quantify the SINR of each receiver type. In up to 20% of cases, the SINR of the single antenna receiver is lower than 0 dB which can potentially harm the connection reliability. Moreover, single antenna receiver has approximately 2 dB lower average (50-th percentile) SINR in the dense urban scenario than in rural and suburban environments, which can be explained by the increased levels of interference due to cell densification. This performance drop is negligible for the MRC and receive beamforming as both methods benefit from the spatial diversity.

Fore each route, there is on average 5 to 8 dB SINR gain of both multi antenna techniques over a single antenna receiver. The average gains in this range were expected as the simulated maximum directional gain of the array was ~8 dB. Only a few snapshots with SINR lower than 0 dB were recorded, which indicates the benefits of using multiple antenna system for improved network connectivity. Slight gains (up to 1.5 dB) of beamforming over MRC are visible especially in the upper tail of the ECDFs, further confirming higher beamforming gains in visually identified regions and similar performance elsewhere. As highway accounted for a substantial part of the second route, the observed beamforming gains are higher than in different environments.

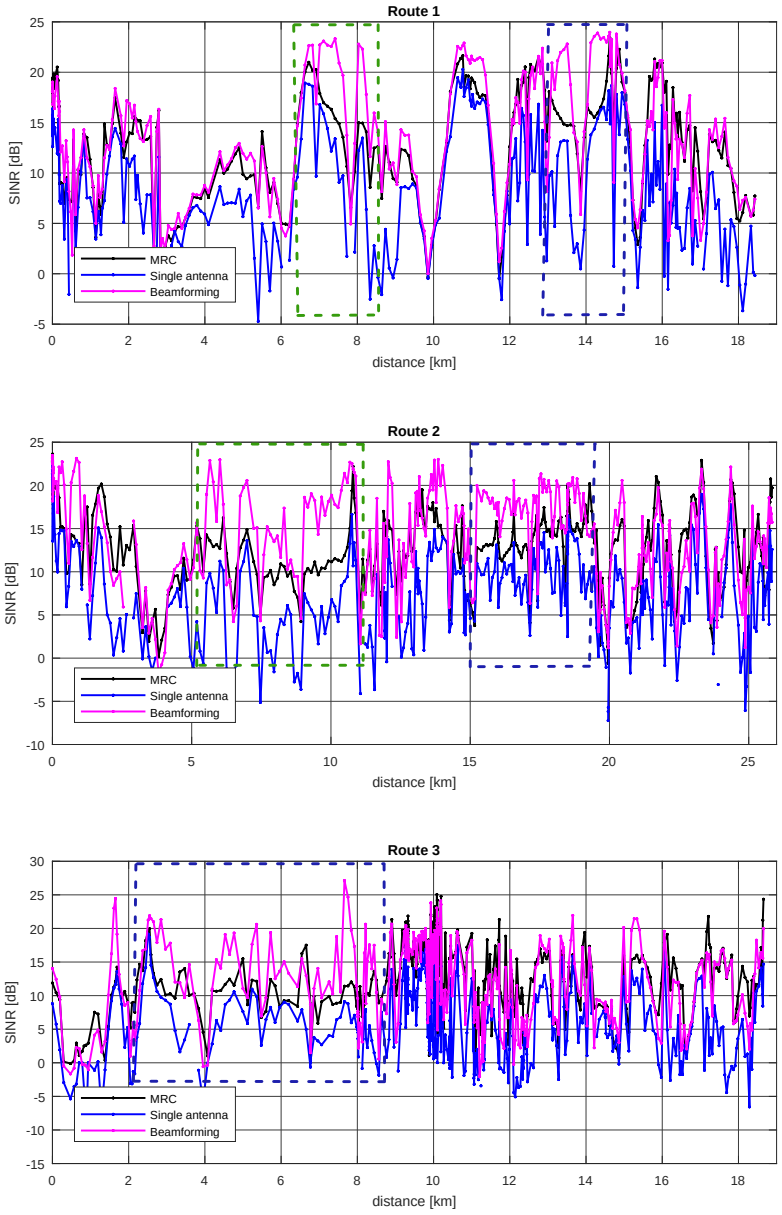

Fig. D.4: Instantaneous SINR for different receiver types measured at routes 1, 2 and 3

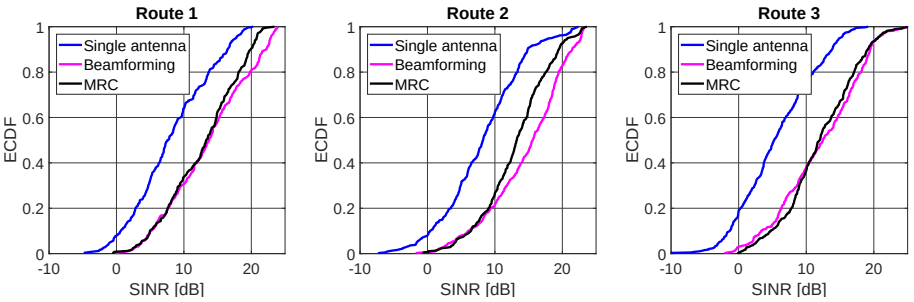

Fig. D.5: Empirical Cumulative Distribution Functions of instantaneous SINR for different receiver types

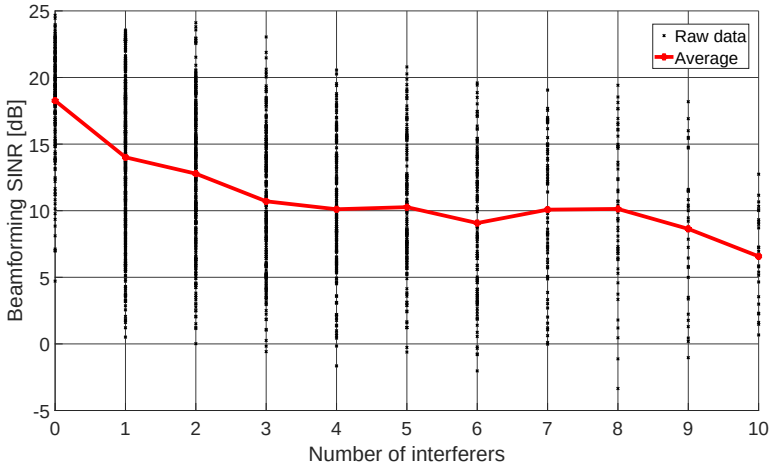

Fig. D.6: Impact of number of interferers on receive beamforming SINR

D.4.2 Impact of interference on the performance of multi-antenna receivers

Trying to better understand the origin of improved beamforming performance with respect to the MRC receiver, in this subsection we focus on the impact of interference on these two receiver types. All results displayed next are generated from the entire set of measurements. Figure D.6 presents how the instantaneous SINR of receive beamforming changes with the number of significant interferers. While black dots represents the measured data, the red line shows the computed mean for each number of interferers. As expected, the lower the number of interferers, the higher the SINR. With fewer interferers, probability of interfering signal being captured within the main lobe of the receiver is generally lower leading to higher SINR.

Figure D.7 shows how the instantaneous beamforming gain over the MRC receiver Δ computed in dB scale as:

$$\Delta = \mathrm{SINR}_{\mathrm{beam}} - \mathrm{SINR}_{\mathrm{MRC}} \tag{D.3}$$

changes with the number of interferers. Looking at the averaged values, it is clearly visible that the performance of both receivers is comparable in a presence of multiple interference sources. Receive beamforming provides up to 2.5 dB average SINR gain when there are no significant interferers decoded and only the sporadic, low power interfering sources are present.

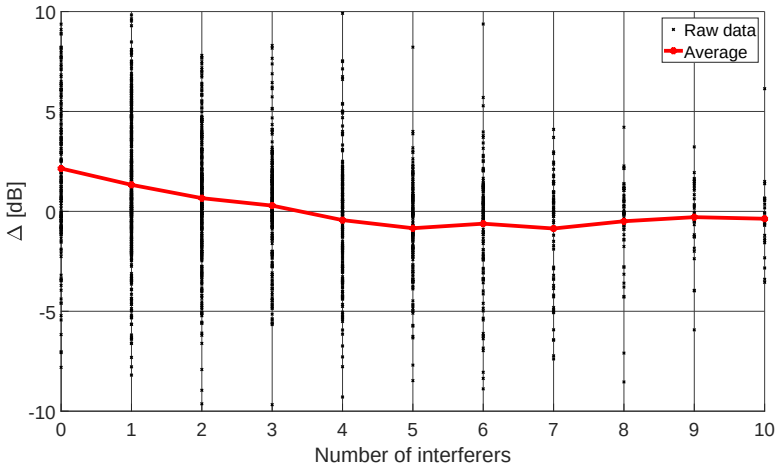

Fig. D.7: Impact of the number of interferers on receive beamforming gains

In order to capture the influence of all reported interferers, Figure D.8 presents how the beamforming gain Δ depends on the DIR, while Figure D.9 presents the histogram of the gains for the special case of snapshots where scanner did not report any interference. Interestingly, beamforming provides higher average gain in cases when DIR is high. Also points corresponding to high beamforming gains visually identified at Figure D.4 in most cases are related to the high DIR. These gains can be intuitively explained as there is a high probability that the AoA of the strongest interferer would be located outside of the main beam of the receiver and due to the lower antenna gain in this direction its power would be reduced. MRC on the contrary does not account for the interference and suffers from its presence. It is expected that the Interference Rejection Combining (IRC) receiver would perform significantly better than MRC in studied scenarios given its capability of suppressing a limited number of relevant interferers. However, it would require an accurate estimate of the interferers' channel responses, which might not be feasible in practice.

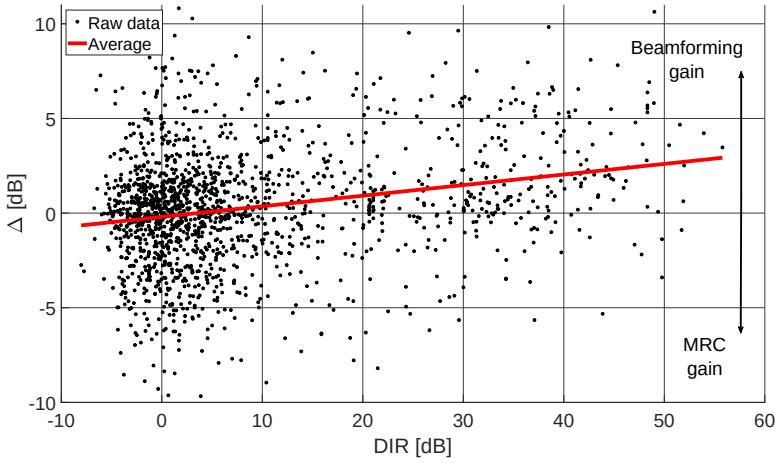

Fig. D.8: Dependence of DIR on receive beamforming gains

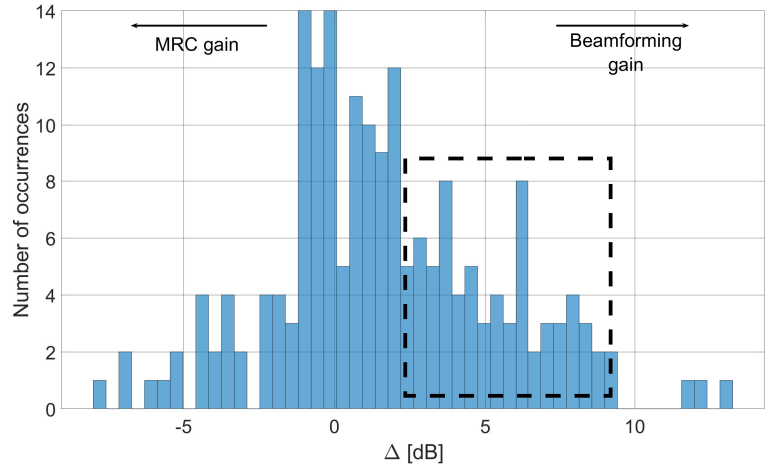

Fig. D.9: Receive beamforming gains when no interference was reported by the scanner

Table D.2: Location of the strongest interfering source

Percentage of snapshots with the interferer coming from the same BS	37%
Percentage of snapshots with the interferer coming from different BS	63%

Histogram presented at Figure D.9 further confirms the assumption that beamforming can provide higher gains with a limited number of interfering sources. Theoretically, if there is no interference, the performance of both receive beamforming and MRC should be identical. This can be observed at the figure as for the most occurrences there is no gain for any of the methods or a very limited gain of MRC. However in reality, there can always be some interference sources which were not decoded by scanner for example due to their low SINR. This situation may not only occur for low power interferers, but also in case of multiple interfering signals with significant power and similar AoA, that cannot be decoded due to their strong mutual interference. In the latter cases, as marked by the black rectangle, beamforming can provide a substantial gain over MRC.

Finally, as an indication for further study, the potential impact of the geographical location of the strongest interfering source on the observed results is studied. As most of the BS towers are usually composed of three cells with antennas pointing towards different sectors, Table D.2 quantifies how often the strongest observed interferer comes from the different sectors of the same BS. Surprisingly, even though different sectors are usually spatially separated (each cell points into another direction) in 37% of the measured cases the strongest interferer is located at the same BS tower. Although no correlation between beamforming gain Δ and location of the interferer was found, this information indicates that if imposed, cooperation between just the different sectors of the same BS should improve the overall system performance.

D.5 Conclusions

In this work, the performance of multi-antenna receiver techniques for C-V2X communications was studied based on data recorded in experimental campaign. The observed 8 dB average SINR gains with respect to a single antenna system are comparable for both MRC and receive beamforming. However as our measurements indicate, instantaneous gains depend on the measured environment. Obtained results indicate superior performance of beamforming techniques over MRC in LoS scenarios (highway and rural areas) while ensuring similar performance in urban environments. Moreover, receive beamforming was found to provide up to 2.5 dB SINR gain over the

MRC receiver in a presence of a strong single dominant interferer. In scenarios with larger number of weaker interferers the performance of both multi antenna receivers was found to be comparable.

As an indication for further study, it has been found that in 37% of the cases, the strongest interfering source was located at the same BS tower. In such cases interference mitigation techniques may be used for signal quality improvement.

References

[1] Z. MacHardy, A. Khan, K. Obana, and S. Iwashina, "V2X access technologies: Regulation, research, and remaining challenges," *IEEE Communications Surveys Tutorials*, vol. 20, no. 3, pp. 1858–1877, thirdquarter 2018.

[2] S. Chen, J. Hu, Y. Shi, Y. Peng, J. Fang, R. Zhao, and L. Zhao, "Vehicle-to-everything V2X services supported by LTE-based systems and 5G," *IEEE Communications Standards Magazine*, vol. 1, no. 2, pp. 70–76, 2017.

[3] "Study on enhancement of 3GPP support for 5G V2X services (release 15)," 3GPP, Tech. Rep. TS 22.886 V15.1.0, 2017.

[4] "Architecture enhancements for V2X services (release 15)," 3GPP, Tech. Rep. TS 23.285 V15.0.0, March 2018.

[5] H. Khan, P. Luoto, M. Bennis, and M. Latva-aho, "On the application of network slicing for 5G-V2X," in *European Wireless 2018; 24th European Wireless Conference*, May 2018, pp. 1–6.

[6] M. Boban, K. Manolakis, M. Ibrahim, S. Bazzi, and W. Xu, "Design aspects for 5G V2X physical layer," in *2016 IEEE Conference on Standards for Communications and Networking (CSCN)*, October 2016, pp. 1–7.

[7] "V2X functional and performance test report; test procedures and results," 5GAA Automotive Association, Tech. Rep. 5GAA P-180106, October 2018.

[8] C. F. Mecklenbrauker, A. F. Molisch, J. Karedal, F. Tufvesson, A. Paier, L. Bernado, T. Zemen, O. Klemp, and N. Czink, "Vehicular channel characterization and its implications for wireless system design and performance," *Proceedings of the IEEE*, vol. 99, no. 7, pp. 1189–1212, July 2011.

[9] "WINNER II channel models," WINNER II Project, Tech. Rep. D1.1.2 ver. 1.1, February 2008.

[10] "METIS channel models," Mobile and wireless communications Enablers for the Twenty-twenty Information Society, Tech. Rep. D1.4 ver. 3, November 2012.

[11] I. Maskulainen, P. Luoto, P. Pirinen, M. Bennis, K. Horneman, and M. Latva-aho, "Performance evaluation of adaptive beamforming in 5G-V2X networks," in *2017 European Conference on Networks and Communications (EuCNC)*, June 2017, pp. 1–5.

[12] T. Izydorczyk, M. Bucur, F. M. L. Tavares, G. Berardinelli, and P. Mogensen, "Experimental evaluation of multi-antenna receivers for UAV communication in live LTE networks," *Globecom workshop on Wireless Networking and Control for Unmanned Autonomous Vehicles*, December 2018.

[13] T. Izydorczyk, F. M. L. Tavares, G. Berardinelli, M. Bucur, and P. Mogensen, "Angular distribution of cellular signals for UAVs in urban and rural scenarios," *Accepted at European Conference on Antennas and Propagation (EuCAP 2019)*, March 2019.

Paper E

On the potential of uplink beamforming in vehicular networks based on experimental measurements

Tomasz Izydorczyk, Gilberto Berardinelli, Fernando M. L. Tavares, Mădălina Bucur and Preben Mogensen

The paper has been published in the
IEEE 90th Vehicular Technology Conference (VTC2019-Fall), 2019.

The layout has been revised.

Abstract

This work evaluates the concept of uplink beamforming for vehicular communications in the sub-6 GHz frequency bands to improve throughput, latency and coverage of the vehicle to Base Station (BS) link. The data recorded in the experimental measurements using live cellular signals are used to study the performance of two direction acquisition methods: the Angle of Arrival (AoA) estimation and downlink-based beam sweep. Next, the feasibility of signal tracking techniques exploiting the location of the vehicle and the BS are investigated to alleviate the need for continuous direction acquisition. The results show that the downlink-based beam sweep leads to higher Signal to Interference and Noise Ratio (SINR) than beamforming based on the estimated AoA. Evaluated tracking techniques are shown to be capable of correctly estimating the beamforming angle for distances in order of hundreds of meters when BS's location is known to the vehicle.

E.1 Introduction

Data traffic patterns in vehicular applications differ widely from the ones generated by typical User Equipments (UEs) [1]. Direct communication between vehicles will be used for communication between proximate vehicles. In addition, cellular technologies can be used for delivering potentially high data rate sensor information and for enabling eventual information exchange among distant vehicles. In such cases, the existing cellular infrastructure will be used to deliver the information requiring the reliable, low latency, high bit rate uplink. As presented in [2], in cellular networks, the uplink coverage radius is generally much lower than its downlink counterpart due to limited transmit power of the device. Limited coverage (especially in the rural and suburban areas), together with large amount of connected vehicles constantly transmitting their sensor data, leads to uplink transmission being the potential bottleneck of the future vehicular communications.

Only few works target the uplink in the vehicular communications. In [3], the usage of Roadside Units (RSU) is discussed as a network element installed to gather data from connected vehicles. In this way, both coverage and congestion problems are solved by introducing additional signal transceivers to enhance network's capacity. However, the challenges still persist as it is hard to believe that RSUs will be globally deployed along all the roads. Beamforming algorithms exploiting millimeter wave frequencies [4] are a promising set of techniques to solve the high uplink throughput requirements imposed on the connected vehicles. However due to the large propagation losses, they might not be able to mitigate the potential coverage holes of the communication system.

The concept of using multi-antenna arrays is proposed in [5]. Authors

note that installation of large antenna arrays, heavily constrained on the smaller vehicles, can be feasible on larger vehicles as trucks or buses. Although the main concept of the work in [5] is to improve downlink connectivity, it is easily extendable to the uplink communications. By using uplink beamforming, one can expect to improve the uplink throughput, reliability of the link or extend the coverage thanks to directional array gain.

These gains will only be achievable in the presence of a strong directional path towards the Base Station (BS) and with transmitter (vehicle) being aware of the direction towards which it should point the beam. In addition, a robust direction tracking procedure will be required to follow the imminent changes in the optimal beamforming angle, which can be challenging to achieve in the practical systems due to multipath propagation. Their applicability may become feasible in the rural and suburban areas with limited number of scatterers. In rich multipath urban scenarios, the potential uplink coverage/throughput bottleneck should be less harmful due to cell (and RSU) densification and therefore beamforming technologies may not be necessary.

In this work we present and experimentally evaluate the novel approach of using beamforming in the 1.8 GHz band for uplink vehicular communications in rural and suburban scenarios. We discuss the potential benefits and drawbacks of using different direction acquisition methods including beam sweeping and Angle of Arrival (AoA) estimation. Further we study two different methods for direction tracking exploiting measured live downlink Long Term Evolution (LTE) signal and Global Positioning System (GPS) information. The main aim is to assess the feasibility of practical implementation and benefits of beamforming, addressing the challenges related to finding the optimal beamformed direction.

The rest of the paper is structured as follows. Section E.2 discusses the potential methods for selection of the uplink beam's direction. In Section E.3 two tracking algorithms are proposed. This is followed by Section E.4 describing the conducted measurement campaign. The obtained results are shown in Section E.5.1 and E.5.2 for direction acquisition and tracking respectively. The work is concluded in Section E.6.

E.2 Acquisition of beamforming direction

Uplink beamforming in sub-6 GHz frequency bands has not been widely utilized in cellular networks due to the device's hardware complexity and a limited gain with respect to other transmission modes [6]. The installation of multiple antennas would entail the need for additional transceiver chains impacting the price and energy consumption of the device. Additional space would be required to physically design antenna arrays with a desired spacing between elements. Even though vehicles are expected not to inherit these

constraints applicable to the typical UEs, a major challenge persists. Vehicle would need to learn the optimal beamforming direction to focus the transmitted signal and benefit from high directional gains. Below, three possible ways of acquiring the beamforming direction are discussed.

Downlink-based AoA estimation

Assuming a cellular network operating in Time Division Duplex (TDD) mode, one can try to estimate the AoA of the received downlink signal based for example on Cell Specific Reference Signals (CRS) using estimation algorithms like Space Alternating Generalized Expectation-Maximization (SAGE) [7]. Then, by assuming channel reciprocity, the same direction would be used for uplink beamforming. This method can also be applied to the networks operating in the Frequency Division Duplex (FDD) mode with both uplink and downlink occupying similar frequency bands as for example LTE bands 3 or 7 [8]. The drawback of the AoA estimation lies in the computational complexity of the estimation algorithms. Also, in the case of FDD networks, the underlining assumption that the main downlink AoA is also the optimal uplink angle may not always be valid.

Downlink-based beam sweep

Another technique utilizing downlink cellular signals for finding the signal's direction is beam sweeping. In this method, a vehicle would use a subset of the possible beams to receive the downlink signals. Assuming the same TDD/FDD constraints as in the previous method, the beam resulting in, for example, the highest Reference Signals Received Power (RSRP) would be used for uplink transmission. Comparing with AoA estimation, beam sweeping should lead to more accurate beam selection, as potential non-idealities of the estimation process, especially in the estimation of weaker multipath components, are avoided. The complexity however still persists as sweeping through multiple beam options would be time consuming.

BS-indicated precoding index

This technique is a mirror image of the methodology used for downlink beamforming in LTE [9]. A vehicle, would transmit its uplink data using a subset of beams. After BS estimates which of the beams would lead to the strongest received Signal to Interference and Noise Ratio (SINR), it would report its choice as a precoding index to the vehicle. This methodology does not set any specific condition even on the FDD bands and assuming slow vehicle's velocity, it should lead to the most accurate results. However, it would

require standardization efforts and implementation in the BS therefore it is not included in the analysis conducted in this paper

E.3 Signal tracking techniques

Due to computational complexity (SAGE) or time required to perform the beam sweep, none of the discussed direction acquisition methods can be repeated with a high frequency. It is rather expected that the chosen direction acquisition method will be accompanied by a tracking algorithm used to estimate the imminent changes of the acquired direction over a short time before next direction acquisition procedure is performed. The valid question is therefore, for how long can the signal be tracked before there is a need for another direction estimation using one of the aforementioned methods? This distance would depend on the environment and is expected to be much longer in the rural and suburban areas rather than dense urban ones where frequent changes of direction are expected due to the multipath propagation. As a part of this work, we experimentally evaluate the length of the tracking distance based on the conducted measurement campaign utilizing live cellular signals. Two different signal tracking techniques are studied depending on information available at the vehicle.

Beam tracking with no GPS information

This simple tracking method, as presented on Figure E.1, assumes that GPS coordinates of the serving cell are not known to the vehicle. At the beginning there is a so-called *warm up* phase. In two positions, separated by a driven distance d, the real direction is acquired using one of the methods presented in Section E.2. Then the change in the beam direction $\Delta\beta$ is computed as the difference between beamformed directions in these two positions. Since the GPS coordinates of the BS are not known, it is assumed that the same change trend will continue and the angle should be adjusted linearly based on the driven distance, as for example after distance $2d$ is driven, the beamformed angle should be adjusted by $2\Delta\beta$. This simple tracking method has some limitations. Only if the distance to the BS is sufficiently long one can assume the angular change of the beam direction will persist. Otherwise, for the same driven distance the angle change would be much lower than $\Delta\beta$ if after the warm up phase the vehicle would start to recede from the BS leading to incorrect estimation of the angle.

Beam tracking with GPS information available

By exploiting the GPS information of the BS, the impact of the distance to the BS can be removed. In this method, as presented on Figure E.2, in each

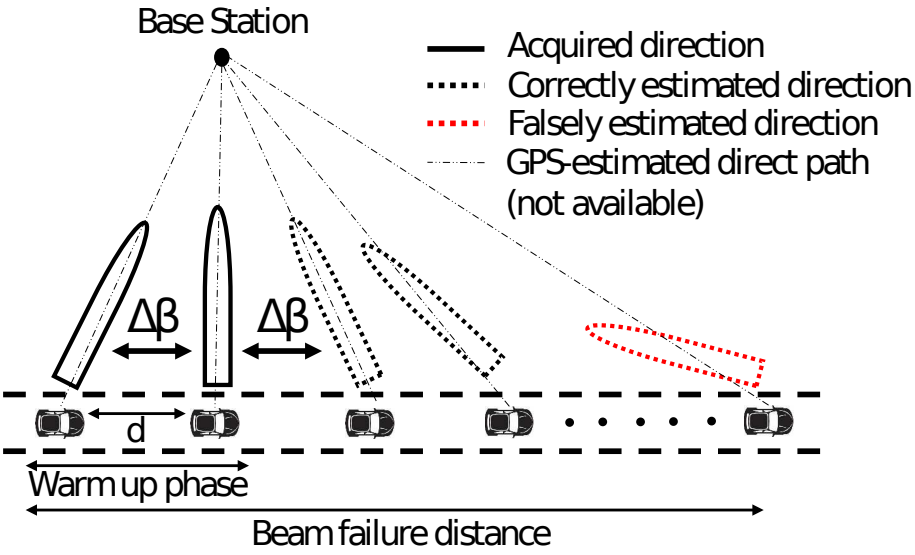

Fig. E.1: Beam tracking exploiting only acquired signal direction

position the direct path towards the BS can be computed based on the GPS coordinates. After initial direction acquisition in the first point, the predicted beamformed angle after distance d is estimated based on the change in the angle of the direct path $\Delta\gamma$. In this method, the angle change $\Delta\gamma$ can be constantly adjusted as the difference between angles of the direct paths in the last two positions removing the impact of the distance to the BS.

E.4 Measurement campaign and post-processing

Given the practical difficulties of obtaining uplink measurements in real cellular networks, the methodology used in this study is based on a measurement campaign where live cellular signals are recorded in the downlink by using a multi-antenna software defined radio setup. The raw measured signals are processed offline, and different direction acquisition methods and signal tracking techniques are studied. Our analysis is based on the assumption that the main signal direction estimated in the downlink can be used for uplink transmission. This holds in case of TDD or FDD modes with sufficiently close operational bands, as highlighted in Section E.2. The downlink SINR is used to compare the direction acquisition techniques, by pointing the beams towards the acquired direction to receive the signal; while downlink-estimated AoA is used to assess the performance of tracking techniques.

The measurement campaign was performed in Aalborg in northern Denmark. In the measurement campaign, the downlink LTE signal from two

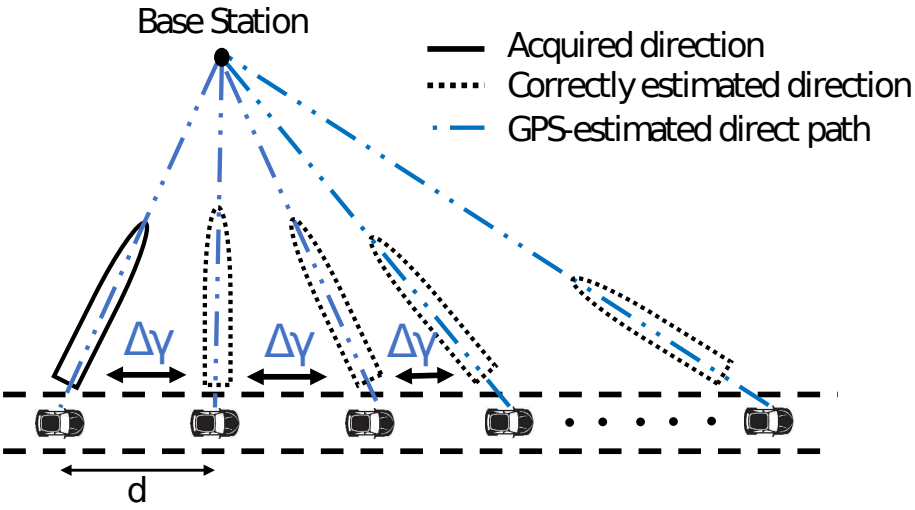

Fig. E.2: Beam tracking exploiting GPS coordinates of the serving cell

Danish mobile operators operating in 1.8 GHz band was recorded using a multi-antenna measurement setup based on the Universal Software Radio Peripheral (USRP) boards thoroughly described in [10]. USRPs provided a set of fully digital receiver chains for a sixteen antennas circular array that was used to record the raw I&Q samples of the LTE signal for the offline post-processing. Every five seconds, a snapshot containing 100 ms of LTE signal was recorded. In total four different routes were driven across suburban, rural and highway scenarios spanning more than 150 km distance [5]. One example of such route is presented on Figure E.3, together with the vehicle used to conduct the measurements.

Post-processing for direction acquisition

After the measurement campaign, in the offline post-processing the direction acquisition methods are studied. For each snapshot recorded in the measurement campaign, after synchronization to the network and channel estimation, the AoA of the incoming signal is estimated using SAGE [11]. After centering the receiver beam at the estimated angle, the SINR of LTE System Information Block 1 (SIB1) control channel is computed. On the other hand, to study the downlink-based beam sweep, the data from each snapshot is independently beamformed using 360 different beams pointed in different directions in azimuth domain. The beam with the highest reported RSRP is used for further decoding of the SIB1 control channel and SINR computation. Finally, since together with the LTE signal, the GPS coordinates of the vehicle were saved, knowing the GPS coordinates of the BS, the angle of the GPS-based

Fig. E.3: The example of the driven route in a suburban environment and the measurement vehicle

direct path towards the serving cell is estimated. The SIB1 SINR is again computed after centering the beam towards the found angle. The same beam shape with Half Power Beamwidth (HPBW) of 22.5º is used for all methods.

Post-processing for signal tracking techniques

Figure E.4 presents the AoA estimated with SAGE together with the computed GPS-estimated direct path towards the BS for a driven fragment of the road, after removing the impact of the vehicle's heading direction. As can be noticed, there are multiple fragments where estimated angle gradually changes with the driven distance and signal tracking seems feasible. As measurements were conducted over large distances, for each driven road there are multiple positions where serving cell changed. This can be noticed on the figure with abrupt changes of the GPS-based geometrical direct path. The first step is to split the recorded data into chunks of continuous snapshots connected the same serving cell. In order to facilitate the studies on tracking techniques, only the chunks of the road containing minimum ten continuous snapshots were used. Please note that due to varied speed of the vehicle, the distance between snapshots is not uniform distributed.

To study the quality of beam tracking algorithms, the metric called *beam failure distance* is defined and shown on Figure E.1. For each snapshot, the difference between the estimated angle using tracking techniques and the real

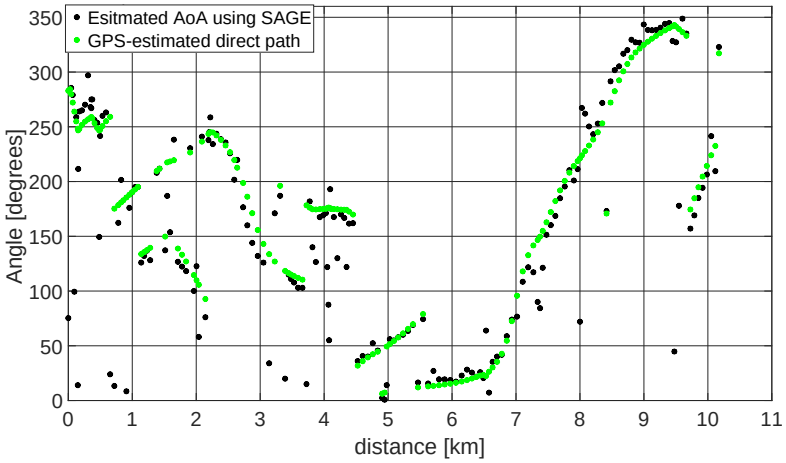

Fig. E.4: The estimated AoA compared with GPS-based to the BS

AoA found based on the direction acquisition of the strongest path estimated using SAGE is computed as a *tracking error*. Assuming the vehicle will center the uplink beam towards the estimated angle, we check if the tracking error is lower than the half of the HPBW. In such a case even though the uplink beam is not precisely centered, more than half of the transmitted energy will propagate towards estimated AoA. In case the tracking error is higher than HPBW, it is assumed that beam tracking failed and the beam failure distance has been reached. In this situation direction acquisition as explained in Section E.2 is required. Please note, that our definition of the beam failure distance is less strict that the beam coherence time defined in [12], as we do not rely on the alignment with the BS's beam but only on its physical location.

E.5 Performance analysis

E.5.1 Acquisition of beamforming direction

Figure E.5 presents the Empirical Cumulative Distribution Function (ECDF) of the computed downlink SINR for the signals beamformed towards the acquired directions using the AoA estimation and downlink-based beam sweeping. Additionally, the performance of blind beamforming towards the GPS-estimated direct path and single antenna receiver are added as a reference to compare the loss with respect to the AoA estimation. Due to the reasons explained in Section E.2, downlink-based beam sweep provides up to 1.6 dB median SINR gain over an AoA-based beamforming and 5 dB gain

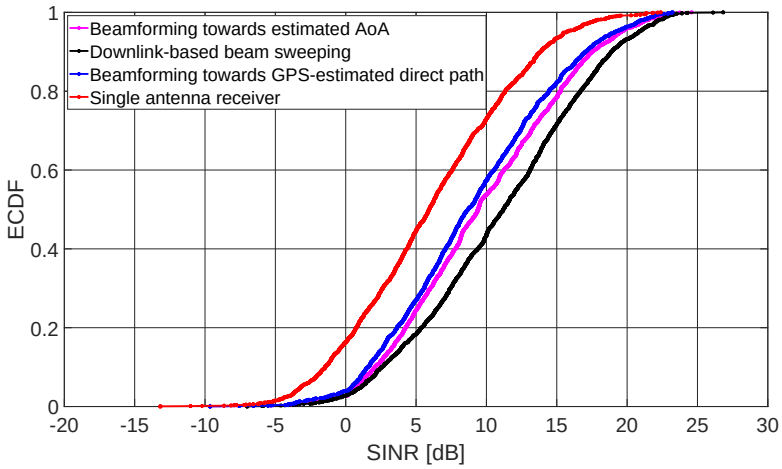

Fig. E.5: Comparison of downlink performance of direction acquisition techniques in suburban and rural scenarios

over a single antenna system. Quite surprisingly, centering the beam towards the estimated AoA provides only a slight gain versus centering the beam on the GPS-estimated direct path. This can be explained, as in more than 70% of the snapshots estimated AoA was approximately the same as the direct path. Please note that measurements were taken in the rural and suburban areas where the likelihood of main AoA coinciding with the direct path is higher than in the dense urban scenarios.

Although, one should not expect that the presented downlink SINR would fully reflect the observed uplink SINR at the BS due to the presence of multiple users and different interference patterns, the presented trends should persist in the rural and suburban areas where interference is limited. Based on the obtained results, it is clear that the downlink-based beam sweep is more reliable method for direction acquisition than AoA estimation. Moreover, if sweeping operation is not possible, centering the beam towards the GPS-estimated direct path to the BS should be considered in place of AoA estimation due to reduced computational cost and similar performance.

E.5.2 Signal tracking techniques

Figure E.6 compares the performance of studied signal tracking techniques for different widths of the beam. The ECDF of the beam failure distance - the distance when tracking error became larger than the half of the HPBW are presented. As expected, for both techniques, the wider the beam, the longer the tracking distance, as better is the tolerance for the small tracking

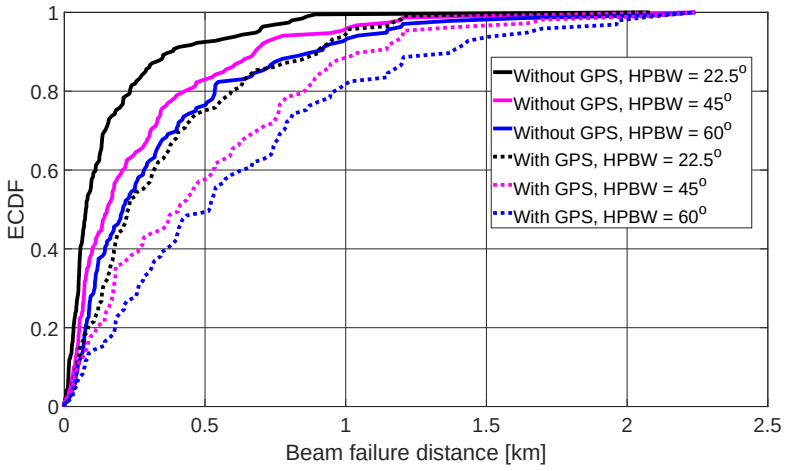

Fig. E.6: Maximum tracking distance in suburban and rural scenarios

Table E.1: Periodicity of direction acquisition methods based on the computed tracking distance for various speeds

Periodicity of direction acquisition						
	With GPS information			**No GPS information**		
Speed/HPBW	60°	45°	22.5°	60°	45°	22.5°
30 km/h	62 s	49 s	27 s	24 s	18 s	9 s
50 km/h	37 s	29 s	16 s	14 s	11 s	5 s
80 km/h	23 s	18 s	10 s	9 s	7 s	3 s
100 km/h	19 s	14 s	8 s	7 s	5 s	2.5 s

errors. This results in a trade-off between directional gain of the array and the tolerance for the direction mismatch. Using the narrowest beam (22.5°) and exploiting the GPS coordinates of the BS, in 50% of the cases the tracking distance is longer than 220 m. With the wider beams, median tracking distance can stretch out to 400 m for 45° HPBW or 500 m if HPBW is 60°. Table E.1 presents the required periodicity of triggering direction acquisition methods for different vehicle speeds computed based on the median beam failure distance.

As can be noticed, there is a significant improvement if the GPS coordinates of the BS are used for the tracking. This can be explained, as in most parts of the driven roads, the distance to the BS was not constant and varied from positions very close to the BS where angle change was large even for small driven distances, up to positions located far away from the serving cell, where this change was negligible. The knowledge of BS's location and

therefore the distance helps to improve the tracking performance such that the expected periodicity of direction acquisition procedure can be extended. In all cases the median tracking distance is in a range of seconds, allowing the time consuming direction acquisition techniques to be performed less frequently or more accurately by, for example, allowing more iterations of SAGE algorithm or more precise beam scan. The upper-bound limits of the tracking performance are constrained by the coverage of the serving cell and the amount of continuous snapshots being recorded.

Focusing on the low tail presented at the Figure E.6, in more than 20% of the cases the tracking distance is shorter than 200 m. This situation can partially be justified, due to the assumed methodology. The tracking error is computed as a difference between estimated angle and computed AoA. For some parts of the road, due to the multipath propagation, the real AoA of one of the first estimated snapshots (after the warm up phase) was computed from the unexpected direction (as can also be seen at the beginning of Figure E.4), leading to instant beam tracking failure. It is expected, that by extending the warm up phase to more than two snapshots or by reducing the distance d between direction estimations the tracking performance would be improved.

E.6 Conclusions

In this paper the concept of uplink beamforming for vehicular communications using sub-6 GHz bands is analyzed. Different methods of direction acquisition and techniques for signal tracking are discussed. Presented concepts are experimentally evaluated based on live LTE signals recorded during extensive measurement campaigns. The results show that beamforming towards the direction found using the downlink-based beam sweep should lead to improved performance over an AoA estimation. In rural and suburban scenarios, the acquired direction was found to be tractable over large distances in the range of hundreds of meters, extending the required direction acquisition periodicity to tenths of seconds. The availability of GPS coordinates of the serving cell can further improve the tracking performance and lead to more than a 100% improvement of tracking distance versus schemes which do not use information on the GPS coordinates of the BS. Results presented in this paper show that the sub-6 GHz uplink beamforming can be a feasible technology to enhance uplink coverage for the vehicular communication.

References

[1] M. Boban, A. Kousaridas, K. Manolakis, J. Eichinger, and W. Xu, "Connected roads of the future: Use cases, requirements, and design considerations

for vehicle-to-everything communications," *IEEE Vehicular Technology Magazine*, vol. 13, no. 3, pp. 110–123, Sept 2018.

[2] Nokia, "White paper: 5G deployment below 6 GHz. ubiquitous coverage for critical communication and massive IoT," https://onestore.nokia.com/asset/201315, 2017.

[3] S. Husain, A. Kunz, A. Prasad, K. Samdanis, and J. Song, "An overview of standardization efforts for enabling vehicular-to-everything services," in *2017 IEEE Conference on Standards for Communications and Networking (CSCN)*, Sept 2017, pp. 109–114.

[4] S. Lien, Y. Kuo, D. Deng, H. Tsai, A. Vinel, and A. Benslimane, "Latency-optimal mmwave radio access for v2x supporting next generation driving use cases," *IEEE Access*, vol. 7, pp. 6782–6795, 2019.

[5] T. Izydorczyk, F. M. L. Tavares, G. Berardinelli, M. Bucur, and P. Mogensen, "Performance evaluation of multi-antenna receivers for vehicular communications in live LTE networks," *Accepted at Vehicular Technology Conference (VTC2019-spring)*, May 2019.

[6] C. F. Mecklenbrauker, A. F. Molisch, J. Karedal, F. Tufvesson, A. Paier, L. Bernado, T. Zemen, O. Klemp, and N. Czink, "Vehicular channel characterization and its implications for wireless system design and performance," *Proceedings of the IEEE*, vol. 99, no. 7, pp. 1189–1212, Jul 2011.

[7] B. H. Fleury, D. Dahlhaus, R. Heddergott, and M. Tschudin, "Wideband angle of arrival estimation using the SAGE algorithm," in *IEEE 4th International Symposium on Spread Spectrum Techniques and Applications Proceedings*, vol. 1, Sept 1996, pp. 79–85.

[8] "Evolved universal terrestrial radio access (E-UTRA); user equipment (UE) radio transmission and reception," 3GPP, Tech. Rep. TS 136 101 V14.3.0, Apr 2017.

[9] "LTE evolved universal terrestrial radio access (E-UTRA) physical layer procedures," 3GPP, Tech. Rep. TS 36.213 version 14.2.0 Release 14, Apr 2017.

[10] T. Izydorczyk, M. Bucur, F. M. L. Tavares, G. Berardinelli, and P. Mogensen, "Experimental evaluation of multi-antenna receivers for UAV communication in live LTE networks," *Globecom workshop on Wireless Networking and Control for Unmanned Autonomous Vehicles*, Dec 2018.

[11] T. Izydorczyk, F. M. L. Tavares, G. Berardinelli, M. Bucur, and P. Mogensen, "Angular distribution of cellular signals for UAVs in urban and rural scenarios," *Accepted at European Conference on Antennas and Propagation (EuCAP 2019)*, Mar 2019.

[12] V. Va, J. Choi, and R. W. Heath, "The impact of beamwidth on temporal channel variation in vehicular channels and its implications," *IEEE Transactions on Vehicular Technology*, vol. 66, no. 6, pp. 5014–5029, Jun 2017.

Paper F

Enhancing vehicular link performance using directional antennas at the terminal

Michel Massanet Ginard, Tomasz Izydorczyk, Preben Mogensen and Gilberto Berardinelli

The paper has been published in the
IEEE GLOBECOM workshops proceedings, 2019.

The layout has been revised.

Abstract

Cellular networks will be one of the main pillars in the development of future vehicular communications. However, Downlink (DL) and Uplink (UL) channels must be improved to cope with the required reliability and high throughput of the coming vehicular use cases. Vehicle side solutions which benefit from the high antenna gains could improve the performance of the UL channel whose coverage is limited by UL transmit power. In this paper we experimentally evaluate the performance of a directional antennas switching system based on live Long Term Evolution (LTE) measurements. A total of more than 150 km have been driven comprising different radio propagation scenarios. The results show considerable improvements of Reference Signal Received Power (RSRP) and Reference Signal Received Quality (RSRQ), together with a reduction of handovers specially in scenarios with high Line-Of-Sight probability. Additionally, it has been found that the UL throughput does not improve with the increase of antenna gain probably due to the UL Power Control mechanism used in LTE.

F.1 Introduction

Future vehicular communication systems will be required to deal with high Uplink (UL) and Downlink (DL) data rate demands together with reliable connectivity. Cooperative sensing and awareness, teleoperated driving or infotainment are some examples in which the required UL throughput can reach up to 25 Mbps [1].

The next 5th Generation (5G) radio technology is expected to cope with a plethora of services with diverse requirements, including vehicular communication [2,3]. Previous studies have proposed the use of Base Station (BS) adaptive beamforming in sub-6 GHz bands [4] and the exploitation of the millimeter wave spectrum [5] to increase the system throughput. However, their practical deployment is subjected to the computation complexity of the Angle of Arrival (AoA) and the reduction of range with the increase of frequency. This could be counteracted by the massive deployment of Road Site Units which would improve the coverage and throughput at the cost of increased number of handovers, latency and cost-inefficiency if deployed in low-populated areas. The use of Vehicle to Vehicle (V2V) communications by means of using surrounding vehicles as relays in order to leverage better channel conditions is proposed in [6]. Nevertheless, its performance is considerably affected in scenarios with low density of vehicles or in congested systems.

Long Term Evolution (LTE) is another suitable system whose already deployed infrastructure, scalability and ubiquitous accessibility make it a potential candidate to serve the vehicular use cases. This technology is

also well-suited to experimentally study potential solutions which would be later applicable in future 5G networks. Authors in [7] have shown the coverage challenge in vehicular scenarios through Reference Signal Received Power (RSRP) measurements. The presented results demonstrate insufficient range for many vehicle data applications. Besides that, UL coverage is even more critical due to the limited UL transmit power.

Alternative solutions applied from the vehicle side become attractive for car vendors due to their possible implementation without standardization. In [8], authors have shown the potential DL Signal to Interference and Noise Ratio (SINR) gains of using receive beamforming on the vehicle side. However, receive beamforming requires expensive and synchronized hardware equipment in addition to high computational complexity of AoA estimation. The use of directional antennas at the vehicles is a well-known [9] alternative to beamforming. Its implementation is much simpler though it presents limitations of the available pointing directions. Although previous approaches have considered the theoretical potential of this solution, upcoming high throughput vehicular use cases claim for the experimental evaluation of its performance.

In this work we experimentally evaluate the use of a switched-based system of directional antennas on the vehicle terminal in both UL and DL. We compare the performance of the switching antenna system with a benchmark case of omni-directional antenna configuration. We conduct measurements of RSRP and Reference Signal Received Quality (RSRQ) by the vehicle terminal in live LTE networks. The measurements include a wide variety of different radio propagation scenarios where the solution could be deployed. Furthermore, we investigate the impact of the antenna gain over the UL throughput and the Handovers (HOs) performance.

The reminder of this paper is structured as follows: Section F.2 describes the measurement equipment and the antenna switching methodology. The campaign itself is described in Section F.3. Section F.4 compares the results of the directional and omni-directional antennas systems analyzing the signal strength and quality, UL throughput and the mobility performance. Then, Section F.5 discusses main findings. Finally, Section F.6 concludes the paper.

F.2 Measurement methodology

F.2.1 Measurement equipment

The measurement equipment consists of a switching antenna system with six directional antennas connected to a LTE modem through a Single Pole, 8 Throw (SP8T) Radio Frequency (RF) switch. The system is controlled by an embedded computer which interacts with the LTE modem, RF switches

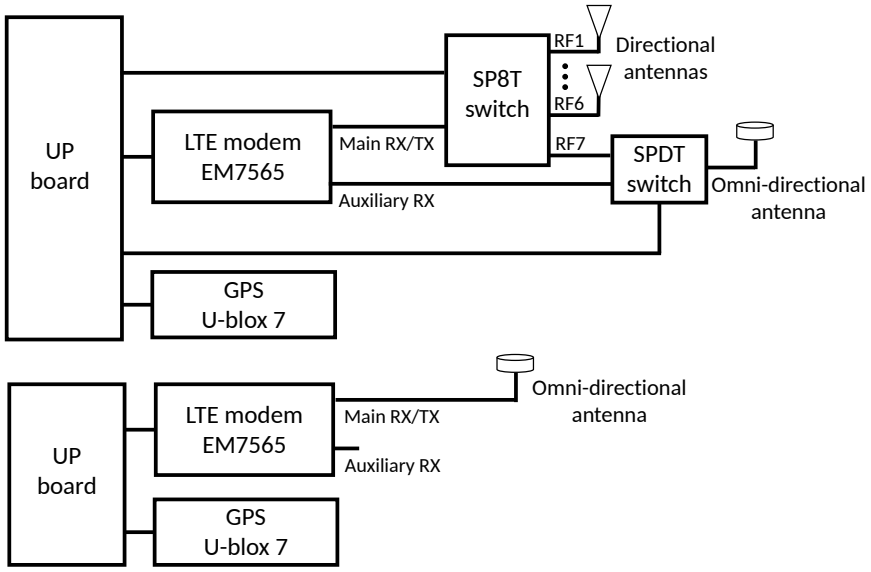

Fig. F.1: Measurement equipment setups for the directional (top) and omni-directional (bottom) antennas configurations

and a Global Positioning System (GPS) receiver. For comparison purposes, a second system is used consisting of an omni-directional antenna attached directly to the second LTE modem. Both systems as shown on Figure F.1 are independent from each other. The antennas of both systems are mounted on the roof of a van as shown on Figure F.2.

Antennas

Six *SENCITY Spot-S Railway Cellular* directional antennas are used. They have 8 dBi of peak gain at the target frequency 1.8 GHz chosen as most densely deployed LTE band in Denmark. The 3 dB beamwidth of each antenna is 70°. As shown on Figure F.3, the antennas are positioned on a roof of the vehicle following the hexagon pattern covering sectors of 60°. Please note that the discrepancy between the nominal 3 dB beamwidth and the width of the sector causes a desired overlap between sectors in case of the potential GPS inaccuracies.

In the second system, an omni-directional *SmartDisc* antenna with a 3.15 dBi gain is utilized. The same antenna model is also used as the supplementary receive diversity antenna in the directional system (Figure F.1). Its purpose is described later in Section F.2.3. Directional antennas have 4.75 dB higher gain than the omni-directional antenna. This difference must be considered in the RSRP and RSRQ performance comparison.

Fig. F.2: A measurement vehicle with the antenna structure on the roof

LTE modem

The *AirPrime EM7565* LTE Cat-12 embedded cellular modem is utilized to provide LTE connectivity and measurement reports of the RSRP and RSRQ of the serving cell. It has one main RF port for DL/UL transmissions and one auxiliary RF port for enabling receive diversity. This downlink-only port, disabled in the omni-directional system as having no effect on the uplink, is used in the directional setup to improve the mobility performance of the modem as explained in the next Section. The modem is set to operate only in the LTE mode at band 3 (1.8 GHz).

RF Switches

Two RF switches are used in the system of directional antennas. The SP8T switch is used for selecting among the six directional antennas. Its input port is connected to the main RF port of the modem and its outputs to the six directional antennas and to the Single Pole, Double Throw (SPDT) switch. The purpose of of the SPDT switch is to interconnect the omni-directional antenna to the auxiliary RF port of the modem as a receive diversity antenna or through the SP8T switch to the main RF port where is used for the initial BS attachment procedure. This procedure will be further addressed in Section F.2.3.

Other modules

For the interaction between hardware modules an *UP board* is used as an embedded controller. Additionally, the *u-blox 7 GNSS* receiver obtains the geographical coordinates and orientation of the vehicle with 5 Hz update rate. These information are later used in the antenna selection process.

F.2.2 Antenna switching methodology

The antenna selection algorithm is based on the known GPS location of the serving BS and the position of the vehicle terminal. The selected antenna is the one which best points in the shortest geometrical direction towards the serving cell. The six antennas are divided in sectors of 60^{o} which define the switching bounds between antennas. The real-time algorithm continuously obtains the serving Cell ID from the LTE modem. For every GPS update, it calculates the angle of the shortest path between BS and the vehicle accounting for its present orientation (direction of travel). The angle is translated into the selection of one of the antenna sectors. Readers can refer to the example illustrated on Figure F.3 to observe how the antenna is selected according to the vehicle orientation and location.

It can be observed that the knowledge of the BS's location is indispensable since without this information proposed methodology could not be applied and would have to be replaced by other techniques like periodic beam-sweeping or AoA estimation. The proposed method assumes that the strongest signal comes from the direct path between the vehicle terminal and the serving cell. This assumption is valid in Line-Of-Sight (LOS) scenarios predominant in rural and suburban scenarios. However when direct path is obstructed (None-Line-Of-Sight (NLOS) conditions, dominant in dense urban deployments), the strongest signal might come from a completely different direction. In these conditions, the performance of the proposed system could degrade. However as shown using ray-tracing simulations in [10], even in NLOS urban scenarios there can be a time-distance correlation of AoA usually still coming from angles similar to LoS.

F.2.3 Initial cell attachment and mobility performance

The use of directional-antennas can influence the initial cell attachment. At the start of the system, the modem has to acquire the LTE connection to the cell which presents the best radio link. Directional antennas might influence the initial attachment by means of the gain into the pointing direction. In a possible unlucky scenario, a modem initialized using a directional antenna in a given direction can attach to a suboptimal far-located cell even though there is a much stronger candidate in a different direction coinciding with the null of the chosen antenna beam pattern. To mitigate this potential suboptimal

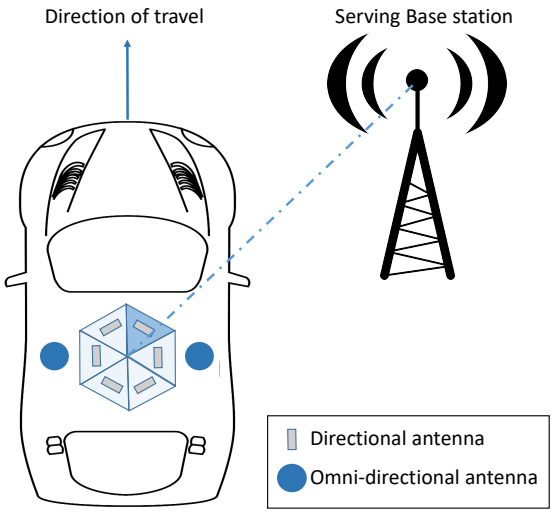

Fig. F.3: Antenna selection with the 6 directional antennas

choice of the serving cell, in this work first the omni-directional antenna is connected to the main RF port of the modem and is used for the initial cell attachment. Only after acquiring the network connectivity, the antenna is switched and the directional one is used towards the direction of the serving cell.

Mobility management is another aspect influenced by using directional antennas. In cellular systems network triggers the HO decision based on the measurement reports from the modem. Using directional antenna would enhance/mitigate the measured neighbor signals power from some directions leading to changed mobility pattern. In some situations, as shown later in this work, it may be a desired behavior as a modem can longer remain connected to the same cell reducing the handover rate. However in some other situations it may downgrade the network performance as the modem would prolong the connection to a weak cell overlooking the more suitable one in the direction where antenna null is located. As a trade-off, in this work the omni-directional antenna used first for the initial attachment, is later connected to the modem's auxiliary RF port. In this way, using receive diversity mode, the modem in its measurement reports, report the best neighbor signal power received among two different antenna ports. In this situation the nulls of the directional antenna are mitigated, however its directionality behavior is preserved. Please note again, that the auxiliary RF port is downlink only and the omni-directional antenna does not influence the uplink studies of this work.

Table F.1: Characteristics of the measured environment [8]

Route index	Measurement environment	Short description
Route 1	Dominant rural and suburban	Small houses and meadows, seldom deployed Base Stations (BS)
Route 2	Highway and urban	Blocks up to the 3rd floor in the urban part, medium density of BS
Route 3	Highway and dense urban	Blocks up to the 6rd floor, high density of BS
Route 4	Suburban	University buildings, high density of BS

F.3 Measurement campaign and post-processing

F.3.1 Measurement campaign

The measurement campaign was conducted in Aalborg, Denmark. Four routes with different radio propagation environments were driven as described in Table F.1. The driven roads comprise a total of more than 150 km and the speed of the vehicle varied from 0 km/h in urbanized areas up to 100 km/h in the highway. Readers can refer to [8] for further details on the driven routes. The LTE connectivity was provided by a Danish network operator whose BSs locations were known. While driving, omni-directional and directional antennas systems were simultaneously measuring RSRP and RSRQ metrics with 500 ms periodicity such that more than 16000 measurements were collected. In both systems, a continuous full-buffer UL transmission was carried out and UL throughput was measured by the controller.

F.3.2 Post-processing

Prior to the analysis, the recorded data is filtered in the post-processing. When a HO occurred, some instances of RSRP and RSRQ were measured before the antenna was effectively switched towards the new BS location. These values have been filtered to ensure that the measured RSRP and RSRQ correspond to the time traces where the directional antenna was pointing into the desired direction. Additionally, the omni-directional and directional systems differ from signal attenuation introduced by the hardware modules between antennas and RF ports (see Figure F.1). Since the RSRP is measured in the modem RF port, the reported values are altered. Hence the RSRP values have been compensated to include the impact of the antenna gain.

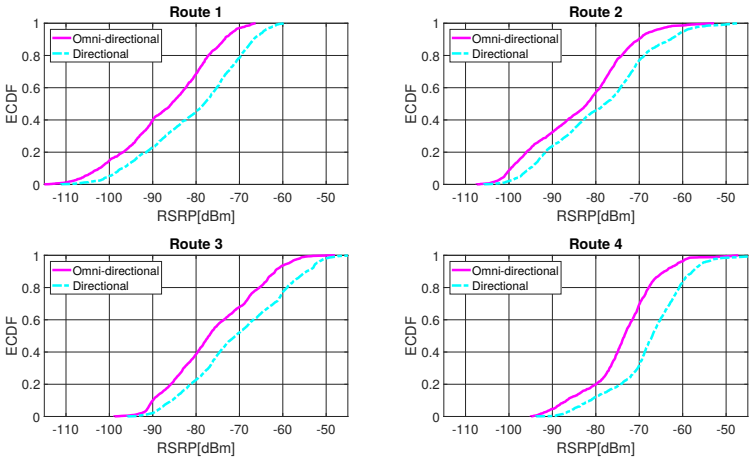

Fig. F.4: ECDFs of the measured RSRP of the serving cell

F.4 Results

F.4.1 RSRP and RSRQ

The following results comparing downlink RSRP and RSRQ for both systems are showed for the time instances in which both systems are connected to the same serving BS (more than 85% of snapshots). The Empirical Cumulative Distribution Functions (ECDFs) of the measured RSRP in the four driven routes are presented on Figure F.4. A continuous gain on the measured RSRP by directional antennas with respect to the omni-directional case can be observed. This gain is slightly reduced in the more urbanized scenarios (Routes 2 and 3) due to higher probability of NLOS. The observed median gains in three routes are slightly higher than expected theoretical antenna gain difference (4.75 dB). This may be due to the constructive fast fading of the channel. The effects of the destructive fading, or the NLOS propagation are mitigated due to the use of an auxiliary omni-directional antenna in the directional system which observes independent channel due to physical separation from the directional system. In general, routes 3 and 4 present the largest RSRP values due to high density of BSs in these scenarios. Route 1 shows the lowest values due to longest distance to the serving BSs common in rural scenarios.

The signal quality enhancement can be assessed by means of the RSRQ. The ECDFs of the measured RSRQ are presented on Figure F.5. With the use of directional antennas, the RSRQ experiences a constant gain over the omni-directional antenna case of approximately 1 dB. Hence, the directional-

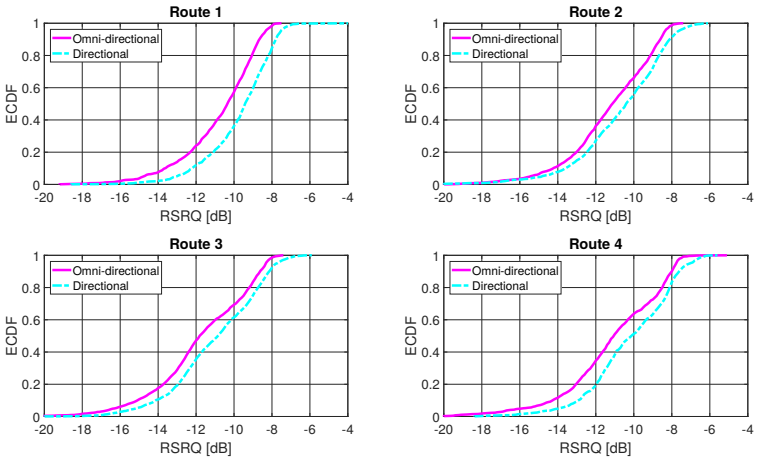

Fig. F.5: ECDFs of the measured RSRQ of the serving cell

ity of the antennas not only improves the signal strength, but also the quality thanks to the attenuation of interfering signals coming from different directions than the serving BS.

F.4.2 UL Throughput

A full-buffer UL transmission let us assess the UL throughput performance. Although, in this work, the instantaneous cell load information was not accessible, due to the sufficient amount of samples, one can assume the similar average load and therefore fair comparison between both antenna systems. The ECDFs of the UL throughput in the different scenarios are shown on Figure F.6. The observed plots show almost no UL throughput improvement with the use of directional antennas, which contradicts the experienced improvement of the DL channel by means of RSRP and RSRQ gains.

The UL throughput performance could be affected by the UL Power Control (PC). In LTE, the Open-loop UL PC scheme [11] is primarily used for compensating the channel Path-Loss (PL). As the network is not aware of the vehicle's antenna system, its directional gain is observed by the reduced PL and fully-compensated by UL transmit power reduction. Only in scenarios with high PL, the transmitted power can reach the maximum allowed value (23 dBm). In those conditions, the UL transmitted power remains constant and a throughput gain should be observed. However, very high PL scenarios correspond to RSRP values much below -100 dBm which are barely experienced in our results.

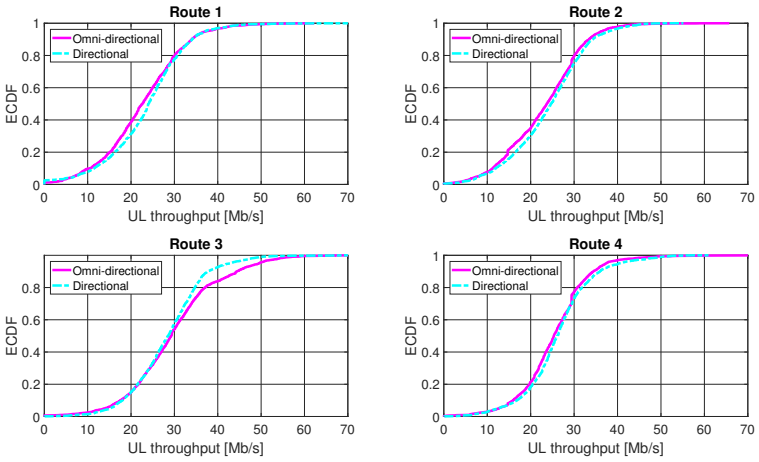

Fig. F.6: ECDFs of the measured UL throughput of the serving cell

F.4.3 Mobility performance

The measured values of RSRP are reported to the network to be used as inputs in the mobility management. The gains in RSRP indicate the improved radio link with serving BS for longer time and can potentially lead to the reduction of observed HOs resulting in lower latency and higher reliability as number of potential failed HOs or radio link failures would also be reduced. The number of performed HOs on each route is shown on Figure F.7. A considerable reduction of HOs of 57.1% and 42.8% is observed in Routes 1 and 4 while almost no reduction is observed in Routes 2 and 3. This is explained by the higher probability of LOS links in Routes 1 and 4 leading to extended attachment to the same cell, whereas in Routes 2 and 3 (the urbanized environments) due to the BS density and NLOS propagation frequent HOs are still observed.

F.5 Discussion

Directional antennas have shown a potential improvement in the DL communication with RSRP and RSRQ gains as well as HO reduction. As expected, higher gains/reduction is observed in the rural and suburban environments where directional systems are expected to be most beneficial. Despite lower gains and no handover reduction in the urban scenario, it is worth to recall that the uplink related coverage and reliability issues are not as harmful as in the rural scenarios as other network-side techniques may be used to eliminate the problem.

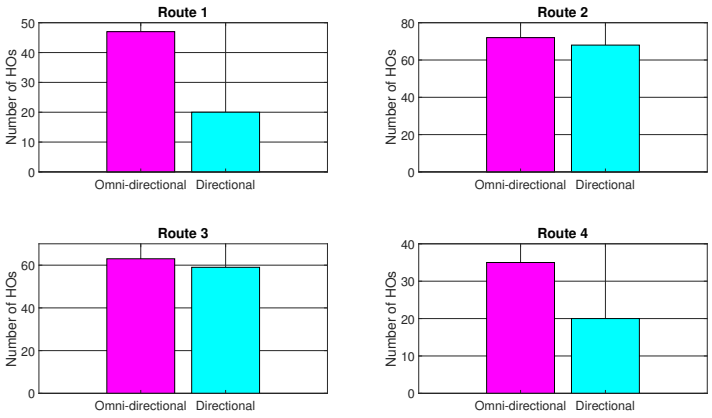

Fig. F.7: Number of successful HOs

The UL throughput performance has experienced no improvement regardless the difference of the antenna gain. This finding is also valid in case any beamforming technique is used in place of directional antennas. It leads to the conclusion that without the network knowledge of the antenna system used by the vehicle, there will be no visible improvement for the car manufacturers of using an advanced antenna system. However, already today, if the network is aware of the problem, communication standards can enable the possibility to circumvent this issue. The so-called user specific closed-loop power control scheme can be used to differentiate users and avoid discounting the transmit power to those benefiting from high antenna gains [11].

F.6 Conclusions

We have experimentally evaluated the performance of a directional antennas switching system implemented in the vehicle terminal. The DL performance has been analyzed with RSRP and RSRQ measurements. Comparing with an omni-directional antenna, directional antennas improved the RSRP in more than 4.75 dB (antenna gain difference) in LOS scenarios. The RSRQ was also improved with an average gain of 1 dB. The improvement of the mobility performance has been corroborated with a HOs reduction of almost 50 % in rural and suburban scenarios. In urbanized scenarios the reduction of HOs is insignificant due to NLOS situations. However, the enhancement of the DL metrics is not translated into an increase of the UL throughput. This is likely due to LTE power control mechanisms which aims at similar receive power levels for all the served UEs.

References

[1] M. Boban, A. Kousaridas, K. Manolakis, J. Eichinger, and W. Xu, "Connected roads of the future: Use cases, requirements, and design considerations for vehicle-to-everything communications," *IEEE Vehicular Technology Magazine*, vol. 13, no. 3, pp. 110–123, September 2018.

[2] S. Husain, A. Kunz, A. Prasad, K. Samdanis, and J. Song, "An overview of standardization efforts for enabling vehicular-to-everything services," in *2017 IEEE Conference on Standards for Communications and Networking (CSCN)*, September 2017, pp. 109–114.

[3] "C-ITS vehicle to infrastructure services: how C-V2X technology completely changes the cost equation for road operators," 5GAA Automotive Association, Tech. Rep., January 2019.

[4] I. Maskulainen, P. Luoto, P. Pirinen, M. Bennis, K. Horneman, and M. Latva-aho, "Performance evaluation of adaptive beamforming in 5G-V2X networks," in *2017 European Conference on Networks and Communications (EuCNC)*, June 2017, pp. 1–5.

[5] S. Lien, Y. Kuo, D. Deng, H. Tsai, A. Vinel, and A. Benslimane, "Latency-optimal mmwave radio access for v2x supporting next generation driving use cases," *IEEE Access*, vol. 7, pp. 6782–6795, 2019.

[6] H. Ishikawa, E. Okamoto, S. Okamoto, H. Okada, and S. Makido, "Performance analysis of uplink v2i cooperative transmission scheme in practical road environments," in *2019 International Conference on Information Networking (ICOIN)*, January 2019, pp. 98–102.

[7] T. Berisha, G. Artner, B. Krasniqi, B. Duriqi, M. Muçaj, S. Berisha, P. Svoboda, and C. F. Mecklenbräuker, "Measurement and analysis of LTE coverage for vehicular use cases in live networks," in *2017 IEEE-APS Topical Conference on Antennas and Propagation in Wireless Communications (APWC)*, September 2017, pp. 260–263.

[8] T. Izydorczyk, F. M. L. Tavares, G. Berardinelli, M. Bucur, and P. Mogensen, "Performance evaluation of multi-antenna receivers for vehicular communications in live LTE networks," *Vehicular Technology Conference (VTC2019-spring)*, May 2019.

[9] R. Kronberger, H. Lindemier, L. Reiter, and J. Hopf, "Smart antenna application on vehicles with low profile array antennas," in *IEEE Antennas and Propagation Society International Symposium*, vol. 2, July 2000, pp. 956–959 vol.2.

[10] F. Ademaj, S. Schwarz, K. Guan, and M. Rupp, "Ray-tracing based validation of spatial consistency for geometry-based stochastic channels," in *2018 IEEE 88th Vehicular Technology Conference (VTC-Fall)*, August 2018, pp. 1–5.

[11] C. Ubeda Castellanos, D. L. Villa, C. Rosa, K. I. Pedersen, F. D. Calabrese, P. Michaelsen, and J. Michel, "Performance of uplink fractional power control in UTRAN LTE," in *VTC Spring 2008 - IEEE Vehicular Technology Conference*, May 2008, pp. 2517–2521.

Paper G

Experimental evaluation of beamforming on UAVs in cellular systems

Tomasz Izydorczyk, Michel Massanet Ginard, Simon Svendsen, Gilberto Berardinelli and Preben Mogensen

The paper has been submitted to
IEEE 92nd Vehicular Technology Conference (VTC2020-Fall), 2020.

The layout has been revised.

Abstract

The usage of beamforming in Unmanned Aerial Vehicles (UAVs) has the potential of significantly improving the air-to-ground link quality. This paper presents the outcome of experimental trial of such a UAV-based beamforming system over live cellular networks. A testbed with directional antennas has been built for the experiments. It is shown that beamforming can extend the signal coverage due to antenna gain, as well as spatially reduce interference leading to higher signal quality. Moreover, it has a positive impact on the mobility performance of a flying UAV by reducing handover occurrences. It is also discussed, in which situations beamforming should translate into the uplink throughput gain.

G.1 Introduction

Unmanned Aerial Vehicles (UAVs) will require a reliable and high uplink throughput communication link to ensure flight's safety and serve foreseen use cases such as package delivery or surveillance [1]. For example, up to 50 Mbps of continuous uplink throughput will be required to send uncompressed video from a UAV to a cloud for machine learning image processing [2].

Cellular systems including Long Term Evolution (LTE) are a potential candidate to cope with the stringent requirements and provide worldwide connectivity to UAVs. However increased Line of Sight (LoS) probability towards interfering base stations due to lack of obstructions in the Air-to-Ground (A2G) channel results in a Signal-to-Interference plus Noise Ratio (SINR) reduction [3]. In the downlink, the interference will result in lower service reliability for a UAV, while higher uplink interference radiated by a UAV to the network will result in decreased performance of other incumbents of the cellular systems, such as ground users or other UAVs.

There are many proposed solutions on how to deal with interference while maintaining UAV connectivity. In [4] and [5] authors discuss how massive Multiple Input Multiple Output (MIMO) and 3D beamforming at the base stations can be utilized for UAV connectivity. In [6] and [7] authors claim that Non-Orthogonal Multiple Access (NOMA) and cell-free massive MIMO can outperform 3D beamforming and provide even better UAV connectivity. Finally, there are multiple [8,9] attempts to optimize the path of a flying UAV in order to contain the radiated/absorbed interference.

Use of multiple antenna techniques at a UAV, such as beamforming, is yet another foreseen solution which in addition does not require any network hardware changes. Simulations in [10] showed the potential of UAV-side beamforming to boost signal strength while spatially reducing interference towards unwanted directions. However this benefits were only shown in

simulation and no experimental validation is available in the literature.

Practical implementation of a beamforming system is a non-trivial task due to space/weight/power constraints of the UAV. Use of directional antennas is one possible simplification of beamforming. Although it reduces the arbitrary number of directions to the number of antennas, it facilitates the development time and cost of the hardware platform, accelerating research activities.

In this work, a complete design of a flexible UAV testbed using directional antennas for beamforming evaluation is presented and further used in a measurement campaign to understand the promises of uplink directional communication for cellular-connected UAVs. The contributions of this paper are twofold. First, to the best of the authors knowledge, it is the first paper explaining in detail the hardware implementation of a UAV-based directional antenna's switching system. Second, this paper contains the measurement results of a first trial of beamforming-enabled UAV flying over real cellular networks, discussing insights and potential benefits of this technology.

The rest of the paper is structured as follows. In Section G.2 the high-level system design is presented together with the remarks on the flexibility aspects of the platform. It is followed by Section G.3 focused on the implemented beam steering algorithm. Section G.4 describes the results of a measurement campaign conducted using live cellular networks. The discussion on potential benefits of uplink beamforming is made in Section G.5.

G.2 System Design

The proposed system was designed to operate using live cellular networks with the target of being used for a number of different research activities from Path Loss (PL) measurements and interference characterization up to uplink throughput studies. The system as presented in Figure G.1 is composed of an antenna array, consisting of six directional patch antennas and a monopole omni-directional antenna. Two Radio Frequency (RF) switches, an embedded computer and a LTE modem complement the design. When flying, the system can either operate autonomously with the mission (trajectory, switching algorithm, data transmission etc.) programmed on the embedded computer or directly controlled from the ground using Secure Shell (SSH) connection. This design was initially inspired by [11], where an array of directional antennas was used to establish WiFi connectivity.

The testbed was mounted using a customized carbon fiber structure on a DJI M600 drone. Its total weight is approximately 2 kg, allowing for more than 35 minutes of continuous flight time. It can be powered using a simple power bank as all components accept a standard 5V power source. The final assembled setup is shown in Figure G.2.

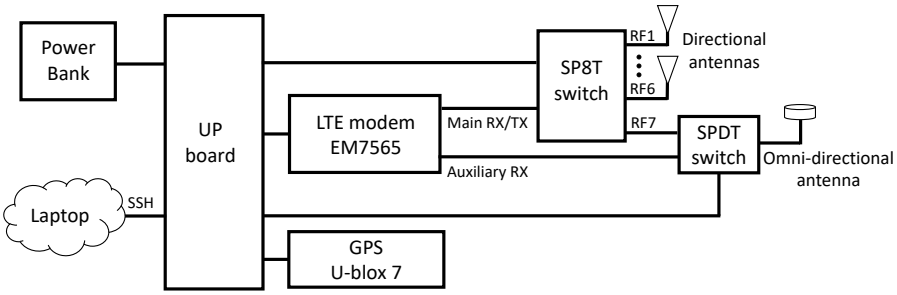

Fig. G.1: Schematic of the designed testbed

Fig. G.2: Assembled setup on a UAV

Two RF Switches are used. Single Pole 8 Throw (SP8T) switch connects all antennas (omni and directional) to the main antenna port of the LTE modem. Single Pole Double Throw (SPDT) switch connects the omni-directional antenna to its auxiliary port. Switches are controlled by the embedded computer built based on Intel's *UP board*.

The cellular modem used in the platform is a *Sierra Wireless EM7565*. Please note that the modem is not only used to provide the network (and SSH) connectivity, but it is also used to provide valuable network information which can be used for research purposes. These include among others measurement reports from up to eight cells, quantified as Reference Signals Received Power (RSRP), Reference Signal Received Quality (RSRQ), Received

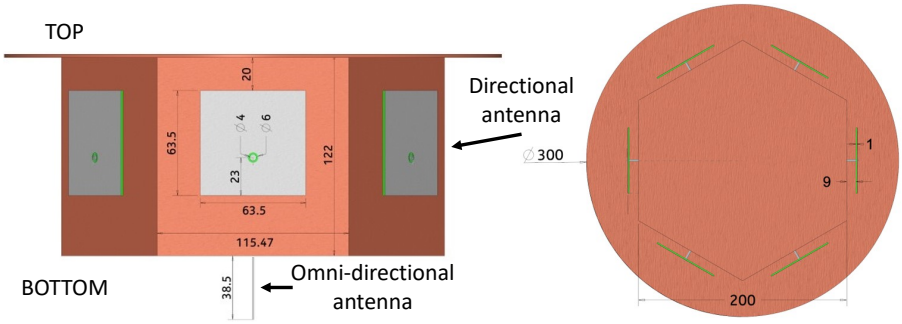

Fig. G.3: Designed antenna array side and top view

Signal Strength Indicator (RSSI) and SINR. Moreover the information of the serving cell is accessible and can be used, for example to quantify a number of network handovers.

In this work, the modem is set to operate in LTE-only mode in the desired band 3 (1.7 GHz uplink and 1.8 GHz downlink frequencies). The auxiliary antenna port can be used as a receive diversity port as explained later in Section G.3. It can be activated within a modem using AT commands. GPS information is acquired from the *Ublox-7* GPS module connected to the embedded computer and is used to provide real-time location and heading orientation to the system.

G.2.1 Antenna design

The antenna array is composed of six identical patch antennas deployed on a hexagonal cylinder-like structure. In this way patch antennas are equally spaced and pointing at different directions, as shown in Figure G.3. Figure G.4 (left side) presents the simulated radiation pattern of one directional antenna using CST studio with the designed Half Power Beamwidth (HPBW) of approximately 70^o giving a desired, slight overlap between different patches. The elevation angle is approximately 61^o. The directivity of the final design is 6.9 dB with a realized gain of 6.4 dB. The bigger ground plane located behind each patch antenna helps to increase the front to back ratio to above 15 dB and the Side Lobe Level to -10 dB.

The omni-directional antenna located at the ground plane at the bottom of the cylinder is a simple monopole. It provides approximately 2 dB gain as shown on the right side of Figure G.4. The simulated S11 parameters of both antennas are shown in Figure G.5. Only one patch antenna is shown as the others are considered to be identical. As shown, the designed antennas cover the frequency range from 1.7 GHz to 1.9 GHz (with the magnitude of S11 below -15 dB) where both uplink and downlink of LTE band 3 are located.

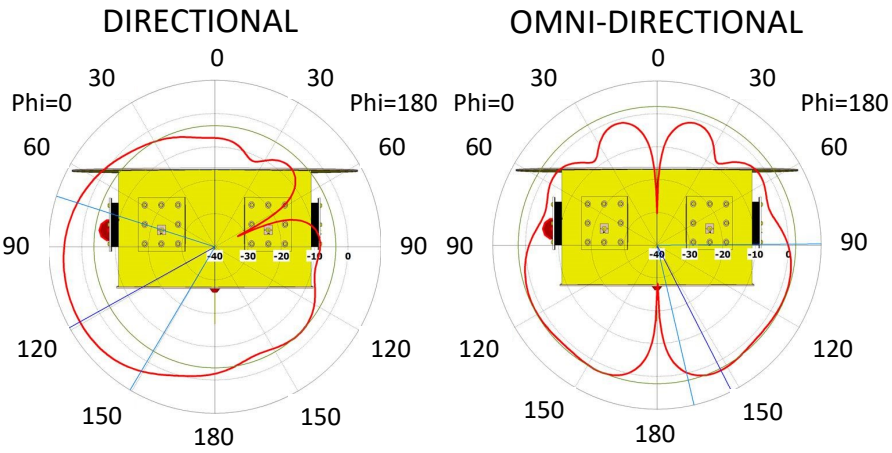

Fig. G.4: Simulated far field antenna pattern for both antenna types

All antennas are connected with the RF switches using the SMA cables of the same length placed inside the designed structure.

G.2.2 Design flexibility

UAV measurements are usually costly and time consuming, therefore flexibility and versatility of the measurement platform are desired. The modular design of the testbed facilitates changes of only single elements in case different frequency bands or antenna configurations are to be studied. This can greatly reduce the development time since most of the hardware elements can be reused.

Another example of flexible design is the addition of a monopole omnidirectional antenna. Very often experimental results of beamforming are to be compared with a reference antenna. By adding this antenna at the design phase, the potential set of measurements can be maximized without the need to exchange the hardware or even land the UAV.

G.3 Beam switching algorithm and mobility management

The beam switching algorithm implemented in this testbed relies on three key information. Serving Cell ID provided by the LTE modem, together with the known a priori list of GPS coordinates of Base Stations (BSs) are used to identify the location of a serving cell. By knowing the instantaneous GPS location and heading of the UAV, the antenna which points towards the direction of

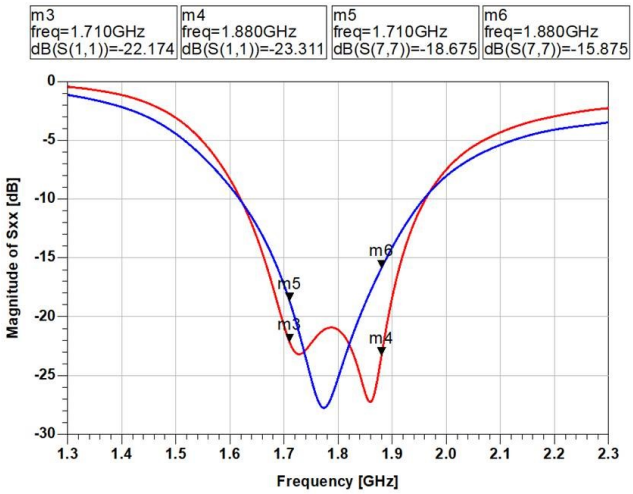

Fig. G.5: Simulated S11 parameters for patch antenna (red) and monopole (blue)

the desired BS is selected. In the LoS-dominant scenarios, often observed in cellular-connected UAVs, this kind of simple antenna-selection algorithm can be used without the need for real-time beam training techniques.

Figure G.6 presents the execution of the beam switching algorithm during one of the preliminary validation measurements. During the flight, the UAV approached the serving BS whose position is highlighted in the figure, flying over a straight trajectory. The UAV kept constant heading towards north. Real time computed antenna index was saved for offline analysis. While flying, the chosen antenna changed four times as illustrated in the figure.

Directional antennas may affect the mobility management protocols. In cellular systems, the serving cell of a user is selected based on highest measured and reported RSRP by the modem. The directional antenna pattern would enhance/mitigate signals from neighbor cells located at specific directions leading to potentially suboptimal cell selection. The proposed testbed offers the flexibility to mitigate the occurrences of wrong cell selection by activating the omni-directional antenna on the auxiliary receiving port. In this configuration, the modem reports to the network the highest RSRP value received from the two different antenna ports. The UE can then measure cells over all directions, thus mitigating the effect of the nulls of the directional antenna while preserving its gain in the beam direction.

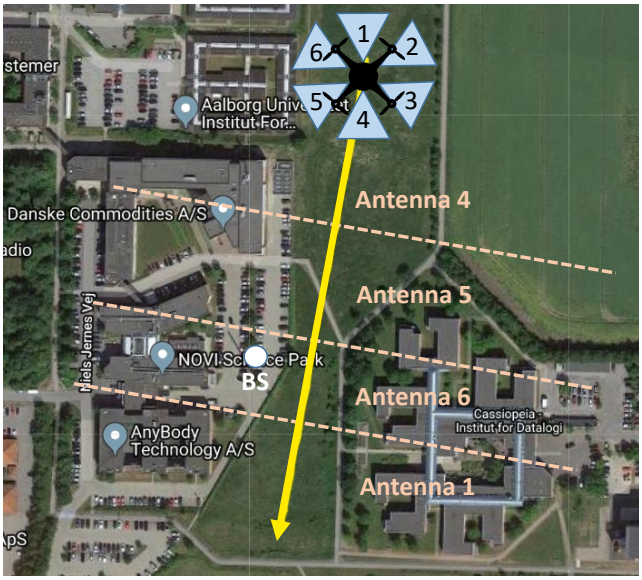

Fig. G.6: Beam switching example with UAV flight path (yellow) and the switching antenna regions

G.4 Measurement campaign

G.4.1 Measurement scenario

The target of the measurement campaign was to understand the impact of beamforming on a UAV's uplink performance when connected to the cellular networks. The measurement campaign took place in the city center of Aalborg, Denmark. Full buffer uplink transmission was implemented in the measurement system, in which a large file was uploaded to a local server. To isolate the effect of beamforming from the varied network load, the measurements were taken during night hours, when limited activity of the ground users was experienced.

Two UAV flights were conducted over the same path shown in Figure G.7. In the first flight, the UAV was using the real-time chosen directional antenna, together with omni-directional antenna activated on the auxiliary receiving port. During the second flight, only the omni-directional monopole antenna was used connected to the main antenna port. Both flights were performed during one mission without landing the UAV. The mission was repeated for two different heights: 10 m (imitating a ground-level scenario) and 40 m (maximum height allowed by the regulations due to airport proximity). UAV flew with a constant speed of 10 km/h and throughout all flights its heading was kept constant towards north regardless of the moving direction. To

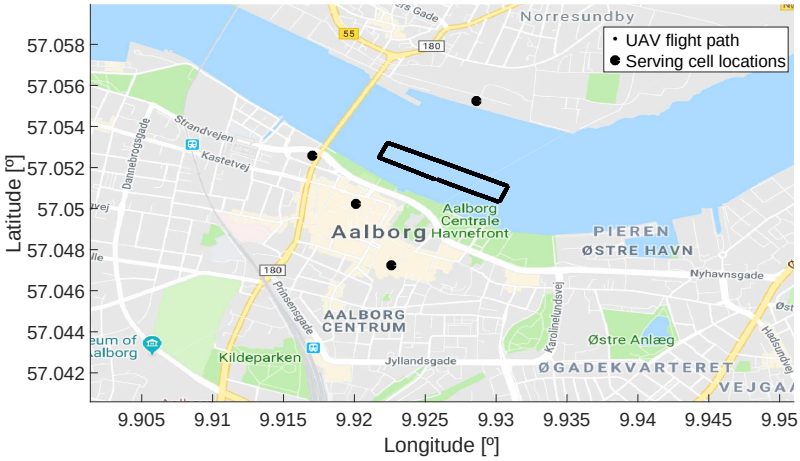

Fig. G.7: Executed flight path

facilitate understanding, in Figure G.7, black dots represent the location of serving cells observed during measurements. Each dot represent a cell tower with a three sectors (cells) of a mobile network.

G.4.2 Results

While flying, every 200 ms the LTE modem installed on a UAV reported some LTE metrics measured with the selected antenna. First, downlink RSRP and RSRQ are studied to show the effect of antenna directionality.

The Empirical Cumulative Distributed Function (ECDF) of the recorded downlink RSRP for both antenna systems is presented in Figure G.8. A continuous RSRP gain by the directional antennas with respect to the omni-directional case can be observed. This, together with median RSRP gains of approximately 6.5 dB, corresponds to the directional antenna gain, therefore validating the proper execution of the beam switching algorithm. In general observed values of RSRP decreased with height proving that the deployed cellular systems are optimized for the ground communication.

Second studied metric is downlink RSRQ as presented in Figure G.9. The shown results lead to an interesting remark. There is no gain in RSRQ for directional antenna system if a UAV is flying at 10 m while there is a substantial gain observed at 40 m. The reason for this is the increased benefit of spatial interference mitigation observed at higher heights. When flying above rooftops, strong interfering signals from a large number of cells become visible leading to RSRQ decrease when omni-directional antenna is used. Conversely, due to spatial interference filtering when UAV is using a directional

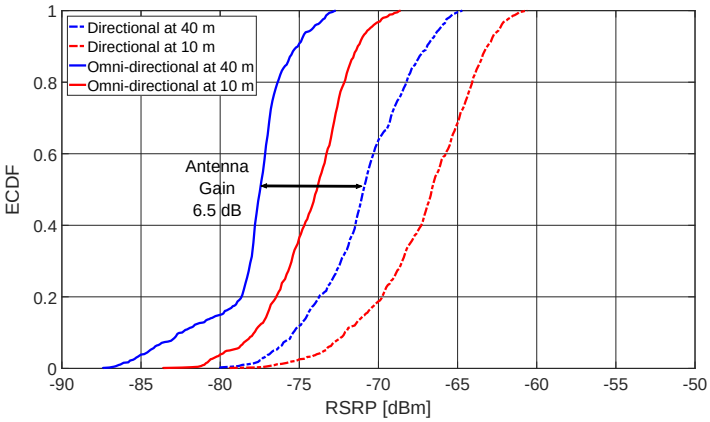

Fig. G.8: ECDF of the measured RSRP of the serving BS

antenna, the RSRQ values increased leading to a 3 dB gain. Higher RSRQ usually leads to higher order modulation and coding schemes being used at the transmitter and therefore translates into improved data rates. At the low heights, the impact of interference is negligible and observed RSRQ values are similar regardless of the antenna system.

After studying downlink metrics, next in Figure G.10, the ECDF of uplink throughput is considered. Not surprisingly the results follow the ones observed in [12], where similar study was conducted for vehicular communication. As the entire flight was carried in the high RSRP regime, due to uplink power control operating in the linear region, the directional antenna gain was compensated by the network issuing lower uplink transmit power in the directional antenna case. At a first glance, the shown results indicate, that there is no user-centric benefit of using high directional antennas at the UAV. However, as discussed later, the potential benefits will become visible if UAV flies in the low RSRP regime or when number of UAVs in the same region is increased.

Finally, the impact of directional antennas on the network mobility is studied in Figure G.11, where total number of handovers per flight is presented for all four flights. Here, one can observe that, when using directional antennas, the total number of handovers can be reduced with respect to a UAV flying at the same height with an omni-directional antenna. This is due to the capability of the UAV to maintain connectivity to the same cell by pointing the antenna towards its direction. At 10 m the total number of handovers was reduced from 12 to 5, while at 40 m, there were no handovers when using directional antennas, as the UAV kept connectivity to the same cell throughout the entire flight!

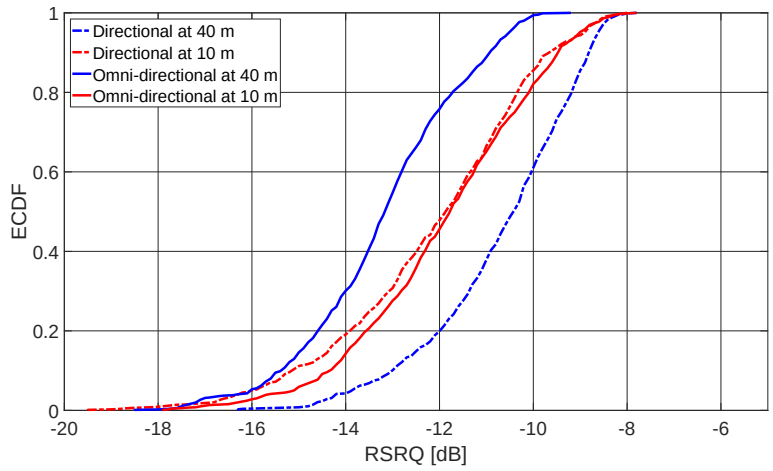

Fig. G.9: ECDF of the measured RSRQ of the serving BS

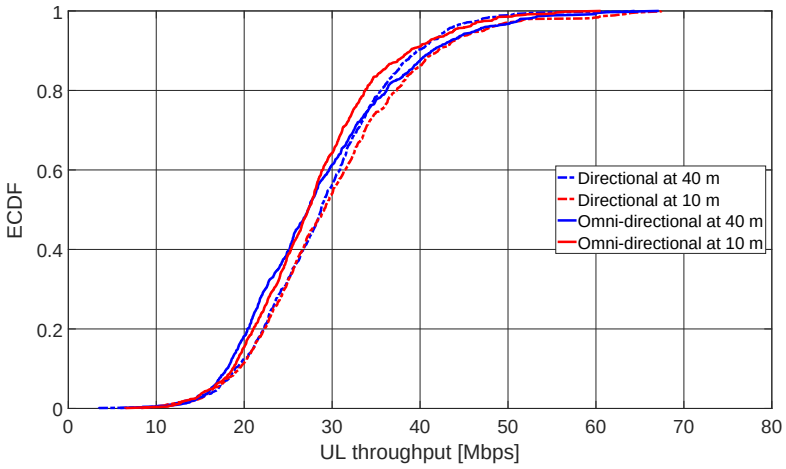

Fig. G.10: ECDF of the measured uplink throughput of the serving BS

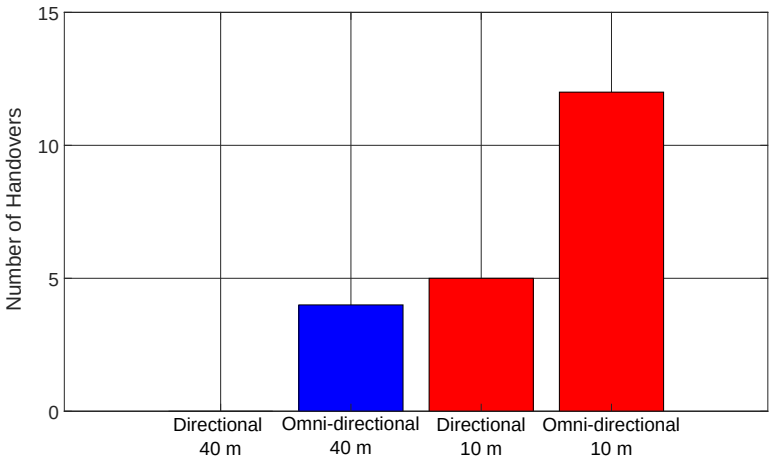

Fig. G.11: Number of handovers observed during measurements

G.5 Conclusions and Discussion

In this work, a multi-functional UAV platform for beamforming experimentation is presented and used in a measurement campaign using live LTE network. Although using only six antennas (directions) may seem as a limitation when studying beamforming performance, it is worth to note that one can steer the UAV in an arbitrary direction and therefore point the beam towards all the possible angles, as UAV's heading information is acquired from the GPS.

G.5.1 Uplink throughput improvements

Presented measurement results indicate that even when equipped with beamforming system, a UAV is not benefiting from uplink throughput improvement due to uplink power control compensating the higher antenna gain. It is worth to note that such gains are instead expected to be observed in the low coverage scenario (as cell edge or even network edge - as seashore). In such cases, a UAV will transmit with maximum power and uplink power control will not be able to fully compensate the antenna gain. This will lead to beamforming gain translating to coverage extension and thus relative throughput improvement.

The conducted measurements consisted of only a single flying UAV. It is expected that with more UAVs, their radiated uplink interference will impact the observed uplink throughput. As a potential future work, we recommend conducting experiments or simulations showcasing the impact on the net-

work performance of multiple UAVs equipped with beamforming capabilities. Our hypothesis is that, the spatially shaped interference would not only result in the improved downlink RSRQ of each UAV, but will also result in improved uplink SINR levels at the base stations (with respect to UAVs with omni-directional antennas) leading to higher uplink throughput.

G.5.2 Beamforming impact on mobility

As presented in the previous section, beamforming can help reducing the number of handovers due to longer connection to the same serving cell. This may be seen both as positive (less handovers means better reliability and lower latency since service interruptions during handover time are avoided) but also as negative (longer connectivity can potentially result in better cell being disregarded). In this measurements a naive beamforming strategy was used. It is expected, that when using other beamforming strategies, as for example interference aware RSRQ-based beam switch, beamforming can be used to steer the connectivity towards less interfered directions, possibly resulting in improved network performance.

References

[1] S. Hayat, E. Yanmaz, and R. Muzaffar, "Survey on unmanned aerial vehicle networks for civil applications: A communications viewpoint," *IEEE Communications Surveys Tutorials*, vol. 18, no. 4, pp. 2624–2661, 2016.

[2] P. Chandhar and E. G. Larsson, "Massive MIMO for connectivity with drones: Case studies and future directions," *IEEE Access*, vol. 7, pp. 94 676–94 691, 2019.

[3] "Study on enhanced LTE support for aerial vehicles (release 15)," 3GPP, Tech. Rep. TR 36.777 V0.4.0, November 2017.

[4] Y. Zeng, J. Lyu, and R. Zhang, "Cellular-connected UAV: Potential, challenges, and promising technologies," *IEEE Wireless Communications*, vol. 26, no. 1, pp. 120–127, February 2019.

[5] G. Geraci, A. Garcia-Rodriguez, L. Galati Giordano, D. López-Pérez, and E. Björnson, "Understanding UAV cellular communications: From existing networks to massive MIMO," *IEEE Access*, vol. 6, pp. 67 853–67 865, 2018.

[6] W. Mei and R. Zhang, "Uplink cooperative NOMA for cellular-connected UAV," *IEEE Journal of Selected Topics in Signal Processing*, vol. 13, no. 3, pp. 644–656, June 2019.

[7] C. D'Andrea, A. Garcia-Rodriguez, G. Geraci, L. G. Giordano, and S. Buzzi, "Analysis of UAV communications in cell-free massive MIMO systems," *IEEE Open Journal of the Communications Society*, vol. 1, pp. 133–147, 2020.

[8] S. De Bast, E. Vinogradov, and S. Pollin, "Cellular coverage-aware path planning for UAVs," in *2019 IEEE 20th International Workshop on Signal Processing Advances in Wireless Communications (SPAWC)*, July 2019, pp. 1–5.

[9] T. Chi, Y. Ming, Tseng, S. Kuo, and C. Liao, "Civil UAV path planning algorithm for considering connection with cellular data network," in *2012 IEEE 12th International Conference on Computer and Information Technology*, October 2012, pp. 327–331.

[10] H. C. Nguyen, R. Amorim, J. Wigard, I. Z. Kovács, T. B. Sørensen, and P. E. Mogensen, "How to ensure reliable connectivity for aerial vehicles over cellular networks," *IEEE Access*, vol. 6, pp. 12 304–12 317, 2018.

[11] S. R. Boroujeni, Z. Li, and S. Safavi-Naeini, "A smart beam-switching multi-antenna system for UAV," in *2017 IEEE International Symposium on Antennas and Propagation USNC/URSI National Radio Science Meeting*, July 2017, pp. 1389–1390.

[12] M. M. Ginard, T. Izydorczyk, P. Mogensen, and G. Berardinelli, "Enhancing vehicular link performance using directional antennas at the terminal," in *2019 IEEE Globecom Workshops (GC Wkshps)*, December 2019, pp. 1–5.

Paper H

Achieving high UAV uplink throughput by using beamforming on board

Tomasz Izydorczyk, Gilberto Berardinelli, Preben Mogensen, Michel Massanet Ginard, Jeroen Wigard and István Z. Kovács

The paper has been published in the
IEEE Access, 2020.

The layout has been revised.

Abstract

High-throughput unmanned aerial vehicle (UAV) communication may unleash the true potential of novel applications for aerial vehicles but also represents a threat for cellular networks due to the high levels of generated interference. In this article, we investigate how a beamforming system installed on board a UAV can be efficiently used to ensure high-throughput uplink UAV communications with minimum impact on the services provided to users on the ground. We study two potential benefits of beamforming, namely, spatial filtering of interference and load balancing, considering different beam switching methodologies. Our analysis is based on system-level simulations followed by a series of measurement campaigns in live Long-Term Evolution (LTE) networks. Our results show that using UAV-side beamforming has a great potential to increase uplink throughput of a UAV while mitigating interference. When beamforming is used, even up to twice as many UAVs may be served within a network compared with UAVs using omni-directional antennas, assuming a constant uplink throughput target. However, to fully exploit the potential of beamforming, a standardized solution ensuring alignment between network operators and UAV manufacturers is required.

H.1 Introduction

Unmanned aerial vehicle (UAV) communications have shown potential to enable a plethora of new services, such as delivery of goods or infrastructure inspection [1]. Reliable and ubiquitous command and control (C2) connectivity everywhere in the air is required to support beyond visual line of sight flights [2]. The C2 link itself may however not be sufficient to satisfy some demanding use cases as surveillance or real-time video broadcasting UAVs. In such scenarios, a minimum guaranteed uplink bit rate of 10 Mbps is required to satisfy the demands of transmitting video frames in high definition to the cloud servers [3], [4].

Cellular networks have been recognized as the most promising wireless technology to serve UAVs [5]. Due to their almost everywhere deployment, as well as favorable signal propagation characteristics at lower frequency bands, cellular networks have been shown to be capable of meeting the requirements imposed by the C2 communication link [6]. However, due to increased line of sight (LoS) probability of the air to ground (A2G) channel, uplink streaming UAVs may create immense uplink interference toward multiple base stations (BSs), impacting their observed uplink signal-to-interference-plus-noise ratio (SINR) [7]. This impact is expected to be even more severe when the predicted number of UAVs flying simultaneously over the same region (e.g., city) grows, harming not only the selfish uplink demands of other UAVs but negatively impacting the coexistence with ground user equipments (GdUEs),

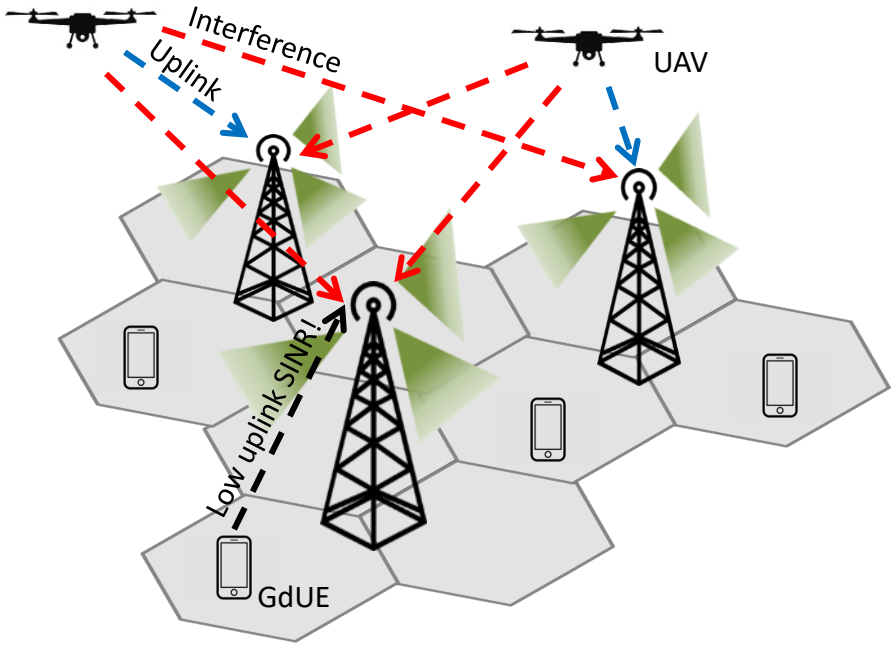

Fig. H.1: Impact of uplink interference created by flying UAVs

as presented in Figure H.1.

Different techniques aiming at coping with increased interference levels and providing UAV connectivity have been proposed in the literature. Massive multiple input multiple output (MIMO) with 3D beamforming capabilities assumed at the BSs is proposed among others in [8], [9] and [10]. By pointing the beams toward the flying UAVs, the potential communication link can be strengthened, while other links may observe reduced interference as the beams are pointed in different directions. Interference coordination among multiple cells is proposed in [11]. The work in [12] further extends the concept of interference mitigation and investigates the possible UAV assistance in the process. The 3rd Generation Partnership Project (3GPP) within the Release 15 studies on UAV enhancements for Long-Term Evolution (LTE) [13] proposes among others a UAV-specific power control settings such that highly interfering UAVs can be issued to lower their transmit power and therefore reduce the interference.

Although all of the mentioned solutions show the potential of serving a future flying UAV, they may require hardware changes at the network side. This, especially in the early deployment phase, when only a limited number of UAVs are expected, may be costly and not profitable. Furthermore, even

when the number of flying UAVs increases, UAVs should be able to fly anytime and anywhere, demanding large investments in the cellular networks.

Implementing a beamforming system on board UAVs is recognized as an alternative solution in [14] and [15]. The authors show the effects of the directional antenna pattern on observed interference and SINR levels, indicating the potential benefits of this solution. They also indicate that it is much cheaper to invest in UAVs, and it may allow them to fly anywhere. However, both works are limited only to the performance of the C2 link, without considering high uplink throughput communication.

In this work, the potential of UAV-side beamforming to satisfy high uplink throughput demands of UAVs is thoroughly investigated using both system-level simulations and experimental measurements over live cellular networks. The main focus is to show how beamforming can be used to spatially filter the radiated interference and in effect improve the uplink performance of UAVs while ensuring fair coexistence with GdUEs. Additionally, the potential of beam steering for load balancing is studied, showing how a UAV's uplink throughput can be improved by steering the beam toward the directions of less interfered/loaded cells. To achieve this goal, a Reference Signal Received Quality (RSRQ)-based beam switching algorithm is proposed and compared with conventional Reference Signal Received Power (RSRP)-based beam switching. Finally, both presented concepts are validated during a series of measurement campaigns using a real UAV with a set of directional antennas and connectivity to live LTE networks.

The rest of this paper is structured as follows. In Section H.2, the expected benefits of using beamforming are explained followed by a presentation of two studied beam switching algorithms. Further, in Sections H.3 and H.4, the system-level simulation settings and results are presented, respectively. Section H.5 presents the results of the measurement campaign, further validating the performance of UAV-side beamforming. Discussion and recommendations reflecting on the obtained results are provided in Section H.6. The work is concluded in Section H.7.

H.2 The benefits of beamforming on board a UAV

A beamforming system installed on a UAV can bring many potential benefits stemming from not only antenna gain but also directionality. These benefits can be grouped into two categories: spatial filtering of interference and load balancing due to beam steering. Both are further described below, focusing on uplink (UAV to BS) communication link.

- **Spatial filtering of interference:** Due to high LoS probability, a transmitted signal from a UAV will be received by many cells, effectively reducing their uplink SINR and thus leading to decreased uplink through-

put of their users. The problem becomes more severe if there are multiple UAVs flying over the same region. Their uplink interference will accumulate leading to even worse overall system performance in the affected cells.

Using beamforming and focusing the signal toward the direction of a serving cell, a UAV can minimize the amount of radiated energy toward other BSs located outside of the main antenna beam. This principle is known as spatial filtering of interference [16]. By spatially filtering the interference, only a limited number of cells, coinciding with the direction of the main beam will be interfered. Limiting interference will lead to higher uplink SINR levels observed in the network and thus improved uplink throughput for the users in these cells - both GdUEs and UAVs.

- **Spatial load balancing:** Any user of the cellular network may experience connection to high and low loaded cells, which lead to different achievable throughput. Flying UAVs will require a constant, high uplink throughput to meet the demands of some use-cases. However, UAVs, as all other users in the network, can be attached to a high loaded cell, which is not able to meet UAV communication requirements.

  By using beamforming on board a UAV, the freedom of choosing the beamforming direction can be used for spatial load balancing. By steering the beam away from a loaded cell, a UAV's uplink throughput can potentially be improved as the network may perform a handover to a different cell. Although load balancing is practically available in the network even without beamforming [17], it requires cooperation between multiple cells to know their instantaneous load. In this article, we demonstrate how beamforming together with RSRQ-based beam switching can be used to achieve load balancing without the cooperation requirements imposed on cellular networks.

H.2.1 Studied UAV beam switching algorithms

In this article, two UAV beam switching algorithms are studied. First, the RSRP-based beam switching method is used. In this case, a flying UAV instantaneously selects the beam resulting in the highest RSRP, providing a handover threshold Δ_{A3} is satisfied [18]. Such beam selection ensures the cell with the strongest received signal power is used.

To showcase load balancing properties, RSRQ-based beam switching is also implemented. In this case, a UAV chooses the beam based on the highest RSRQ, which is defined as the ratio between the measured RSRP and the total received power including desired and interfering signals [19]. Figure H.2 explains how the RSRQ metric captures the effects of network load

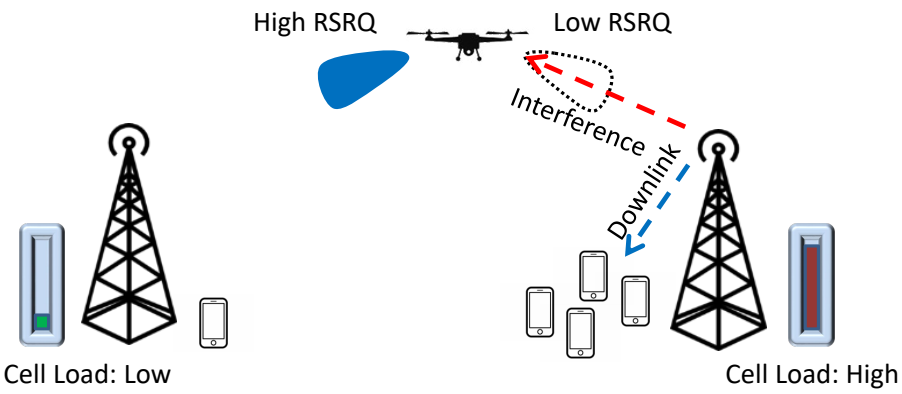

Fig. H.2: The principle of using RSRQ-based beam switching for load balancing

and can be used for load balancing purposes. As presented in the figure, a flying UAV is located in the proximity of a high loaded cell, which does not have sufficient available resources to meet the UAV's uplink demands. When the loaded cell is serving its ground users, the flying UAV receives these downlink transmissions as interference, effectively reducing the measured RSRQ toward this direction. However, when the UAV is pointing its beam toward a more distant but less loaded cell, even though the distance to the cell is larger, the amount of observed interference is limited, resulting in a higher RSRQ; therefore, a connect to the less loaded cell is made.

H.3 System-level simulation settings

In the first part of this article, system-level simulations are used to show the potential impact of beamforming in multi-UAV scenarios. A dynamic system-level simulator thoroughly described in [14] is used. To best show the practical aspects of the proposed results, a real network topology of a Danish network operator was implemented in the simulator, with real locations, heights, antenna patterns and orientations of more than 150 cells representing the city of Aalborg and its suburbs. Contrary to the work in [14] focusing on a rural network and sub-GHz frequency bands, in this article, the implemented network represents a system deployed at a 1.8 GHz carrier frequency and 20 MHz bandwidth.

A height-dependent UAV channel model derived in [20] is used in the simulator. The channel model used for GdUEs is the urban macro model from 3GPP specifications [21]. Further, we consider open-loop power control. The algorithm can be described as follows:

$$P_{UL} = \min\{P_{UL}^{max}, P_0 + \alpha RSRP_{est} + 10\log_{10} M\}, \tag{H.1}$$

Table H.1: Parameters used in system-level simulations

Parameter	Value
Simulation area	40x40 km
Network layout	Real imported network layout
Number of cells	162
System bandwidth	20 MHz
Carrier frequency	1800 MHz
Total number of GdUEs	Scenario dependent, 750 or 1200
UAV's flying height	40 m
GdUE's height	1.5 m
UAV's velocity	Scenario dependent, 30 km/h or hovering
GdUE's velocity	Pedestrian speed (5km/h)
UAV's channel model	Height-dependent model [20]
GdUE's channel model	Urban Macro
Uplink traffic	Full buffer model
Max uplink transmit power	23 dBm
Uplink power control P_0	-58 dBm per PRB (180 kHz)
Uplink power control α	0.75
Handover event	A3 with Δ_{A3}=3 dB
Number of iterations	100
Length of one iteration	20 s

where P_{UL} and P_{UL}^{max} represents the used and maximum allowed uplink transmit powers, respectively. $RSRP_{est}$ and M represent the estimated RSRP and number of scheduled uplink resource blocks. Finally, P_0 and α are two network controlled parameters, which are adjusted in this simulation with respect to the imported network layout such that most of the users can transmit with lower power than P_{UL}^{max}. Table H.1 summarizes the most relevant settings of the simulator.

Flying UAVs are equipped with six directional antennas and a switching system, as described in [14] and presented in Figure H.3. Each of the six antennas points toward a different direction and has a beamwidth of 60°. All antennas have 6.6 dBi directional gain and -13 dB front-to-sidelobe ratio. The antenna system orientation is fixed with respect to the fuselage.

H.3.1 Considered scenarios

To show the benefits of beamforming, three different scenarios are studied, as summarized in Table H.2. First, Scenario 1 focuses on the potential of beamforming for spatial filtering of interference. A low-loaded network is designed with a target of two average active GdUEs per cell moving with

Table H.2: Scenarios studied using system-level simulations

Scenario	Research target	Possible use-case	Number of UAVs	GdUEs distribution	UAV distribution
Scenario 1	Spatial filtering of interference	Last-mile package delivery	1 - 100 UAVs	Low load (Average 2 active users per cell), random movement at 5 km/h	UAVs drawn uniformly, random flight patterns at 30 km/h
Scenario 2	Load balancing	An event with real-time TV broadcasting	1 - 5 UAVs	Low load (Average 2 active users per cell, random movement at 5 km/h) plus a crowded region (50 GdUEs drawn in a 100 m^2 square corresponding to average 17 active users per cell, static)	UAVs drawn randomly over a crowded region, hovering
Scenario 3	Joint effect of spatial filtering and load balancing	A UAV flying in a highly populated area during rush hour	1 - 100 UAVs	Medium load (Average 3.5 users per cell, random movement at 5 km/h) and five crowded regions (50 GdUEs drawn in a 100 m^2 square corresponding to average 17 active users per cell, static) distributed across the map	UAVs drawn uniformly, random flight patterns at 30 km/h

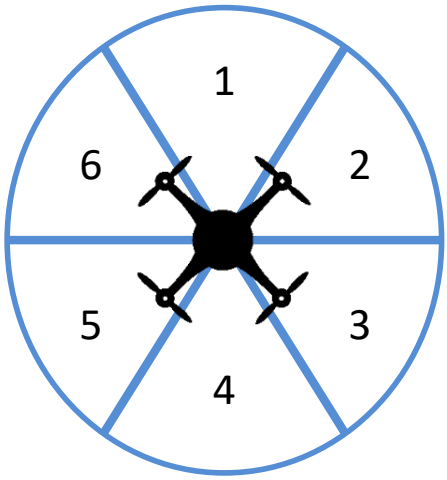

Fig. H.3: Modeled antenna beam configuration of a UAV

pedestrian speed. Different numbers of flying UAVs are dropped within the simulated area. UAVs fly at 30 km/h in a random direction at 40 m height. This setup emulates the envisioned package delivery scenario and represents last-mile delivery service.

Scenario 2 focuses on showcasing the spatially controlled load balancing using beamforming. For this reason, a 'crowd' of static 50 GdUEs is generated in the 100 m$\times$100 m central, most urban region with a limited number of UAVs drawn at 40 m height hovering right above the crowd. The remaining GdUEs are drawn uniformly within a network, considering low load as in Scenario 1. This scenario emulates any event in which many users are located in a certain place and flying UAVs are used to either monitor or for real-time broadcasting of video footage.

Finally, in Scenario 3, the focus is placed on the worst case scenario in which a loaded network is generated. In addition, five randomly placed crowded events, as described in the previous scenario, are drawn and are happening simultaneously. UAVs are drawn randomly within the frame of the city and behave as in Scenario 1.

Two different beam switching algorithms are used in all three scenarios as explained in Section H.2. For comparison, in all three scenarios, the case of UAVs using omni-directional antennas is also studied. Each scenario is repeated 100 times. In each iteration, UAVs and GdUEs are randomly repositioned and move with the assigned scenario-dependent velocity for 20 s.

H.3.2 Measurement KPIs

To understand the impact of beamforming on the performance of UAVs and GdUEs, the following key performance indicators (KPIs) are considered:

- **UAV-originated uplink interference over thermal noise (IoT):** The overall uplink interference quantified per cell, normalized such that 0 dB represents the average IoT when no UAVs (only GdUEs) are available in the network.
- **Uplink SINR:** Average uplink SINR of users with active uplink transmissions. Studied separately for UAVs and GdUEs.
- **Uplink throughput:** Average uplink throughput. Studied separately for UAVs and GdUEs. Because the main objective of this work being to study the performance of beamforming to meet high uplink throughput demands of UAVs, a 10 Mbps target is used in some analysis. This represents the minimum requirements for real-time video streaming.

H.4 Simulation results

H.4.1 SCENARIO 1 - spatial filtering of interference

First, the focus is on spatial filtering of uplink interference using beamforming as described in Section H.2 and labeled as Scenario 1. Figure H.4a presents the average levels of UAV-originated uplink IoT averaged over different cells. With more flying UAVs, the overall IoT values increase as more uplink transmissions are made. Spatial filtering of interference becomes visible when a larger number of UAVs is simultaneously flying, with more than 4 dB reduction of interference power for the case of 100 UAVs. Both beam switching algorithms result in a similar IoT increase. The slightly lower average IoT levels in the case of RSRP-based beam switching are a result of the uplink power control algorithm, as in Equation (H.1), where path loss is estimated based on $RSRP_{est}$. RSRP-based switching always selects the beam with the best RSRP, leading to the lowest uplink transmit power and therefore lowest radiated interference.

Second, in Figure H.4b, the uplink SINR values averaged over all flying UAVs are shown. The impact of spatial filtering can be seen. The results are clearly correlated with the IoT results discussed earlier. With a larger number of UAVs, increased interference leads to reduced SINR values with a more than 5 dB SINR drop for 100 UAVs.

Finally, the impact of interference and reduced SINR on uplink throughput of the UAVs can be seen in Figure H.4c. The overall throughput values drop with more UAVs in the network. Spatial filtering of interference

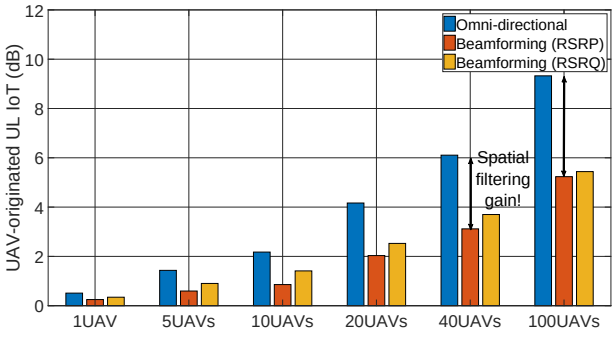

(a) Rise of UAV-originated uplink Interference observed by the cells

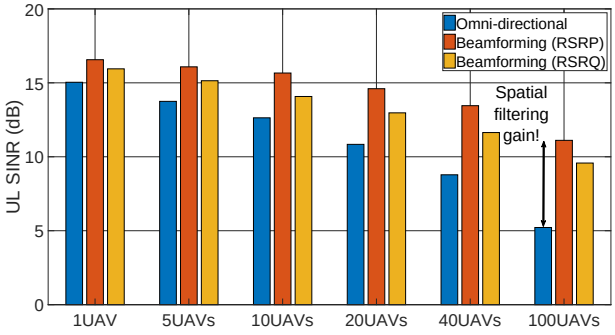

(b) Uplink SINR of flying UAVs

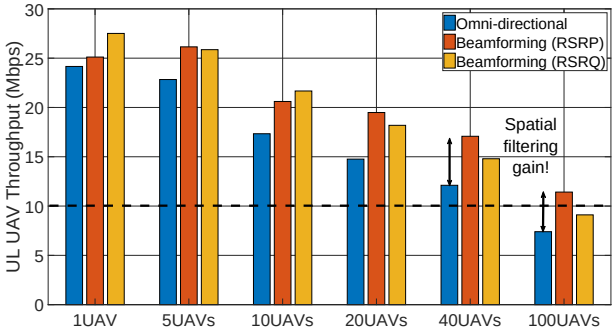

(c) Average uplink throughput of flying UAVs

Fig. H.4: Simulation results of scenario 1

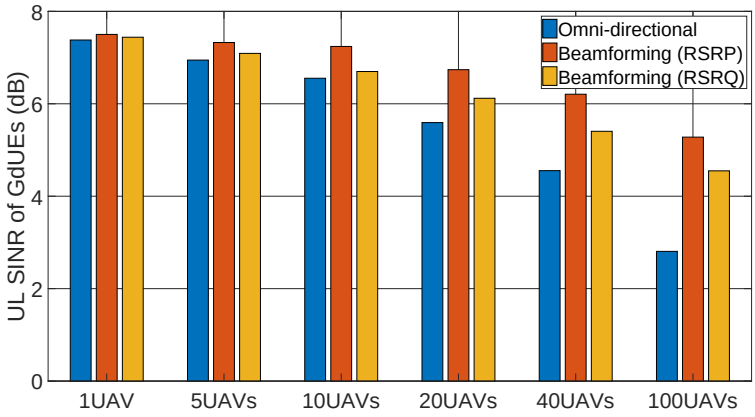

Fig. H.5: Average uplink SINR of ground users

impacts the observed throughput values, leading to improved performance. Some interesting observations can be made. With only a single flying UAV, uplink throughput observed with an omni-directional antenna and using RSRP-based beam switching is almost identical and is consistent with the measurement results presented in [22]. This is because, with only a single UAV, spatial filtering of interference is not yet visible as there are no other interfering UAVs to affect the performance. In addition, uplink power control compensates the antenna gain leading to the same average uplink throughput.

Given a low-loaded network, even with 40 UAVs, the benchmark 10 Mbps uplink throughput, marked using the dashed line, is exceeded regardless of the antenna system. However, with more UAVs, only using beamforming, the target value can be achieved. Finally, this figure also indicates that about two times more UAVs can be supported in the network when beamforming is used compared to omni-directional UAVs assuming the same uplink throughput target.

A fair coexistence between flying UAVs and GdUEs is necessary for smooth adoption of UAVs into the cellular paradigm. To showcase how beamforming impacts the performance of ground users, Figure H.5 presents the average uplink SINR of all GdUEs. Similarly to Figure H.4b, the SINR values drop with more UAVs. However, due to spatial filtering of interference, the drop is reduced if UAVs use beamforming. The improved uplink SINR can be translated into better overall uplink throughput ensuring improved performance of GdUEs in the presence of UAVs.

H.4.2 SCENARIO 2 - impact of spatially controlled load balancing during a crowded event

The potential of using beamforming for load balancing while flying over a crowded event is discussed in this subsection. Figure H.6 presents the observed values of uplink SINR and uplink throughput for 1, 2 and 5 flying UAVs. By studying only a limited number of UAVs, the effect of load balancing can be isolated from the spatial filtering effect discussed previously. The SINR values for both beamforming strategies are similar regardless of the number of UAVs. However, the uplink throughput in the case of RSRQ-based beamforming is twice the throughput when RSRP-based beam switching is used. This indicates the potential of using RSRQ as a beam switching metric to improve load balancing properties.

Note that the overall SINR and throughput of UAVs are still relatively low, even when RSRQ-based beam switching is used. This can be explained as follows. When a UAV is able to connect to a relatively low loaded cell, such cell is still likely to be one of the closest physically located cells. In such a case, all the GdUEs located in a crowd are still causing a significant uplink interference to the UAV's serving cell, limiting its SINR and the UAV's uplink throughput.

The impact of spatially controlled load balancing on the GdUE's performance is rather limited with respect to the already studied spatial filtering and therefore not shown in the paper. If a UAV is connected to the same cell, it competes for an already limited set of resources with GdUEs, limiting their potential uplink throughput. If a UAV is connected to a low loaded cell located in close proximity, it acts as an interferer to the cell serving GdUEs, effectively reducing their uplink SINR.

H.4.3 SCENARIO 3 - Performance of spatial filtering and load balancing in a loaded network

Finally, the potential of beamforming is studied in the presence of a loaded network with multiple events happening in different places. As in Scenario 2, Figure H.7 presents the average uplink SINR and throughput for different numbers of flying UAVs. Both spatial filtering of interference and load balancing effects are visible when analyzing the uplink throughput results. Not surprisingly, spatial filtering gains are dominant when a larger number of UAVs is flying and interfering the network.

Load balancing gains are a major reason for throughput improvement with a limited number of UAVs, when interference-based load balancing can still be used to connect to a low loaded cell. The load balancing gains disappear however with a very high number of UAVs and result in similar uplink throughput to the one obtained using RSRP-based beam switching as fewer

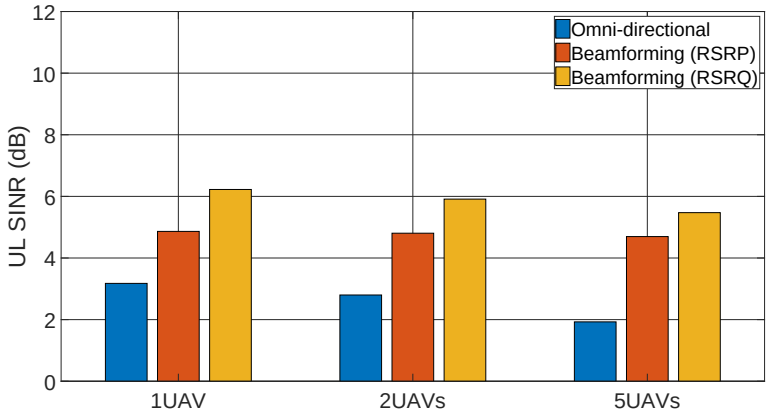

(a) Uplink SINR when UAVs fly in loaded cell

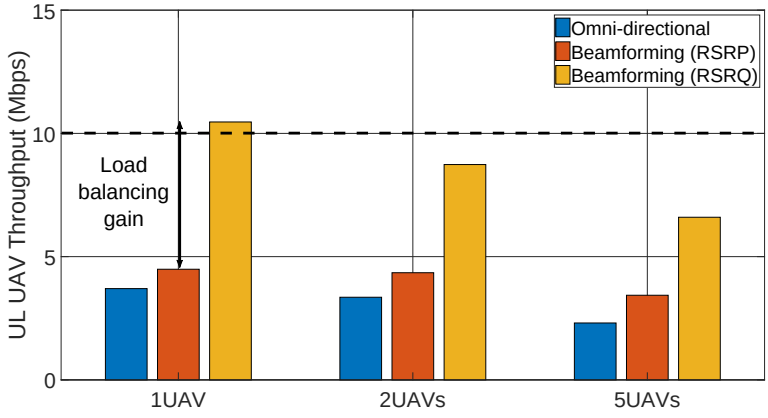

(b) Uplink throughput when UAVs fly in loaded cell

Fig. H.6: Simulation results of Scenario 2

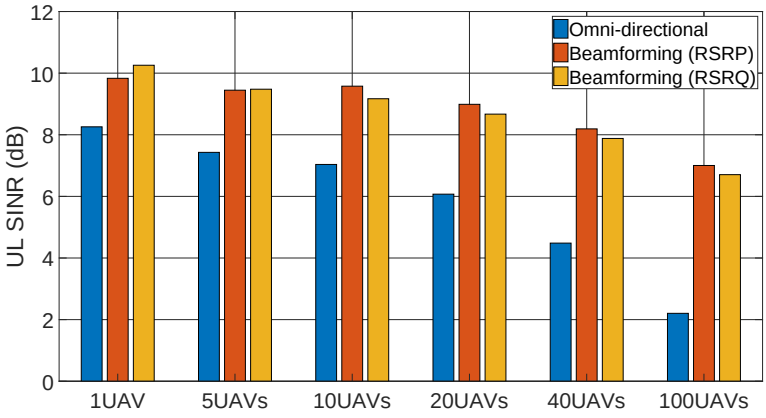

(a) Uplink SINR of flying UAVs in a loaded network

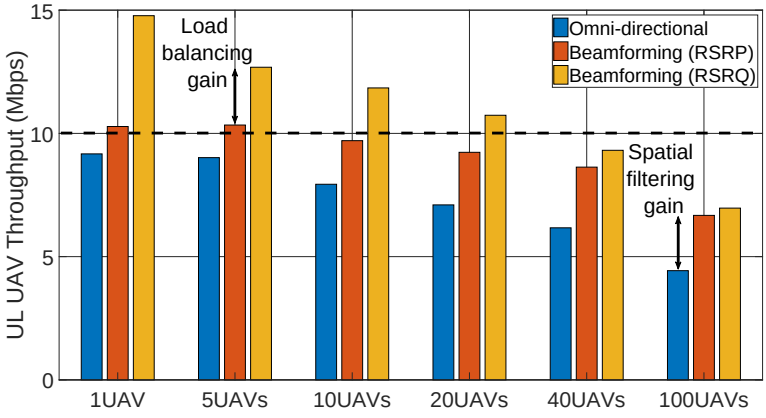

(b) Average uplink throughput of flying UAVs in a loaded network

Fig. H.7: Simulation results of Scenario 3

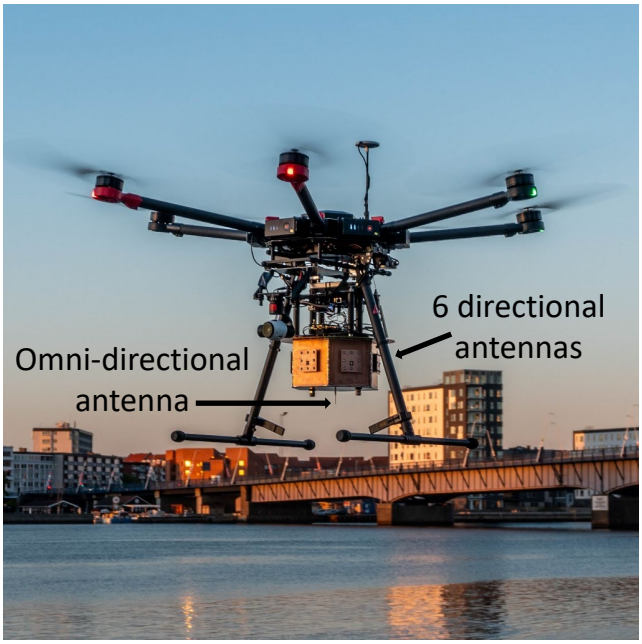

Fig. H.8: Active UAV during one of the measurement campaigns

and fewer cells remain low-loaded and interfered.

To obtain the target 10 Mbps uplink throughput, an RSRQ-based beamforming strategy is to be used even with a limited number of UAVs. The overall network load is indeed too high to achieve the target when omni-directional antennas or RSRP-based beamforming is used.

H.5 Experimental measurement campaigns

After disclosing the potential of uplink beamforming using system-level simulations, a set of measurement campaigns was conducted to experimentally validate the spatial filtering of interference and load balancing properties of beamforming as well as to analyze UAV-GdUEs coexistence.

The measurements were conducted using the platform presented in [22], consisting of a UAV with six directional antennas, one omni-directional antenna and an LTE modem, as presented in Figure H.8. The antennas used in the measurement system are virtually identical with the model used in the previously described simulations. Both measurement campaigns were conducted using a real LTE network deployed at 1.8 GHz with UAVs flying over the same region (and network) as implemented in the system-level simulator and presented in Figure H.9.

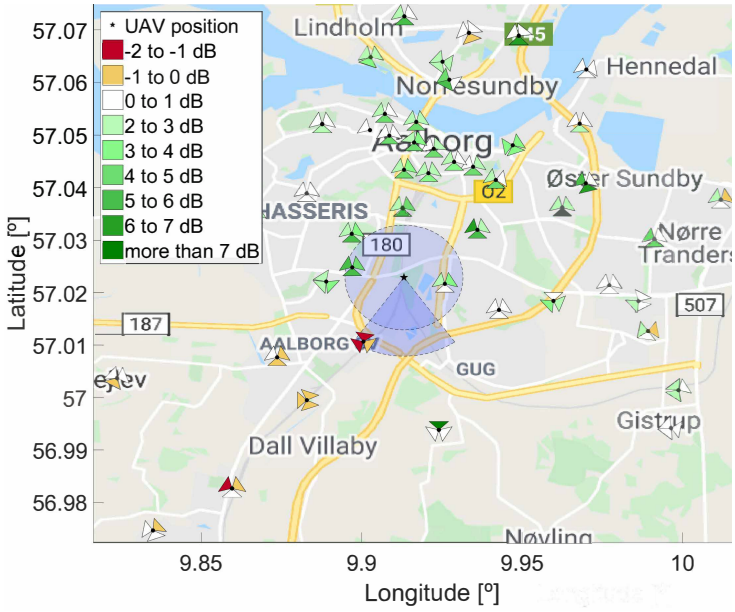

Fig. H.9: Map of Aalborg, presenting the uplink Δ_{IoT} observed at different cells

Due to practical restrictions, this initial measurement campaign was conducted using only a single flying UAV. Nevertheless, as argued in Section H.4, even a single flying UAV is sufficient to experimentally validate the presence of spatial filtering or load balancing.

H.5.1 Validation of spatial filtering of interference

The first measurement campaign focused on validating in practice the spatial filtering of interference. The goal of this study is to compare the uplink IoT levels observed within a network in the case that a UAV is using omni-directional transmission or beamforming. To achieve this goal, two thirty-minute flights were performed in Aalborg, Denmark, in which a UAV hovering at 100 m constantly executed a full-buffer uplink transmission. During the first flight, the UAV used the omni-directional antenna, while during the second flight, transmission was beamformed toward a predefined direction. The IoT information was obtained based on network IoT KPI data provided by the network operator. The measurements were taken during nighttime hours, in which the overall non-UAV interference in the network is negligible.

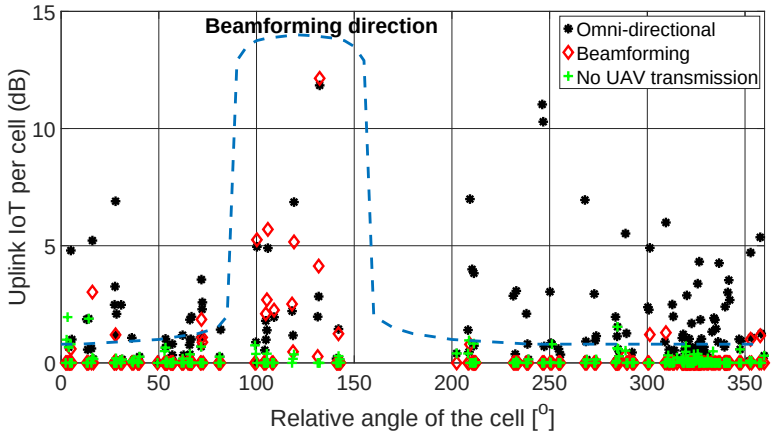

Fig. H.10: Experimentally observed spatial interference mitigation when using beamforming

To validate the spatial filtering, the average interference increase Δ_{IoT} is computed in dB as follows:

$$\Delta_{\text{IoT}} = \text{IoT}_{\text{Omni}} - \text{IoT}_{\text{Beamforming}} - \text{IoT}_{\text{No UAVs}}. \tag{H.2}$$

Figure H.9 presents the obtained Δ_{IoT} values per cell across the network. The UAV position together with the antenna patterns are presented. The obtained results are visualized using a color code, in which green colors represent cells where the omni-directional antenna created higher levels of interference than the directional antenna ($\Delta_{\text{IoT}} > 0$dB); red colors represent cells which where interfered more using the directional antenna ($\Delta_{\text{IoT}} <$ 0dB). The darker the colors are, the larger the difference.

The obtained results give visual indication that omni-directional transmission creates more spatially spread interference than beamforming. In some cells, omni-directional transmission create more than 7 dB higher interference than the beamforming system. Only a limited number of cells observe higher interference when beamforming is used. However, even in these cases the increase in interference is limited and does not exceed 2 dB.

In Figure H.10, similar results obtained using different beamforming directions are presented. The results are presented in terms of total IoT per cell located at a relative angle with respect to the flying UAV. When a UAV uses an omni-directional antenna, cells located in every direction are being interfered. However, when using beamforming, only cells located within the main beam observe interference higher than 4 dB. Moreover, within the main beam direction, the interference levels observed for the very same cells when using both antenna systems are comparable. Due to uplink power control, beamforming can therefore spatially filter interference without increasing it

in the direction of the main beam.

Finally, the average IoT when there are no UAV transmissions is presented to further indicate that when measuring during nighttime hours, most of the interference observed in the network is initiated by a flying UAV, and the impact of GdUE-originated interference can be omitted from the analysis.

H.5.2 Validation of load balancing

The target of the second measurement campaign was to showcase the potential of using beamforming for load balancing while ensuring the coexistence between UAVs and GdUEs. Similar to Scenario 2 of the simulations, measurements were used to show the possibility of triggering a network handover when switching the beamforming direction, thus escaping a loaded cell to improve UAV uplink throughput. Four Release 13-compatible, Cat. 18 mobile phones [23], with installed Qualipoc [24] software to measure network parameters were used as GdUEs. They were all located in the same place and connected to the same cell. All phones were programmed for a full buffer uplink transmission such that a loaded cell was created (referred to later as *cell A*). A UAV was set to hover at 40 m right above the GdUEs, also performing a full-buffer uplink transmission.

For the first 15 minutes, the flying UAV was using an omni-directional antenna and based on the recorded logs, it attached to the same cell as the GdUEs (cell A). Further, for the next 15 minutes, the UAV was programmed to use the directional antenna pointing in the opposite direction of the location of cell A. Eventually, the change in the antenna system triggered a handover procedure to a different cell (referred to later as *cell B*).

This beam switching[1], although simplified, resembles the RSRQ-based beam switching, as studied in the simulation phase. By pointing the beam away from cell A, a network handover toward cell B was triggered. The conducted measurements reflect similar conditions as in Scenario 2 from the system-level simulations; as in both cases, a UAV flew directly over a group of GdUEs.

Figure H.11 presents the empirical cumulative distribution function (ECDF) of recorded UAV uplink throughput during the measurements, while in Figure H.12, the ECDF of the GdUE uplink throughput is presented. It is clearly visible that both types of devices benefit from load balancing. Initially, the UAV observes low uplink throughput because it was connected to a loaded cell A. The median throughput of the UAV increases approximately five times after handover to cell B is performed.

Similar behavior is observed regarding uplink throughput of GdUEs. The low throughput due to a large number of active devices (4 GdUEs and 1 UAV)

[1]Please refer to [22] for details of how the switching was implemented.

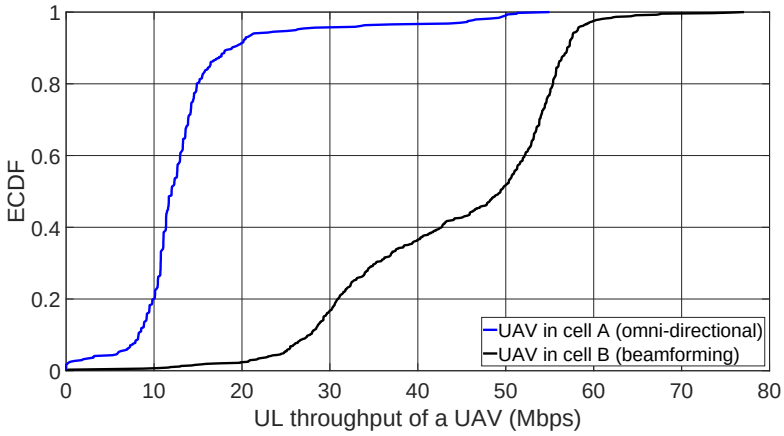

Fig. H.11: Uplink throughput of the UAV during load balancing experiments

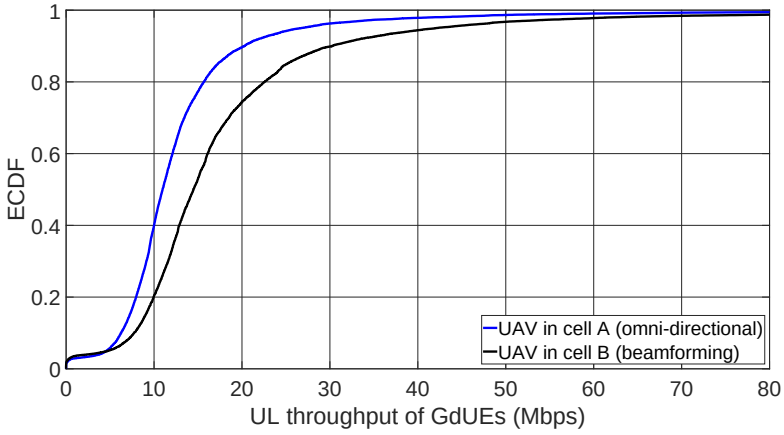

Fig. H.12: Uplink throughput of the GdUEs during load balancing experiments

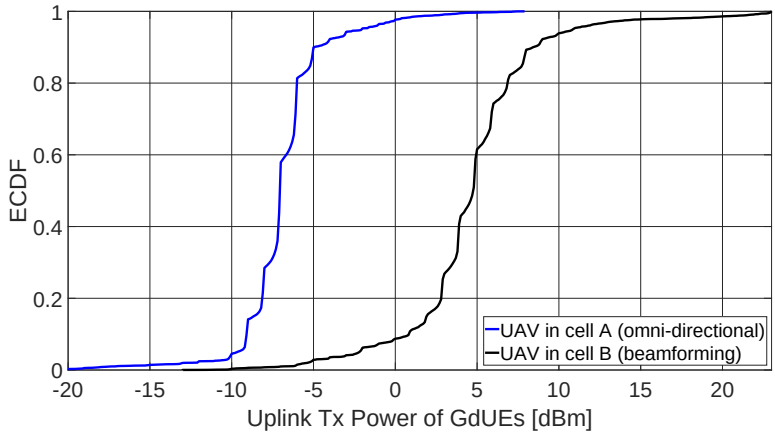

Fig. H.13: Uplink transmit power of the GdUEs during load balancing experiments

increases by more than 12% when the UAV switches cell and frees the resources. Theoretically, the throughput should increase by 25%. The lower gain is due to the interference generated by the UAV to cell A. Figure H.13 presents the ECDF of uplink transmit power for all GdUEs. There is more than a 10 dB increase in the average transmit power when the UAV transitions from being a user of the same cell to an interferer (handover from cell A to cell B).

Although the actual power control policy implemented in a real network is unknown, the obtained results indicate that the UAV uplink transmission to cell B resulted in strong interference to cell A, and all GdUEs in cell A were set to a higher uplink transmit power to compensate otherwise decreased uplink SINR. We believe that the real network is using an SINR estimate to make fast adjustments of the UE uplink transmit power on top of the usual open-loop power control based on $RSRP_{est}$. However, in the performed simulations, these fast adjustments were not implemented. Nonetheless, our obtained experimental results are aligned with the results reported by other researchers in [25].

H.6 Discussion and recommendations

In the remainder of this article, we summarize our findings, discuss their impact and provide some guidelines on the potential future improvements needed for seamless integration of UAVs within a cellular network. The experimental results provided in Section H.5 validated the concepts studied using system-level simulations presented in Section H.4. In the authors'

opinion, they provide valuable information on how today's network can handle UAV traffic and show that there is still a lot to be done to meet all UAV requirements within a cellular network framework.

UAV-side beamforming has shown a great potential to mitigate uplink interference by spatially directing the uplink transmission only in a desired direction. This behavior leads to improved uplink throughput of flying UAVs and ensure fair coexistence with GdUEs. Bearing in mind that there are multiple network-side interference mitigation techniques already in use or proposed, UAV-side beamforming should be regarded as a complementary technique, further used to reduce interference. The promises of beamforming are also clearly visible when a UAV is flying in a high traffic cell. In this situation, beamforming can be used to steer the connectivity and potentially improve UAV uplink throughput with limited interference impact on the nearby cells.

H.6.1 UAV-controlled beamforming

In the simulations and during the described experiments, a mobile network (simulated or real-world) did not possess any knowledge of flying UAVs and their beamforming capabilities[2]. In such a situation, it is up to the UAV to choose the desired beamforming direction. During the simulations, beam switching was performed considering RSRP or RSRQ metrics. During the measurements, due to limitations of the used modem, the executed beamforming direction was chosen manually based on the analysis of network topology.

Leaving the beamforming decision to the UAV itself, although already providing visible gains, is clearly suboptimal from both UAV and mobile network operator perspectives. A UAV, even if a smart beamforming algorithm is implemented, would have to assume the beamforming direction without any guarantees that it is beneficiary. As an example, during the measurement campaign validating load balancing, the UAV might direct the beam toward a cell that is even more loaded, or even worse, in the direction where there are no cells at all. Although eventually a UAV may find a correct beamforming direction (by performing trial and error beam sweeps), while sweeping, the uplink throughput requirements of a UAV may not be satisfied.

When the beamforming decision is taken by the UAV, the potential spatial interference reduction gains are also suboptimal. Assuming a multi-UAV scenario, it may happen that each UAV chooses its beamforming direction independently in such a way that the interference radiating from all UAVs will accumulate in a certain geographical region. In the worst case, the

[2]While performing the measurements, we used a regular SIM card with a commercial data plan

highly interfered region, would observe similar interference as if all UAVs are equipped with an omni-directional antennas.

H.6.2 Network-assisted beamforming

To fully embrace the potential of beamforming on the UAVs, a network needs to not only possess the knowledge but also be in control of beamforming decisions of each UAV. If the network has the capabilities to signal the beamforming direction to each UAV present within a certain geographical area, highly optimized interference and load balancing procedures can be used. If multiple UAVs are present, an optimized network would be able to redirect their beams over base stations located at directions for which mutual harm is avoided.

A load balancing procedure would become beneficial if a UAV demands constant high uplink throughput. Due to the larger amount of visible cells by a UAV, the network would be able to proactively redirect a UAV to a cell in which the trade-off between low cell load and potential impact on GdUEs is satisfied. By doing so, the demands of the UAV can be satisfied and coexistence with GdUEs improved[3]. One example can be a UAV flying over a city center and being connected to a cell located in the suburban or residential area with a lower load.

Network assistance will also become beneficial during crowded events. In Scenario 2 of the simulations presented in Section H.4.2, due to high uplink IoT, a UAV flying over a crowd of users observed limited uplink throughput, not matching the minimum 10 Mbps target. It is expected that with network assistance, a handover to a cell with low IoT can be made and the minimum throughput target can be achieved.

H.6.3 UAV-specific uplink power control

Another way that the network can benefit from UAV-sided beamforming is by introducing a UAV-specific uplink power control. Please note that as of Release 15, a UE-specific power control is already available and can be used to differentiate the uplink power assignments for the particular group of users [26]. Considering UAVs with beamforming capabilities as one of such groups, a network can create unique power control settings embracing directional gains.

Assuming a power control policy in which a group of UAVs with beamforming capabilities can transmit their uplink signals with higher power compared with regular power control settings, stronger signals will be received by the serving cell allowing higher-order modulation to be used at a UAV and

[3]Contrary to the performed measurements in Section H.5.2, where using UAV-controlled beamforming, UAV demands were satisfied with the risk of increasing intercell interference.

therefore improving uplink throughput. This gain comes at the expense of increased interference radiated within the main beam of the UAV. However, this extra interference can be in some situations tolerated by the network if the beam direction is carefully controlled and steered in the potentially less loaded directions.

H.7 Conclusions

High-throughput uplink UAV communication is a necessary technology component needed to fully benefit from UAVs flying in our skies. In high load scenarios or with many UAVs flying over the same geographical region, cellular networks may not be able to match these stringent requirements. By implementing a beamforming system on a UAV, its efficient usage may complement network efforts in providing high uplink throughput for UAVs. In this article, we have analyzed potential scenarios in which such a beamforming system would become beneficiary. As a result of the conducted simulations and experiments, we indicated the limitations of the current generation of cellular networks and provided possible guidelines on how to efficiently integrate high uplink-demanding UAVs into the cellular paradigm.

H.8 Acknowledgment

We would like to thank TDC, Denmark for supporting this work via sharing the network topology and IoT information.

References

[1] Y. Zeng, Q. Wu, and R. Zhang, "Accessing from the sky: A tutorial on UAV communications for 5G and beyond," *Proceedings of the IEEE*, vol. 107, no. 12, pp. 2327–2375, December 2019.

[2] S. Hayat, E. Yanmaz, and R. Muzaffar, "Survey on unmanned aerial vehicle networks for civil applications: A communications viewpoint," *IEEE Communications Surveys Tutorials*, vol. 18, no. 4, pp. 2624–2661, 2016.

[3] P. Chandhar and E. G. Larsson, "Massive MIMO for connectivity with drones: Case studies and future directions," *IEEE Access*, vol. 7, pp. 94 676–94 691, 2019.

[4] S. Qazi, A. S. Siddiqui, and A. I. Wagan, "UAV based real time video surveillance over 4G LTE," in *2015 International Conference on Open Source Systems Technologies (ICOSST)*, December 2015, pp. 141–145.

[5] X. Lin, V. Yajnanarayana, S. D. Muruganathan, S. Gao, H. Asplund, H. Maattanen, M. Bergstrom, S. Euler, and Y.-P. E. Wang, "The sky is not the limit: LTE for unmanned aerial vehicles," *IEEE Communications Magazine*, vol. 56, no. 4, pp. 204–210, April 2018.

[6] "LTE unmanned aircraft systems trial report," Qualcomm, Tech. Rep. v1.0.1, May 2017.

[7] R. Amorim, H. Nguyen, J. Wigard, I. Z. Kovács, T. B. Sørensen, D. Z. Biro, M. Sørensen, and P. Mogensen, "Measured uplink interference caused by aerial vehicles in LTE cellular networks," *IEEE Wireless Communications Letters*, vol. 7, no. 6, pp. 958–961, December 2018.

[8] A. Garcia-Rodriguez, G. Geraci, D. Lopez-Perez, L. G. Giordano, M. Ding, and E. Bjornson, "The essential guide to realizing 5G-connected UAVs with massive MIMO," *IEEE Communications Magazine*, pp. 2–8, 2019.

[9] Y. Zeng, J. Lyu, and R. Zhang, "Cellular-connected UAV: Potential, challenges, and promising technologies," *IEEE Wireless Communications*, vol. 26, no. 1, pp. 120–127, February 2019.

[10] G. Geraci, A. Garcia-Rodriguez, L. Galati Giordano, D. Lopez-Perez, and E. Bjornson, "Understanding UAV cellular communications: From existing networks to massive MIMO," *IEEE Access*, vol. 6, pp. 67 853–67 865, 2018.

[11] W. Mei, Q. Wu, and R. Zhang, "Cellular-connected UAV: Uplink association, power control and interference coordination," in *2018 IEEE Global Communications Conference (GLOBECOM)*, December 2018, pp. 206–212.

[12] W. Mei and R. Zhang, "UAV-sensing-assisted cellular interference coordination: A cognitive radio approach," *IEEE Wireless Communications Letters*, 2020.

[13] "Summary for WI enhanced LTE support for aerial vehicles," 3GPP, Tech. Rep. RP-181644, September 2018.

[14] H. C. Nguyen, R. Amorim, J. Wigard, I. Z. Kovács, T. B. Sørensen, and P. E. Mogensen, "How to ensure reliable connectivity for aerial vehicles over cellular networks," *IEEE Access*, vol. 6, pp. 12 304–12 317, 2018.

[15] T. Izydorczyk, M. Bucur, F. M. L. Tavares, G. Berardinelli, and P. Mogensen, "Experimental evaluation of multi-antenna receivers for UAV Communication in Live LTE networks," in *2018 IEEE Globecom Workshops (GC Wkshps)*, December 2018, pp. 1–6.

[16] B. D. Van Veen and K. M. Buckley, "Beamforming: a versatile approach to spatial filtering," *IEEE ASSP Magazine*, vol. 5, no. 2, pp. 4–24, April 1988.

[17] H. Hu, J. Zhang, X. Zheng, Y. Yang, and P. Wu, "Self-configuration and self-optimization for LTE networks," *IEEE Communications Magazine*, vol. 48, no. 2, pp. 94–100, 2010.

[18] "LTE evolved universal terrestrial radio access (E-UTRA). radio resource control (RRC). protocol specification," 3GPP, Tech. Rep. TS 36.331 Version 15.3.0, October 2018.

[19] "LTE evolved universal terrestrial radio access (E-UTRA). physical layer. measurements," 3GPP, Tech. Rep. TS 36.214 Version 14.2.0, April 2017.

[20] R. Amorim, H. Nguyen, P. Mogensen, I. Z. Kovács, J. Wigard, and T. B. Sørensen, "Radio channel modeling for UAV communication over cellular networks," *IEEE Wireless Communications Letters*, vol. 6, no. 4, pp. 514–517, August 2017.

[21] "Spatial channel model for multiple input multiple output (MIMO) simulations," 3GPP, Tech. Rep. TR 25.996, March 2011.

[22] T. Izydorczyk, M. M. Ginard, S.Svendsen, G. Berardinelli, and P. Mogensen, "Experimental evaluation of beamforming on UAVs in cellular systems," Available at: https://arxiv.org/abs/2003.12010, 2020, submitted for 2020 European Wireless (EW).

[23] "LTE evolved universal terrestrial radio access (E-UTRA). user equipment (UE) radio access capabilities," 3GPP, Tech. Rep. TS 36.306 Version 14.2.0, April 2017.

[24] Rohde and Schwarz, "Using R&S TSMA with swissqual qualipoc android. A wide range of optimization applications," 2016. [Online]. Available: https://scdn.rohde-schwarz.com/ur/pws/dl_downloads/dl_common_library/dl_brochures_and_datasheets/pdf_1/service_support_30/TSMA-QualiPoc_ac_en_3607-3574-32_v0101.pdf

[25] J. Sae, R. Wiren, J. Kauppi, H. Maattanen, J. Torsner, and M. Valkama, "Public LTE network measurements with drones in rural environment," in *2019 IEEE 89th Vehicular Technology Conference (VTC2019-Spring)*, April 2019, pp. 1–5.

[26] C. Ubeda Castellanos, D. L. Villa, C. Rosa, K. I. Pedersen, F. D. Calabrese, P. Michaelsen, and J. Michel, "Performance of uplink fractional power control in UTRAN LTE," in *VTC Spring 2008 - IEEE Vehicular Technology Conference*, May 2008, pp. 2517–2521.

ISSN (online): 2446-1628
ISBN (online): 978-87-7210-645-8

AALBORG UNIVERSITY PRESS